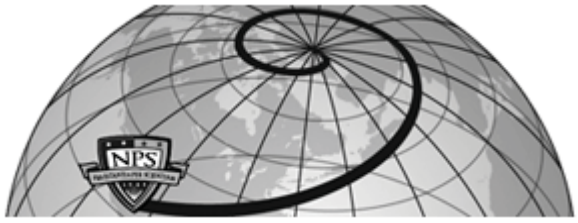

NAVAL POSTGRADUATE SCHOOL

MONTEREY, CALIFORNIA

THESIS

RELATIONSHIP BETWEEN THE SONIC LAYER DEPTH AND MIXED LAYER DEPTH IDENTIFIED FROM U.S. NAVY SEA GLIDER DATA

by

Vance A. Villarreal

September 2014

Thesis Advisor:	Peter C. Chu
Second Readers:	Chenwu Fan
	Ronald E. Betsch

Approved for public release; distribution is unlimited

THIS PAGE INTENTIONALLY LEFT BLANK

REPORT DOCUMENTATION PAGE

Form Approved OMB No. 0704-0188

1. AGENCY USE ONLY *(Leave blank)*	**2. REPORT DATE** September 2014	**3. REPORT TYPE AND DATES COVERED** Master's Thesis

4. TITLE AND SUBTITLE
RELATIONSHIP BETWEEN THE SONIC LAYER DEPTH AND MIXED LAYER DEPTH IDENTIFIED FROM U.S. NAVY SEA GLIDER DATA

5. FUNDING NUMBERS

6. AUTHOR(S) Vance A. Villarreal

7. PERFORMING ORGANIZATION NAME(S) AND ADDRESS(ES)
Naval Postgraduate School
Monterey, CA 93943-5000

8. PERFORMING ORGANIZATION REPORT NUMBER

9. SPONSORING /MONITORING AGENCY NAME(S) AND ADDRESS(ES)
N/A

10. SPONSORING/MONITORING AGENCY REPORT NUMBER

11. SUPPLEMENTARY NOTES The views expressed in this thesis are those of the author and do not reflect the official policy or position of the Department of Defense or the U.S. Government. IRB protocol number ____N/A____.

12a. DISTRIBUTION / AVAILABILITY STATEMENT
Approved for public release; distribution is unlimited

12b. DISTRIBUTION CODE
A

13. ABSTRACT (maximum 200 words)

The mixed layer depth (MLD) represents the upper ocean mixing, and the sonic layer depth (SLD) reveals the capacity of the upper ocean to trap acoustic energy and create a surface duct. A set of sea glider date from the Naval Oceanographic Office is used to identify the MLD and SLD at five locations. The maximum angle method is found to be the best among 17 existing MLD determination schemes of the four major methods (difference, gradient, curvature, and maximum angle). The maximum angle method is also found better than the currently used maximum value method in determining SLD. The optimally determined MLD and SLD by the maximum angle method from the Navy's glider data shows that one can swiftly, accurately, and objectively determine the MLD and SLD for operations in seas around the world.

14. SUBJECT TERMS mixed layer depth (MLD); sonic layer depth (SLD); difference method; gradient method; curvature method; max angle method.

15. NUMBER OF PAGES
117

16. PRICE CODE

17. SECURITY CLASSIFICATION OF REPORT	**18. SECURITY CLASSIFICATION OF THIS PAGE**	**19. SECURITY CLASSIFICATION OF ABSTRACT**	**20. LIMITATION OF ABSTRACT**
Unclassified	Unclassified	Unclassified	UU

NSN 7540-01-280-5500

Standard Form 298 (Rev. 2-89)
Prescribed by ANSI Std. 239-18

THIS PAGE INTENTIONALLY LEFT BLANK

Approved for public release; distribution is unlimited

RELATIONSHIP BETWEEN THE SONIC LAYER DEPTH AND MIXED LAYER DEPTH IDENTIFIED FROM U.S. NAVY SEA GLIDER DATA

Vance A. Villarreal
Lieutenant, United States Navy
B.S., United States Naval Academy, 2007

Submitted in partial fulfillment of the
requirements for the degree of

MASTER OF SCIENCE IN PHYSICAL OCEANOGRAPHY

from the

NAVAL POSTGRADUATE SCHOOL
September 2014

Author: Vance A. Villarreal

Approved by: Peter C. Chu
Thesis Advisor

Ronald E. Bestch
Second Reader

Donald Brutzman
Second Reader

Peter C. Chu
Chair, Department of Oceanography

THIS PAGE INTENTIONALLY LEFT BLANK

ABSTRACT

The mixed layer depth (MLD) represents the upper ocean mixing, and the sonic layer depth (SLD) reveals the capacity of the upper ocean to trap acoustic energy and create a surface duct. A set of sea glider date from the Naval Oceanographic Office is used to identify the MLD and SLD at five locations. The maximum angle method is found to be the best among 17 existing MLD determination schemes of the four major methods (difference, gradient, curvature, and maximum angle). The maximum angle method is also found better than the currently used maximum value method in determining SLD. The optimally determined MLD and SLD by the maximum angle method from the Navy's glider data shows that one can swiftly, accurately, and objectively determine the MLD and SLD for operations in seas around the world.

THIS PAGE INTENTIONALLY LEFT BLANK

TABLE OF CONTENTS

LIST OF FIGURES

THIS PAGE INTENTIONALLY LEFT BLANK

LIST OF TABLES

THIS PAGE INTENTIONALLY LEFT BLANK

LIST OF ACRONYMS AND ABBREVIATIONS

ANNUALEX	annual exercise
ASW	anti-submarine warfare
ASUW	anti-surface warfare
LRI	Liquid Robotics Incorporated
MA	max angle
MLD	mixed layer depth
NAVO	Naval Oceanographic Office
RIMPAC	Rim of the Pacific
RMSD	root-mean square difference
SEASWITI	Southeast ASW Integration Training Initiative
SHAREM	Ship Anti-submarine Warfare Readiness and Evaluation Measurement
SLD	sonic layer depth
SPM	sound speed maximum
SSP	sound speed maximum
SV2	surface vehicle two
SV3	surface vehicle three
SVP	sound velocity profile
QI	quality index
VS	Valiant Shield
USN	United States Navy
USW	undersea warfare
UUV	unmanned underwater vehicles
XBT	expendable bathythermograph

THIS PAGE INTENTIONALLY LEFT BLANK

ACKNOWLEDGMENTS

I would like to offer my most sincere appreciation to Professor Peter C. Chu for his support during my thesis trials. Without your help and supervision I would not have been able to complete it. I would also like to thank Mr. Chenwu Fan for all of your MATLAB help. There were some huge struggles, roadblocks, and, several rewrites of code along the way that I would not have been able to overcome without your expertise. It was an honor and a privilege to be able to work alongside both of you.

I would like to extend my appreciativeness to Mr. Ronald E. Betsch for being my second reader and to the United States Navy for affording me the opportunity to attend NPS and get my Masters of Science in Physical Oceanography.

THIS PAGE INTENTIONALLY LEFT BLANK

I. INTRODUCTION

In this chapter, we will define the mixed layer depth (MLD) and the sonic layer depth (SLD). Next, we will discuss the problem statement, related works, and the objective of this thesis. Lastly, we will describe the organization of the thesis.

A. MIXED LAYER DEPTH

The MLD is the thickness of a surface layer of water that has nearly vertical uniformed temperature, salinity, and density. It is due to turbulent mixing driven by surface momentum and buoyancy fluxes and shear at the base of the mixed layer (Garrett 1996). Since a multiple of forces influence the mixed layer its depth is constantly changing with time and location. The MLD is important because it identifies the penetration depth of turbulence from the ocean surface, and it has a broad array of influences on a variety of upper ocean processes from air-sea exchange (Chen et al. 1994) to biological interactions (Helber et al. 2009) (see Figure 1).

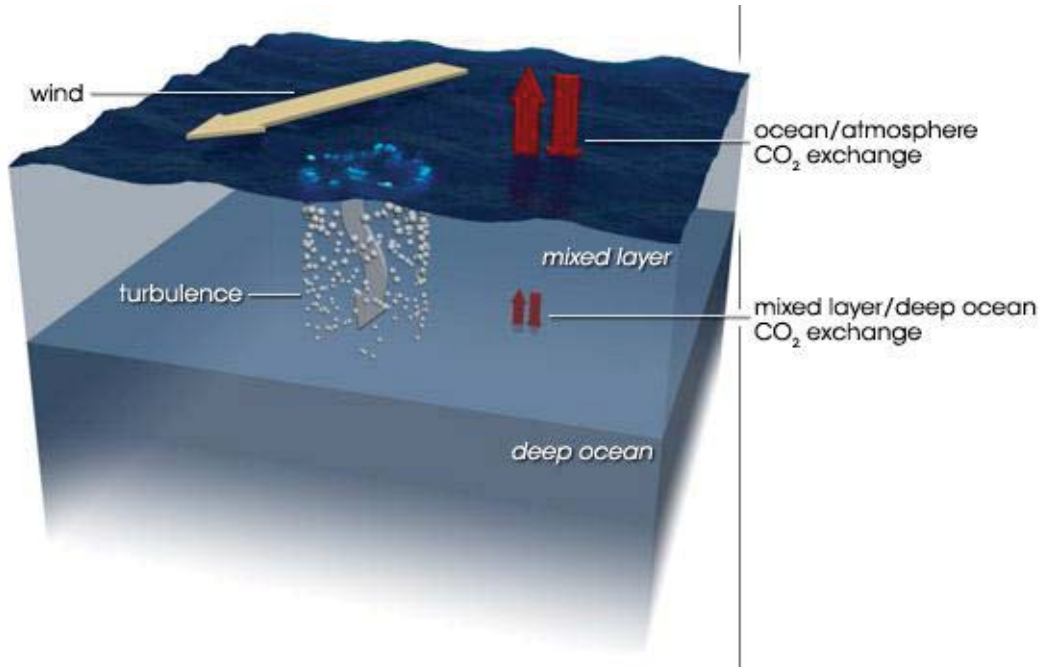

Figure 1. A visual of the mixed layer depth (from Holli 2014).

The United States Navy (USN) has a vested interest in knowing exactly where the MLD is located. The USN operates in the MLD across the globe on a daily basis, whether it be in anti-submarine warfare (ASW) through its ships and aircraft or in anti-surface warfare (ASUW) waged by its submarines. Nearly every platform in the USN will come into contact with the MLD in one way or another.

B. SONIC LAYER DEPTH

The SLD is the vertical distance from the ocean surface to the depth of the sound speed maximum (Helber et al. 2009) (see Figure 2). The sound speed reaches its max speed at the SLD because in the mixed layer temperature and salinity are nearly constant; therefore, the only variable affecting the sound speed is pressure. As sound leaves the mixed layer, temperature starts to take over and the sound speed will decrease due to a decrease in temperature.

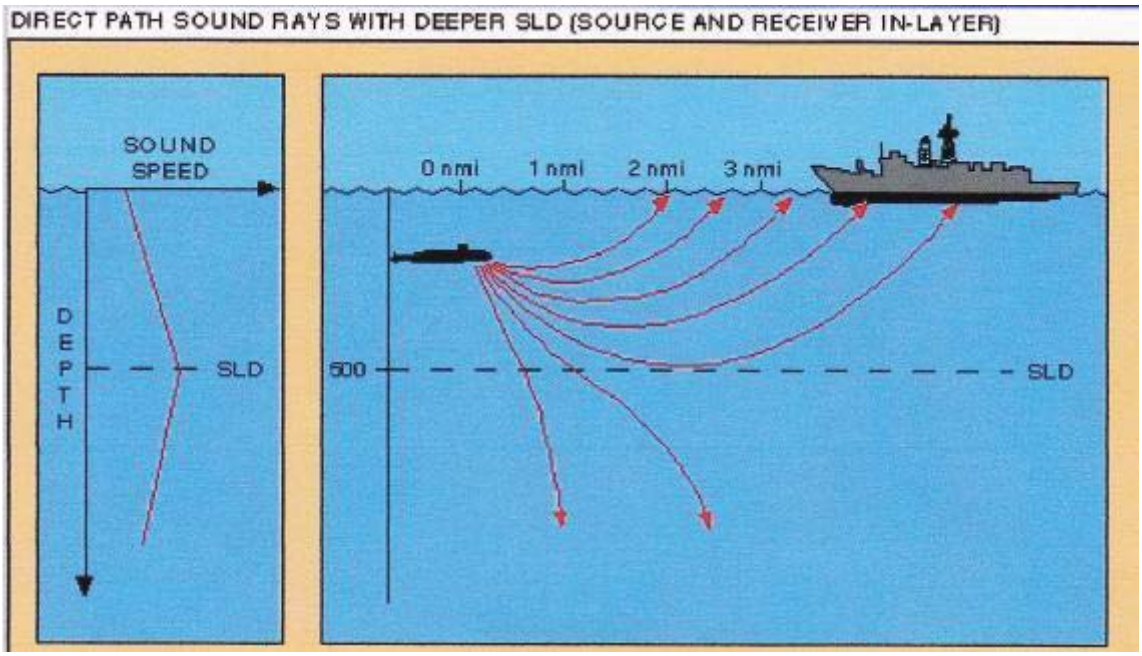

Figure 2. An example of the SLD (from Guest 2014).

The MLD and SLD often coincide since "the sounds speed is locally maximum at the base of the isothermal and/or isohaline surface layer" (Helber et al. 2009). The SLD is important to the USN because it determines the minimum cut off frequency above which

sound tends to be trapped and below which a shadow zone exists. This has a direct impact on where the USN operates its sensors and places its platforms in the water column.

C. PROBLEM STATEMENT

The SLD and the MLD are often assumed to be one and the same. People assume this because the sounds speed often increases down to the bottom of the MLD where a decrease in temperature occurs, resulting in a local maximum of sound speed; however this is not always the case (Helber et al. 2008). The SLD is measured using temperature and salinity while the MLD is measured by using temperature or density. The difference of depth between the MLD and SLD can occur because sound speed is substantially more sensitive to temperature then to salinity compared to density. Depending on the season and location on the globe the MLD and SLD can differ by more than 10 meters (Helber et al. 2008). There are also some substantially different results for the MLD between the different methods that researchers use to determine the MLD.

D. RELATED WORKS

Many different people have looked at different ways to determine the MLD from observational data. There are no fewer than a dozen papers on the subject dating back to 1961 where Defant used the gradient method to determine the MLD. In recent years new methods have emerged to determine the MLD such as optimal linear fitting and the max angle methods from Chu and Fan (Chu et al. 2010b). These methods while more computative intensive have proved to be more accurate and objective then other methods at determining the MLD.

Few papers have compared and contrast the relationship between the MLD and the SLD. Helber et al. (2008) evaluated the MLD using the difference method reference 10m (temperature and density) and the curvature method (temperature) and compared them to the SLD. They did this using a set of global in situ profiles from various platforms gathered by conductivity-temperature-depth recorders for an annual cycle.

E. OBJECTIVE

The objective of this paper is twofold. The first objective is to show that the MLD can be determined fast and accurately from anywhere in the world with certain small restrictions by using a simple algorithm. The second objective is to compare the best method for determining the MLD to the SLD and see how close the results are.

F. THESIS ORGANIZATION

Chapter II gives the background information about the data used in this thesis, location where the data was collected, when the data was collected, and other pertinent information.

Chapter III provides a detailed description about the different methods we to obtain the MLD and SLD. It explains each method step by step and details the limitations and short comings of each one.

Chapter IV gives the findings of the MLD and the SLD from our experiment. It presents the results in several different graphs and illustrations.

Chapter V presents the analysis of our data set of the MLD and compares them to the SLD. It also outlines possible reasons and explanation for the outcome of our experiment.

Chapter VI takes our findings and then explains how it can benefit and impact the USN and its missions. It also shows how the USN could use this information in the future. Next, it summarizes our findings. Lastly, it suggests future area of works that can be researched that are related to our problem statement.

II. DATA

In this chapter we will take a look at where our data set came from. We will take a look at location, date, and other relevant information about our data set.

A. OVERVIEW

The data used in this thesis is from the Naval Oceanographic Office (NAVO) (Mahoney et al. 2009a). The data was obtained from a set of USN sea gliders from 2006 to 2007. The data was collected during five different naval exercises around the world. The locations of these exercises were in the vicinity of the water off of Hawaii, Florida, Guam, Okinawa, and the Ryukyu Island chain. The USN has bases that are close to all of these locations and are constantly operating in these waters.

1. Florida

Two USN sea gliders were deployed off the east coast of Florida by NAVO on the November 14, 2007 through the December 6 of the same year in support of exercise Southeast Anti-Submarine Warfare Integration Training Initiative (SEASWITI) (Mahoney et al. 2009b). The paths taken were the following: Glider 137 (blue line) was deployed at 29.52N, 79.01W (blue circle) and Glider 137 (red line) at 29.51N, 79.00W (red circle) (see Figure 3). Glider 137 moved north. Then it moved northeast and performed four loops before ending at 30.13N, 77.97W (blue star). Its lateral voyage was 237nm. Glider 138 moved northeast and then south (see Figure 4). On its final two legs, it turned north and then northwest ending up 29.45N, 78.40W (red star). Its lateral voyage was 203nm.

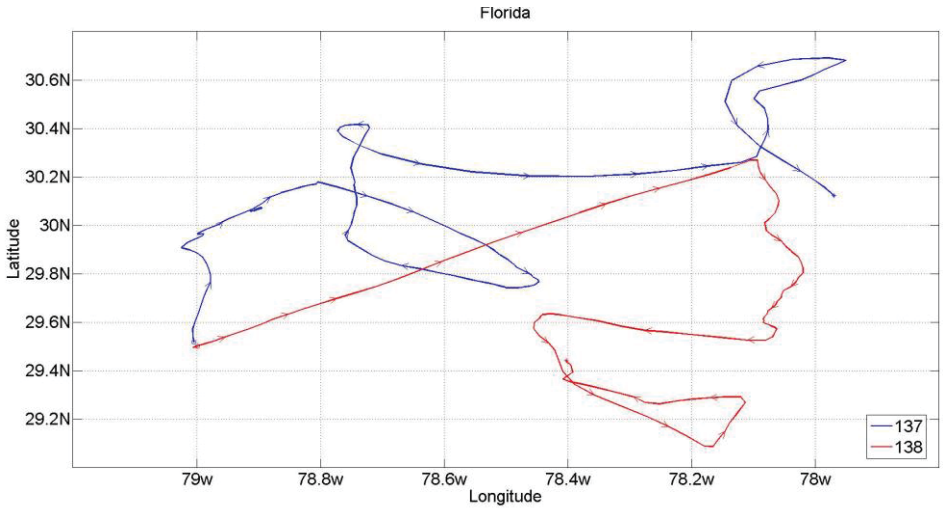

Figure 3. Starting points, path taken, and ending points for gliders 137 and 138.

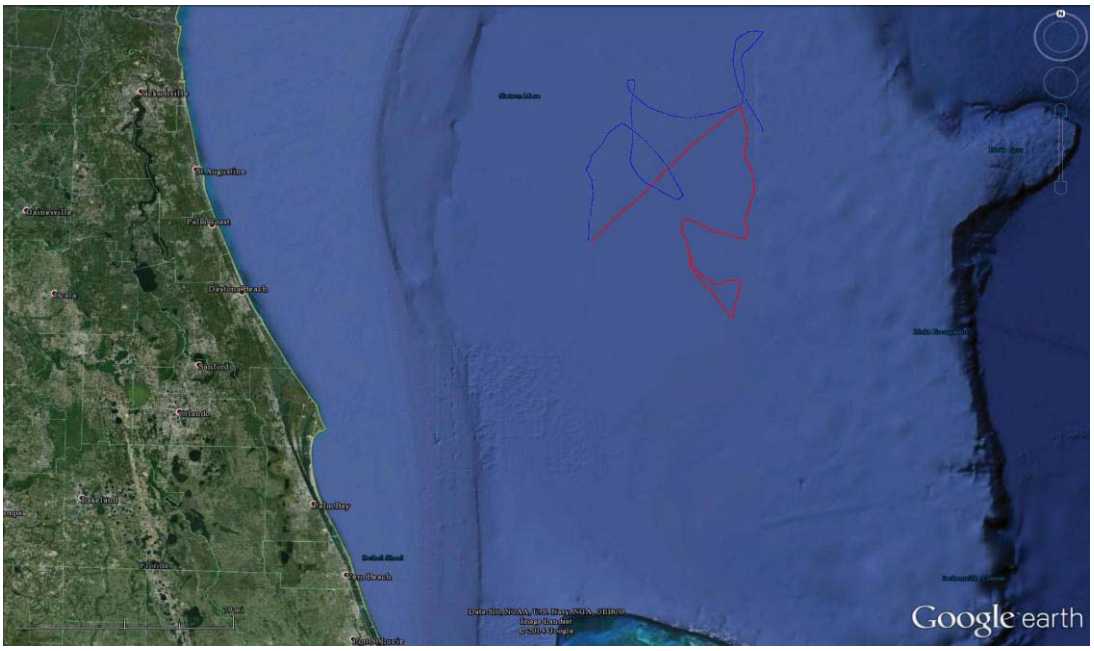

Figure 4. Glider 137 and 138 paths overlaid onto the globe (after Google Earth 2014).

a. Sound Speed Maximum and SLD

The sound speed maximum (SPM) for the different gliders in the Florida data set is pretty consistent. The differences between glider 137 and 138 will result from their being used in different areas of the ocean and on different days. The SPM of the sea

gliders downward profiles are plotted on the top graph in Figure 5. The middle graph is the sea gliders upward profile and the bottom is the two profiles combined. The SPM is between 1534.8 m/s to 1538.7 m/s for both gliders.

Figure 6 is the same layout as the SPM, but the SLD is plotted with respect to time (day). The SLD has huge fluctuations between the two gliders. The minimum SLD for the gliders is approximately 5m while the maximum is around 136m.

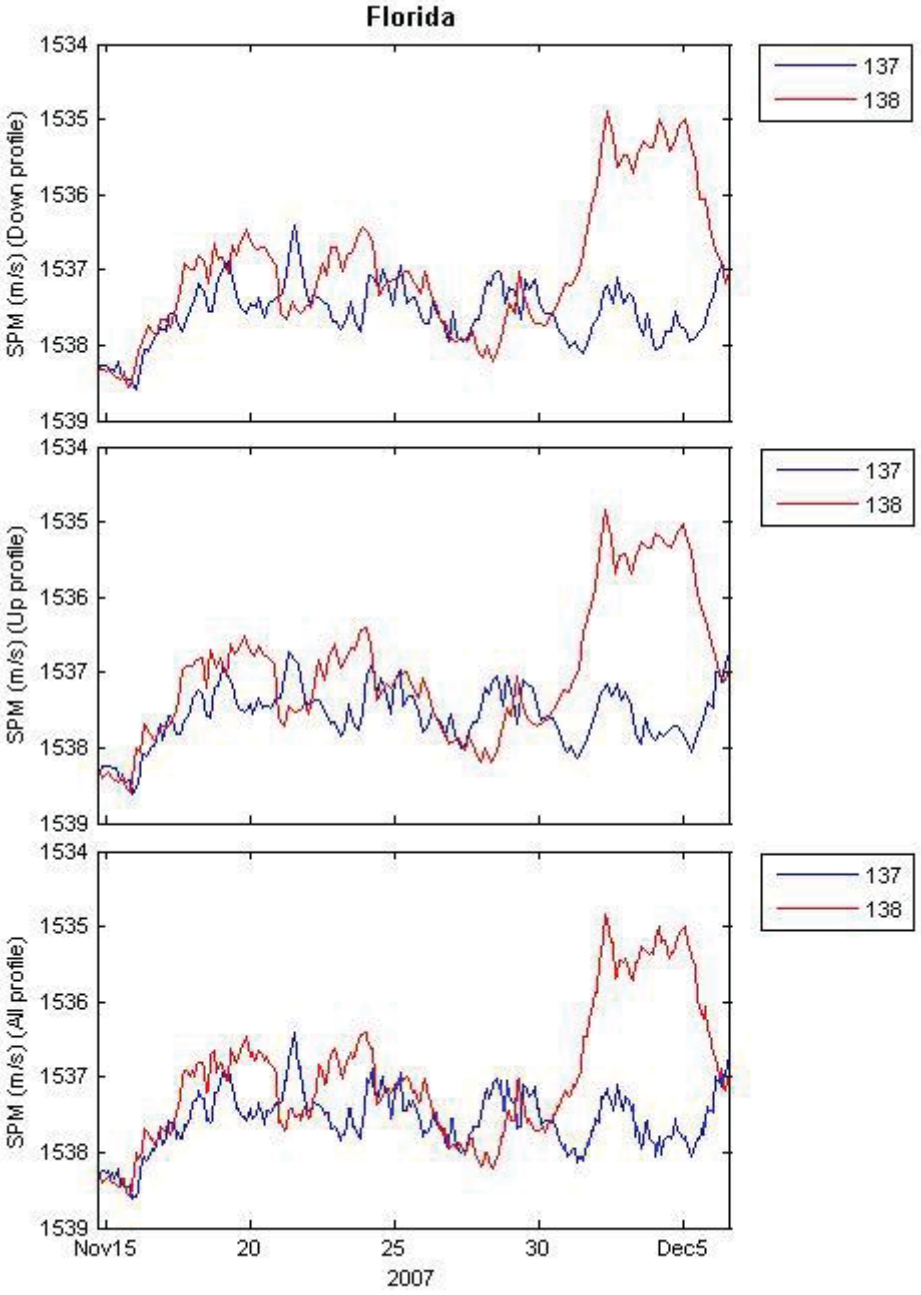

Figure 5. The SPM by day for the Florida data set for the down part of the dives, the upward parts, and both combined.

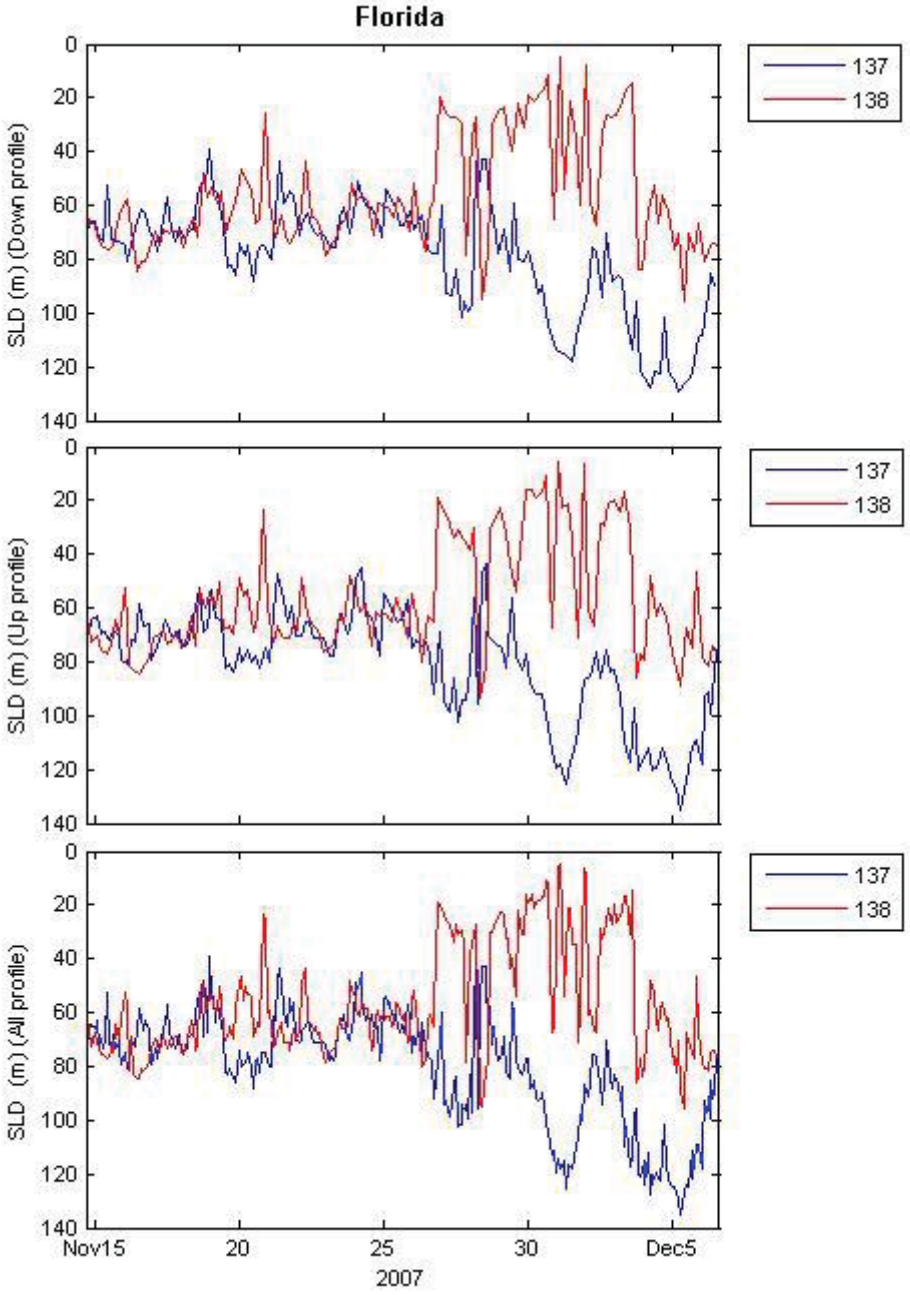

Figure 6. The SLD depth for the Florida data set by day for the downward part of the dives, the upward parts, and both combined.

b. Dive Profile

Figure 7 is the profile of the very first dive of exercise SEASWITI '07. Each dive roughly took between three and four hours to complete.

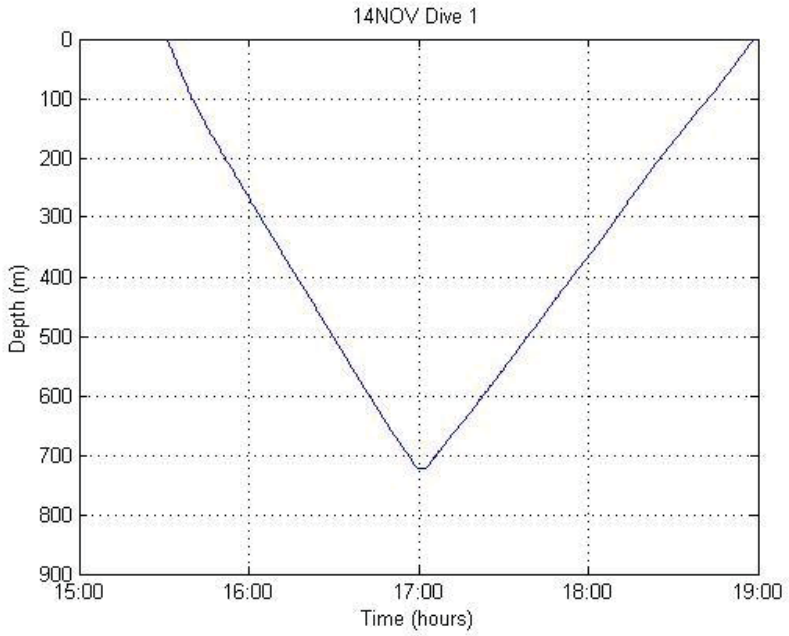

Figure 7. The first dive profile of exercise SEASWITI '07

c. Temperature, Salinity and Sound Speed Profile

Figures 8 and 9 show each of the dive profiles by glider for temperature, salinity, and sound speed (blue lines). The red lines are the average of the respective variables. As one can see from the profiles the blue lines are in a tight grouping. There is also a clear and present mixed layer, thermocline/halocline, and deep layer in each of the figures. At about 90m, there is also a well-defined SLD.

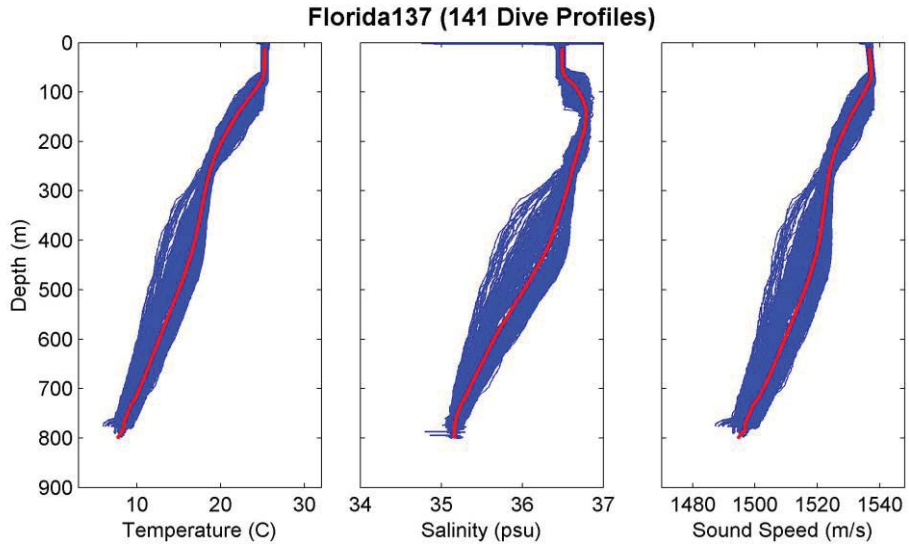

Figure 8. Glider 137 temperature, salinity, and sound speed profiles for 141 dives.

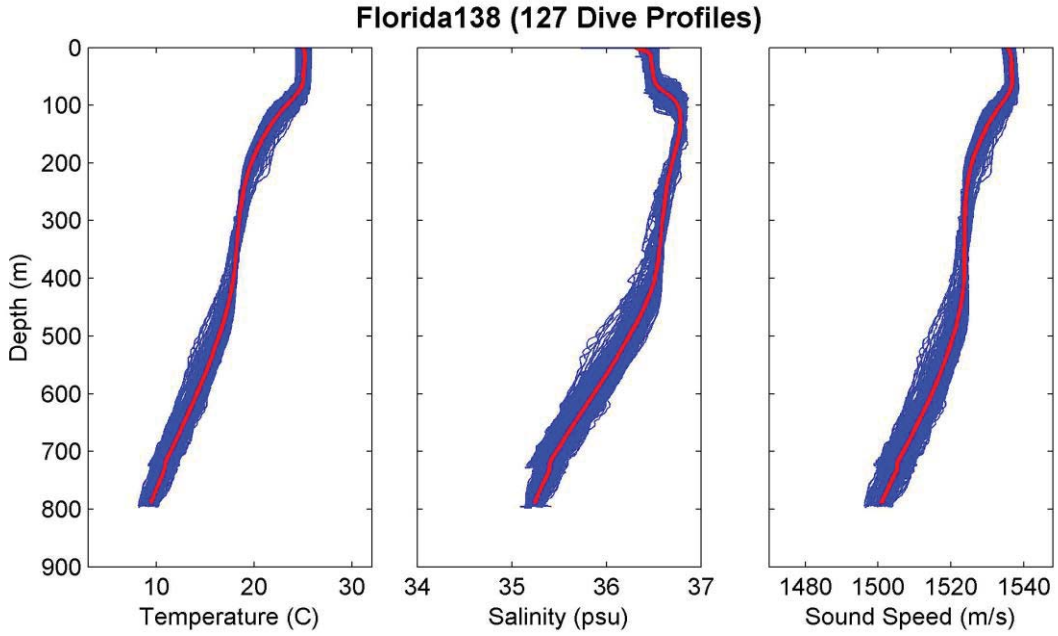

Figure 9. Glider 138 temperature, salinity, and sound speed profiles for 127 dives.

2. Guam

Seven USN sea gliders were deployed off the east coast of Guam by NAVO from the May 9, 2007 through the August 17 in support of exercise Valiant Shield (VS) (Mahoney et al. 2008). The gliders color coding are as follows: 133 (blue line right), 132 (red line right), 133 (black line), 134 (pink line) 135 (green line), 136 (blue line left), and 138 (red line left) (see Figure 10). All start and end points for the glider are indicted by a circle and star respectively. The total lateral distance traveled by the gliders in support of VS07 was 1,141.1nm (see Figure 11).

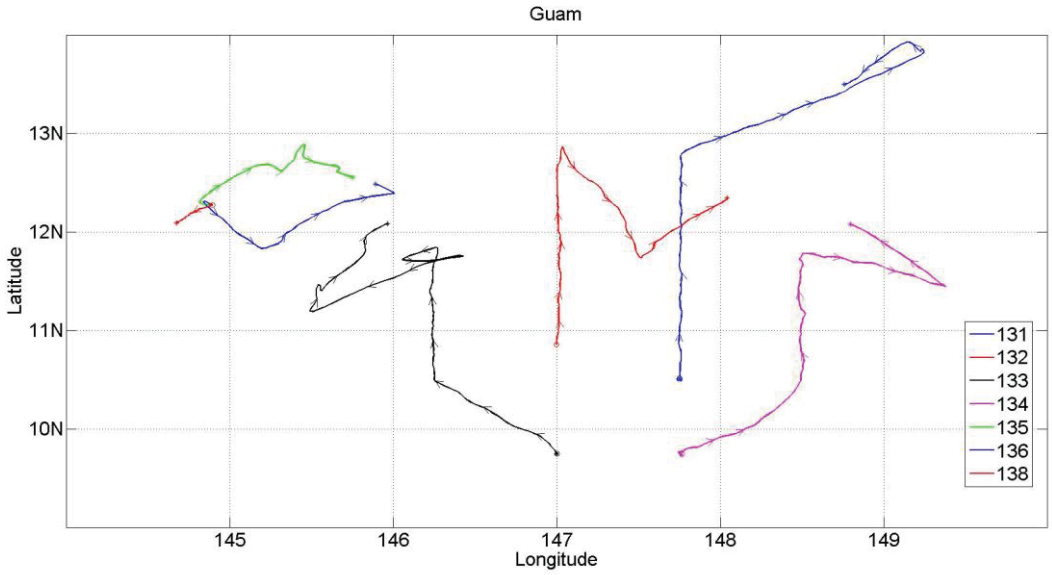

Figure 10. Starting points, paths taken, and ending points for all seven gliders in VS '07.

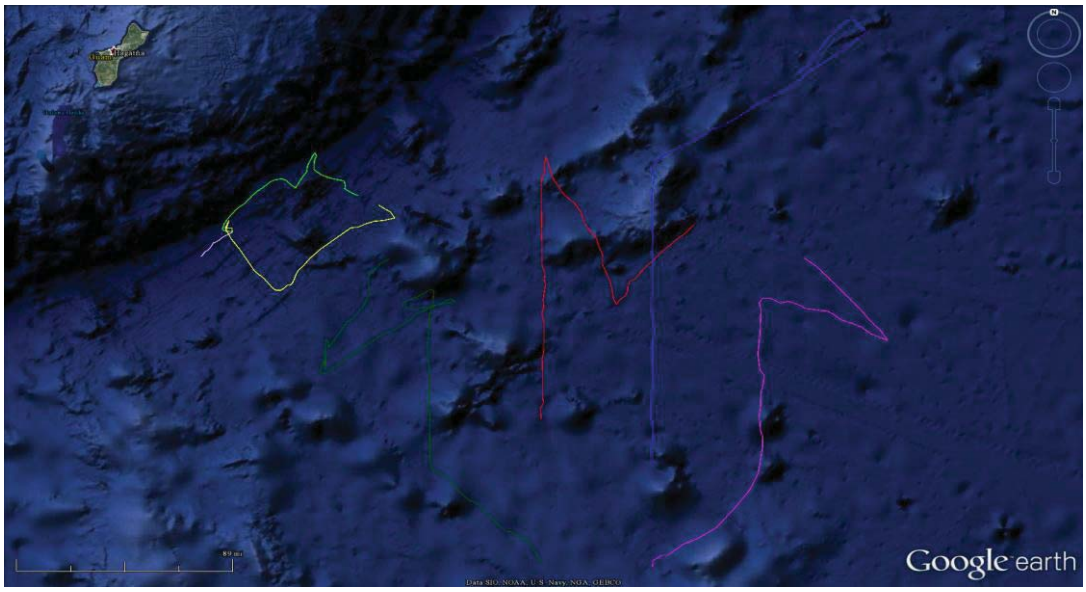

Figure 11. The gliders' path overlaid onto the globe (after Google Earth 2014).

a. SPM and SLD

The SPM for the Guam data set is very tight. There are slight differences between the gliders. The SPM of the sea gliders downward profiles are plotted on the top graph in Figure 12. The middle graph is the sea gliders upward profile and the bottom is the two profiles combined. The sound speed maximum is between 1543 m/s to 1549.5 m/s for the gliders.

Figure 13 is the same layout as the SPM, but we are plotting the SLD depth versus the day. The SLD fluctuates for the gliders.

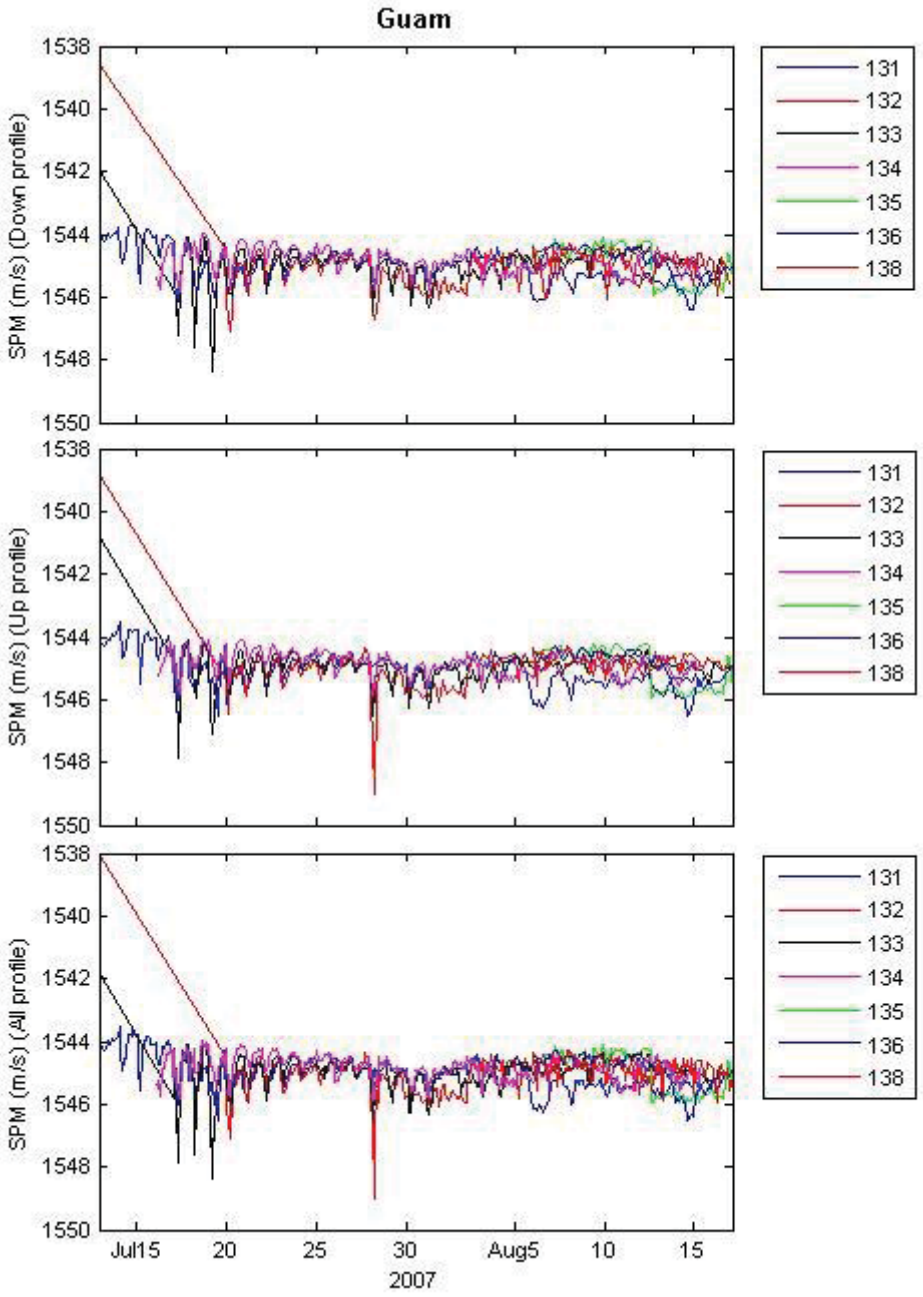

Figure 12. The SPM for the Guam data set by day for downward part of the dives, the upward parts, and both combined.

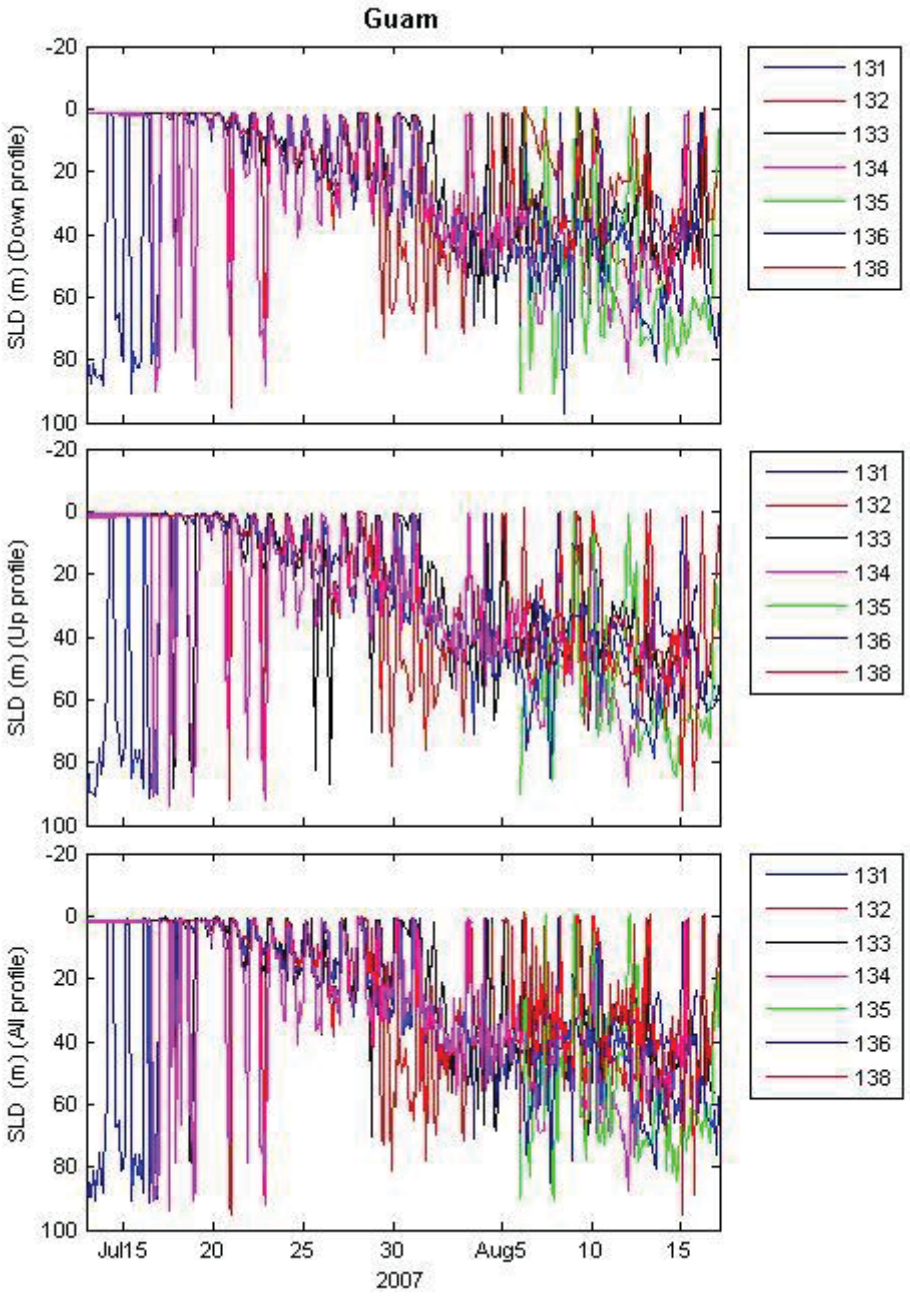

Figure 13. The SLD depth for the Guam data set by day for the downward part of the dives, the upward parts, and both combined.

b. Dive Profile

Figure 14 is the dive profile from 01AUG07. It shows a dive profile that took approximately three and a half hours to go down to 600m and back to the surface.

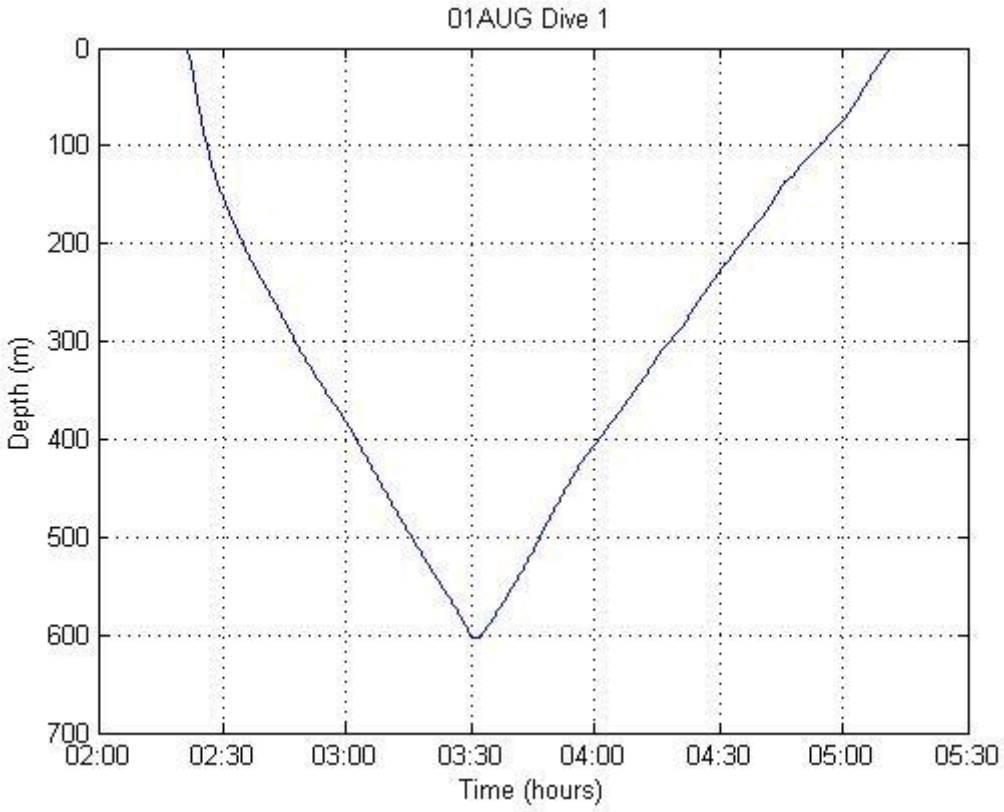

Figure 14. August 1 dive profile of exercise VS ‘07.

c. Temperature, Salinity, and Sound Speed Profiles

Figures 15–21 show each of the dive profiles by glider for temperature, salinity, and sound speed (blue lines). The red lines are the average of the respective variables. As one can see from the profiles, the blue lines for temperature are in a relative tight grouping for the number of each glider’s dive; however, the salinity profiles are more spaced out and stand out especially for Glider138. There is also a clear and present mixed layer, thermocline/halocline, and deep layer in each of the figures. The SLD is well-defined in each of the figures.

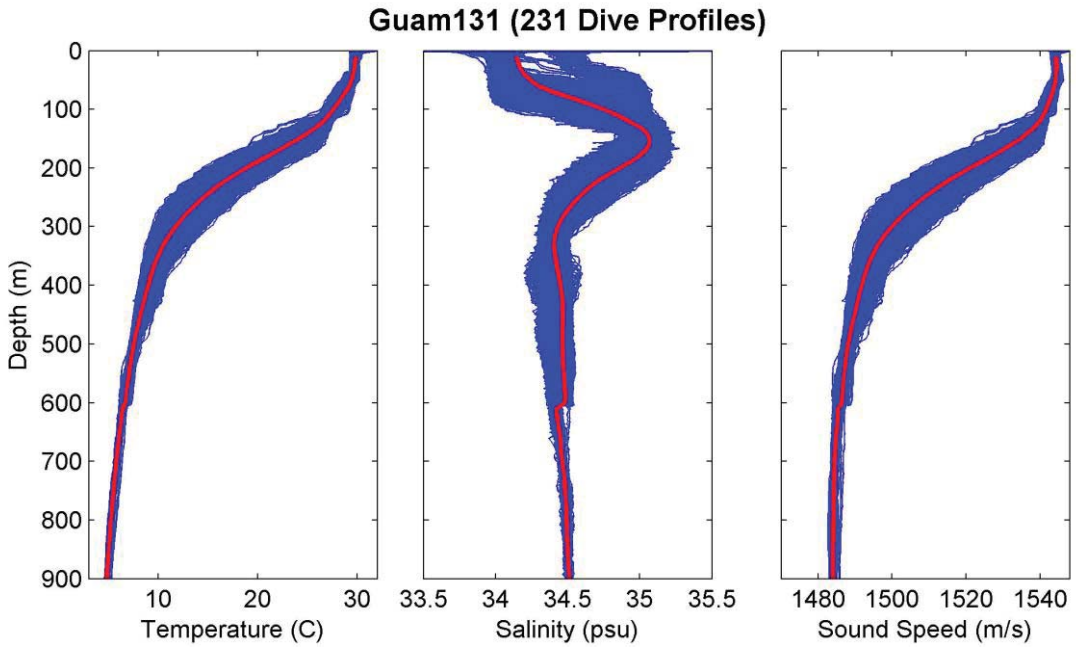

Figure 15. Glider 131 temperature, salinity, and sound speed profiles for 231 dives.

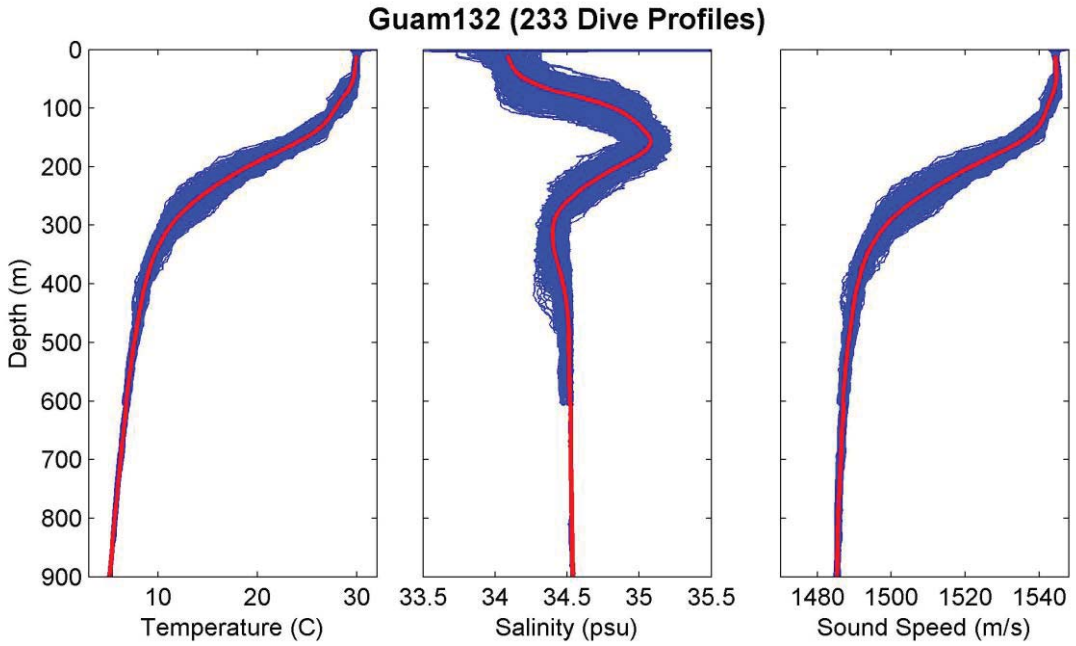

Figure 16. Glider 132 temperature, salinity, and sound speed profiles for 233 dives.

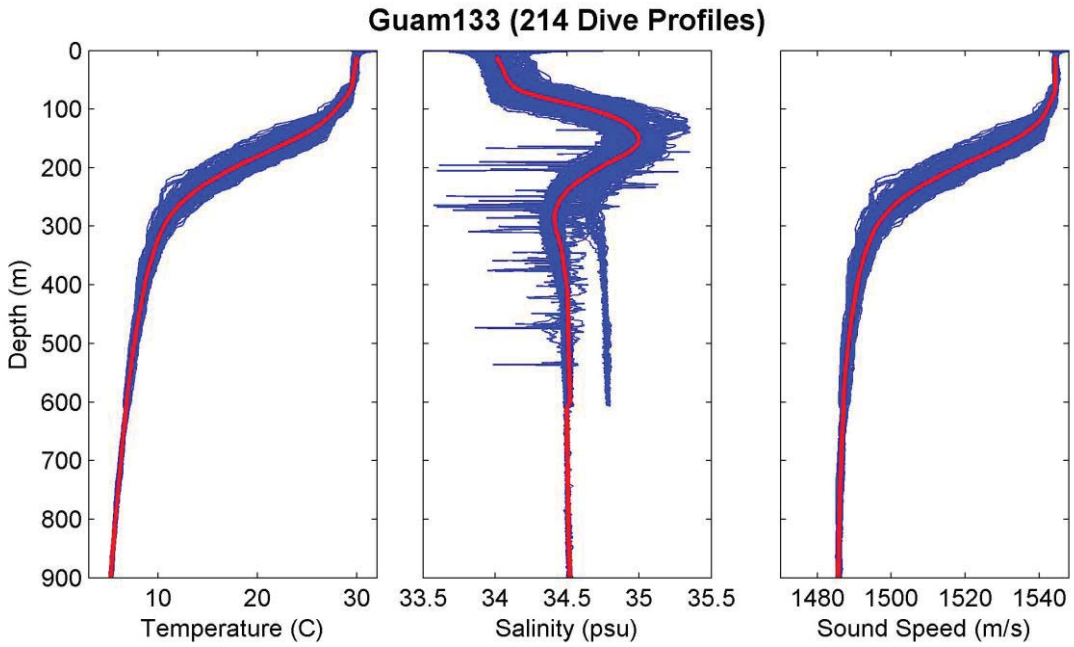

Figure 17. Glider 133 temperature, salinity, and sound speed profiles for 214 dives.

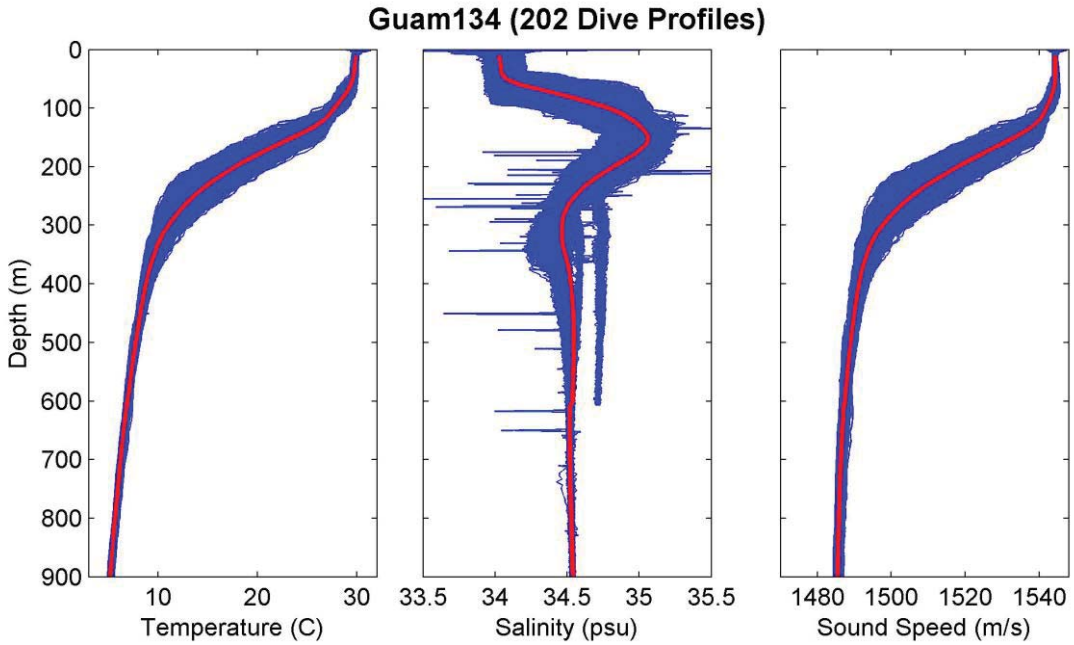

Figure 18. Glider 134 temperature, salinity, and sound speed profiles for 202 dives.

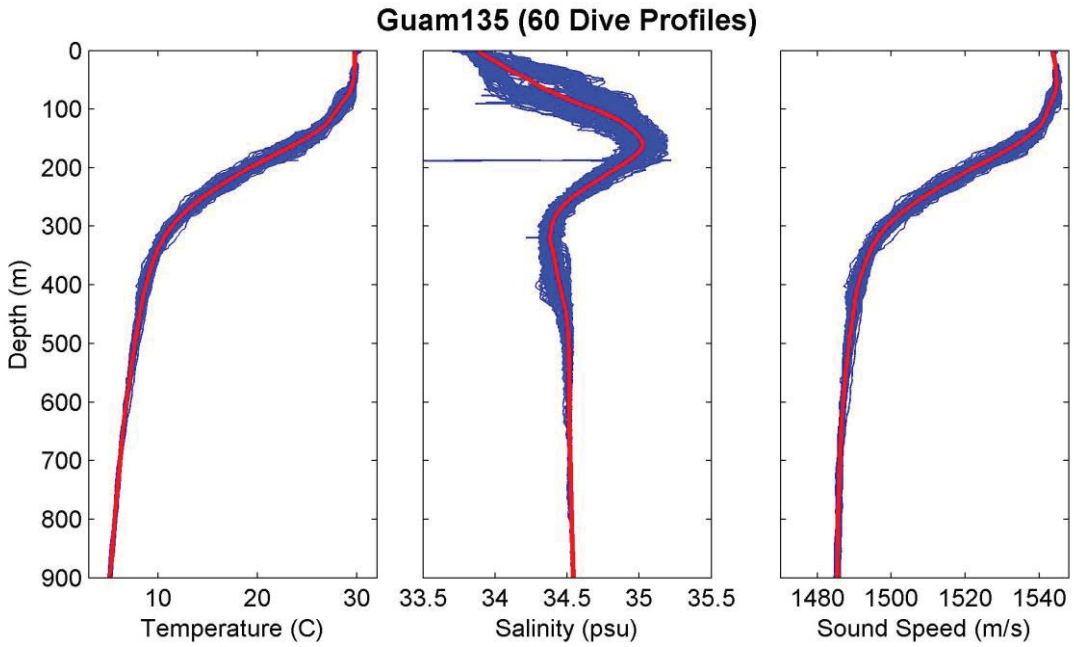

Figure 19. Glider 135 temperature, salinity, and sound speed profiles for 60 dives.

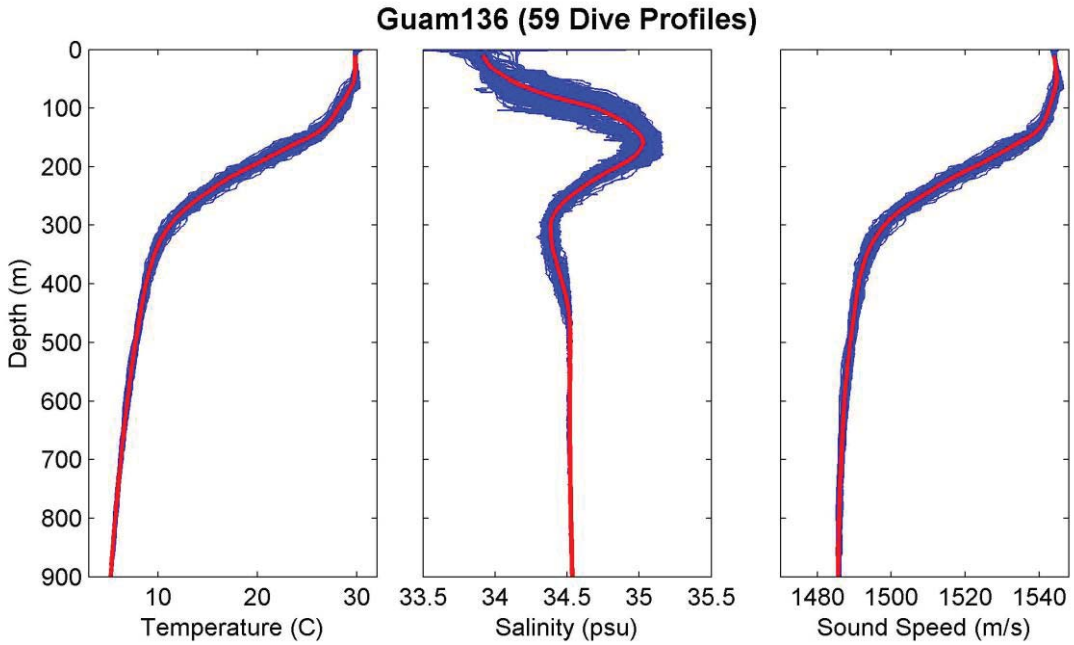

Figure 20. Glider 136 temperature, salinity, and sound Speed profiles for 59 dives.

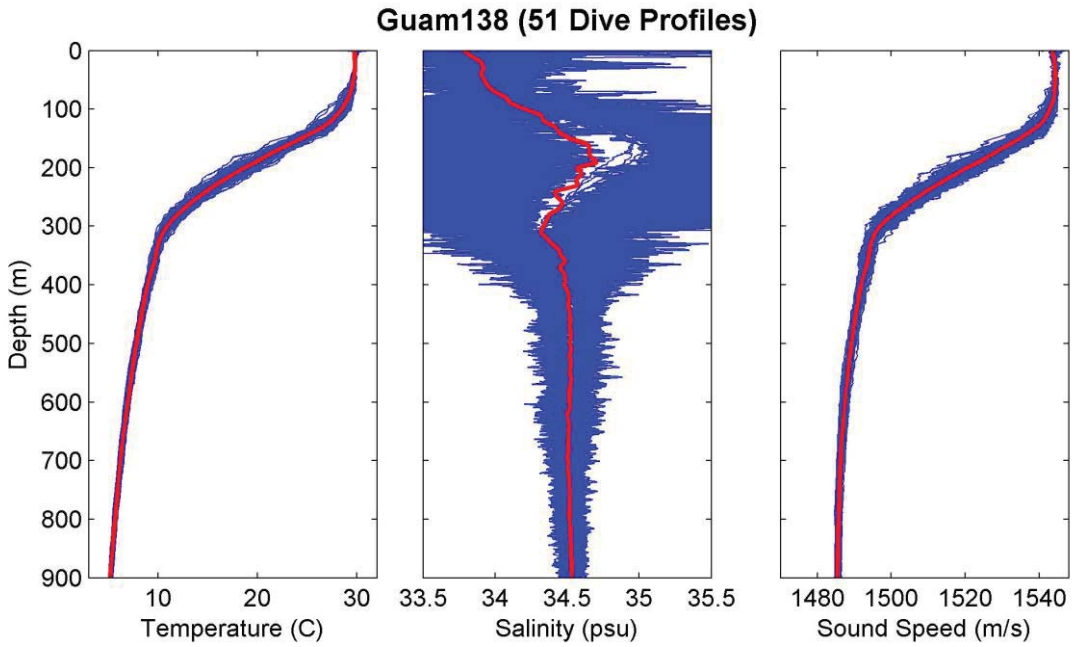

Figure 21. Glider 138 temperature, salinity, and sound speed profiles for 51 dives.

3. Hawaii

Four USN sea gliders were deployed off the west coast of Hawaii on the sixth of June 2006 through the July 24 of the same year in support of Rim of the Pacific (RIMPAC) exercise (Mahoney et al. 2007) (see Figure 22). Glider 111 (blue line), Glider 113 (red line), and Glider 114 (black line) were all deployed in the vicinity of 19.34N, 157.91W (three circles). Glider 115 (pink line) was deployed at 20.35N, 157.27W (pink circle). The three gliders spread out from each other heading north, west, and south from each other and made several different course changes and end up at the respective end points (indicated as blue, red, and black stars). Glider 115 moved west and ended its voyage at 19.99N, 159.37W (indicated by a pink star). The total lateral voyages for gliders 111,113, and 114 respectively were 265.04nm, 99.93nm, and 152.94nm. Glider 115 total lateral voyage was 109.49nm (see Figure 23).

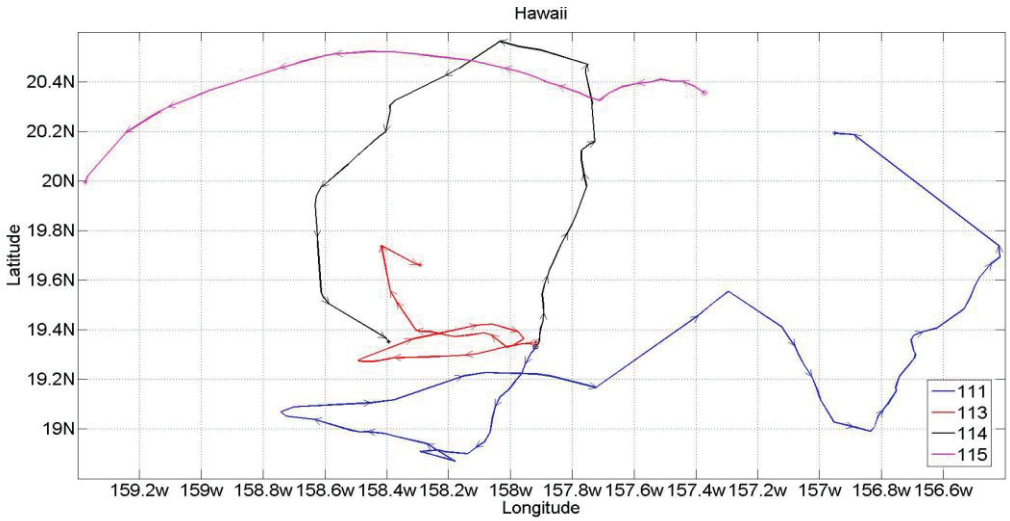

Figure 22. Starting points, path taken, and end points for gliders 111,113,114 and 115.

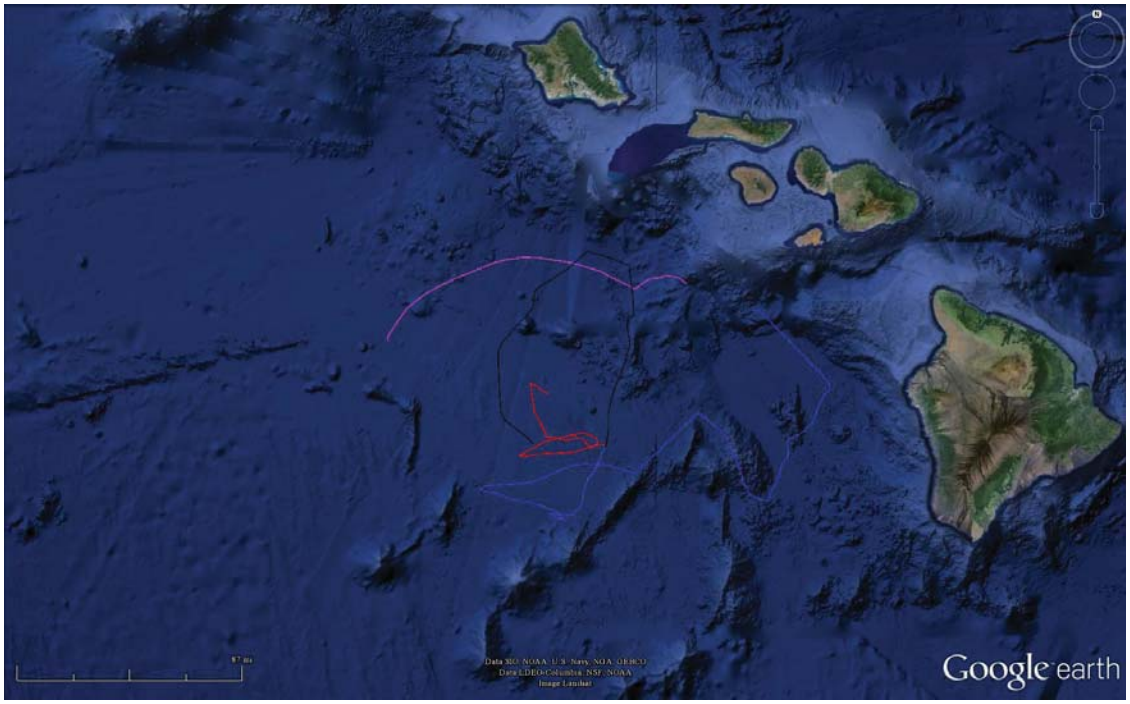

Figure 23. Gliders 111, 113, 114 and 115 paths overlaid onto globe (after Google Earth 2014).

a. SPM and SLD

The SPM for the Hawaii data set is close for the different gliders. It may seem at first glance on the down profile that it is not, but the m/s interval on the y-axis is small.

The SPM of the sea gliders downward profiles are plotted on the top graph in Figure 24. The middle graph is the sea gliders upward profile and the bottom is the two profiles combined. The sound speed maximum is between 1482 m/s to 1545 m/s for the gliders. Figure 25 uses the same layout has the SPM, but we are plotting the SLD depth versus the day. The SLD has major fluctuations between the gliders.

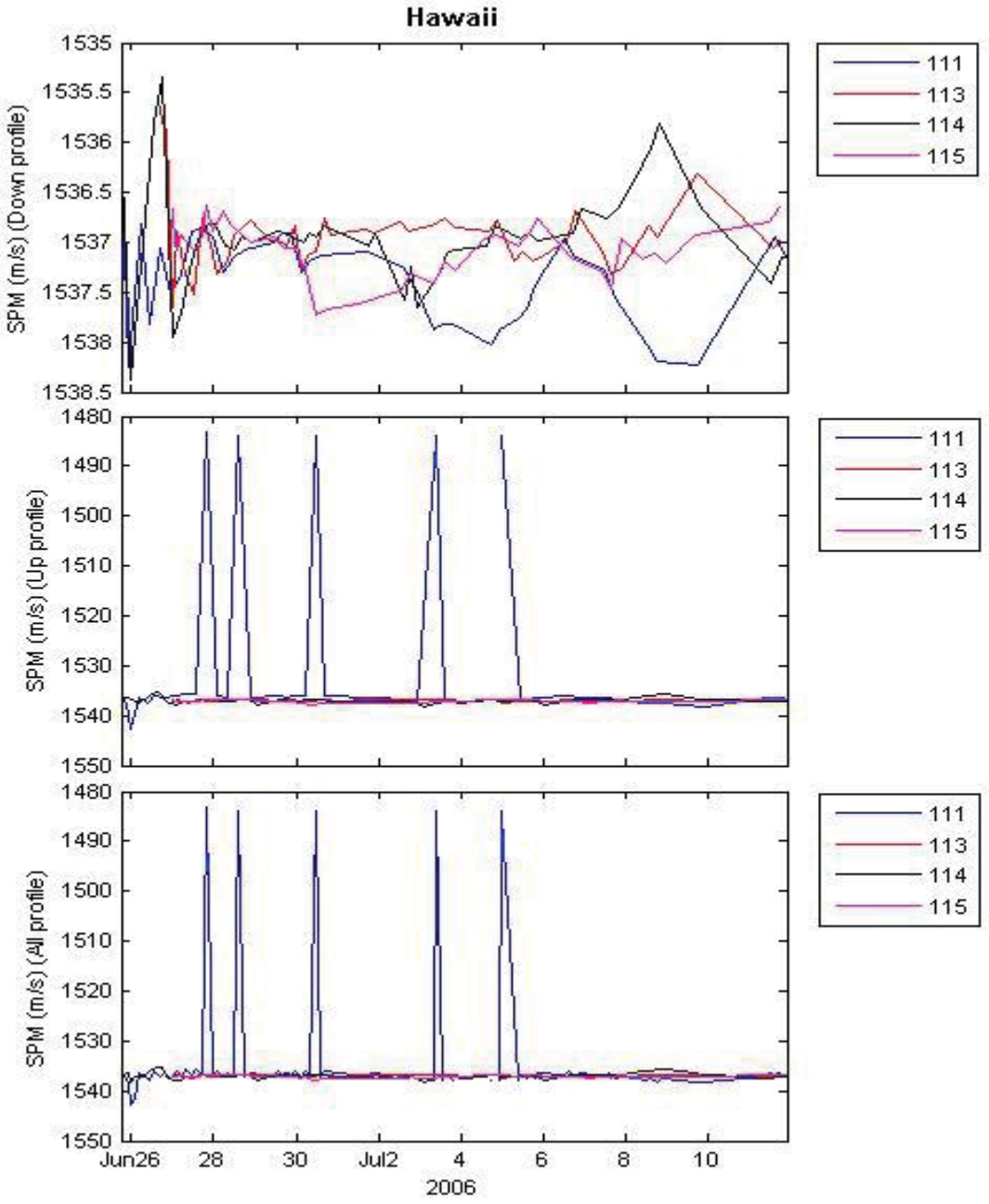

Figure 24. The SPM for the Hawaii data set by day for the downward part of the dives, the upward parts, and both combined.

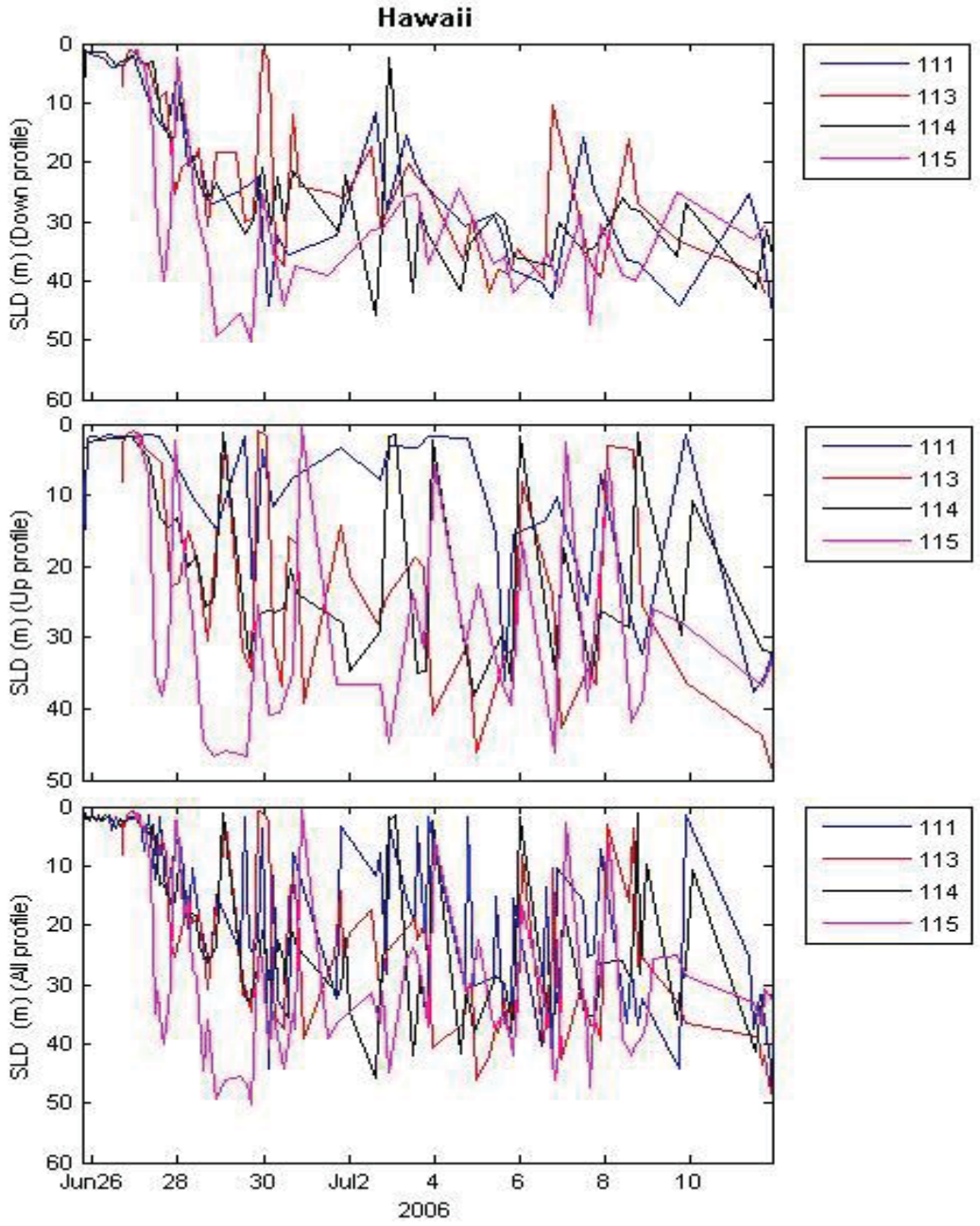

Figure 25. The SLD depths for the Hawaii data set by day for the downward part of the dives, the upward parts, and both combined.

b. Dive Profile

Figure 26 is the dive profile from 29JUN06. It shows a dive profile that took five hours to go down to 920m and back to the surface.

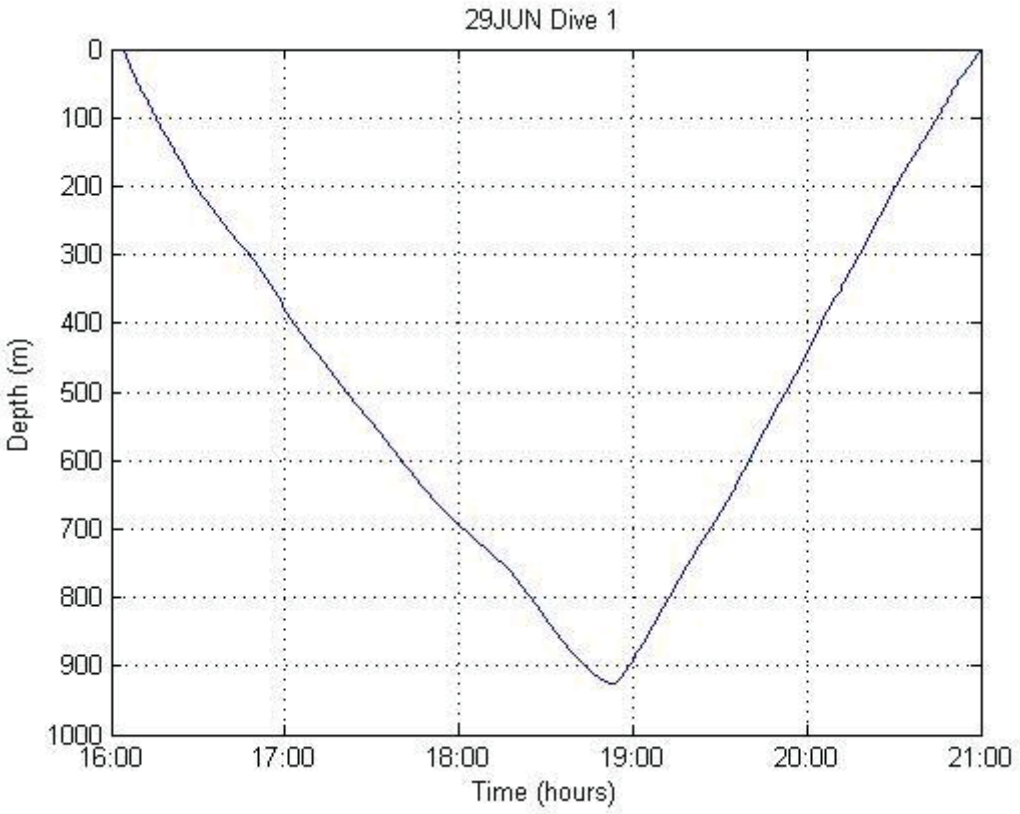

Figure 26. June 29 dive profile for RIMPAC ‘06.

c. Temperature, Salinity, and Sound Speed Profile

Figures 27–30 show each of the dive profiles by glider for temperature salinity and sound speed (blue lines). The red lines are the average of the respective variables. The profiles highlight the tight grouping of the blue lines. There is also a clear mixed layer, thermocline/halocline, and deep layer in each of the figures, and a well-defined SLD at approximately 90m.

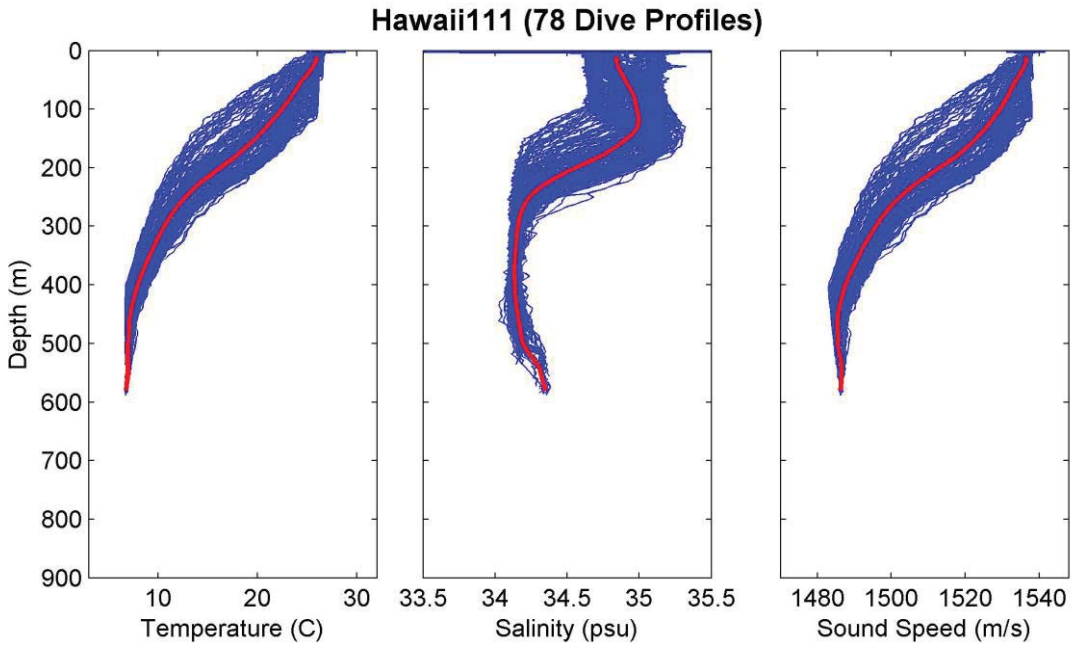

Figure 27. Glider 111temperature, salinity, and sound speed profiles for 78 dives.

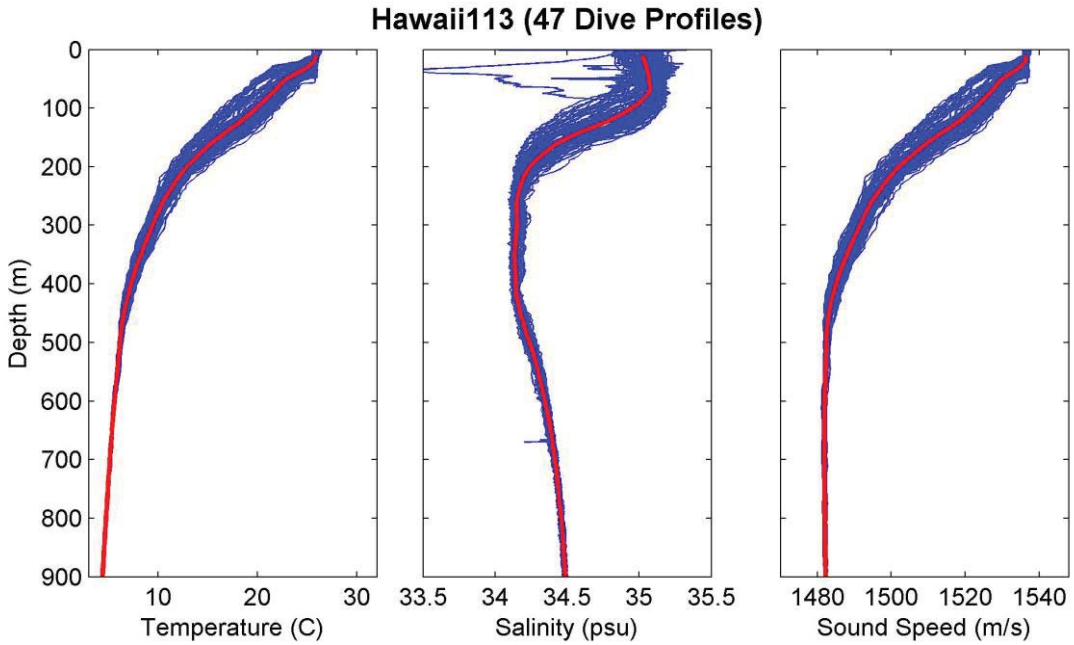

Figure 28. Glider 111 temperature, salinity, and sound speed profiles for 47 dives.

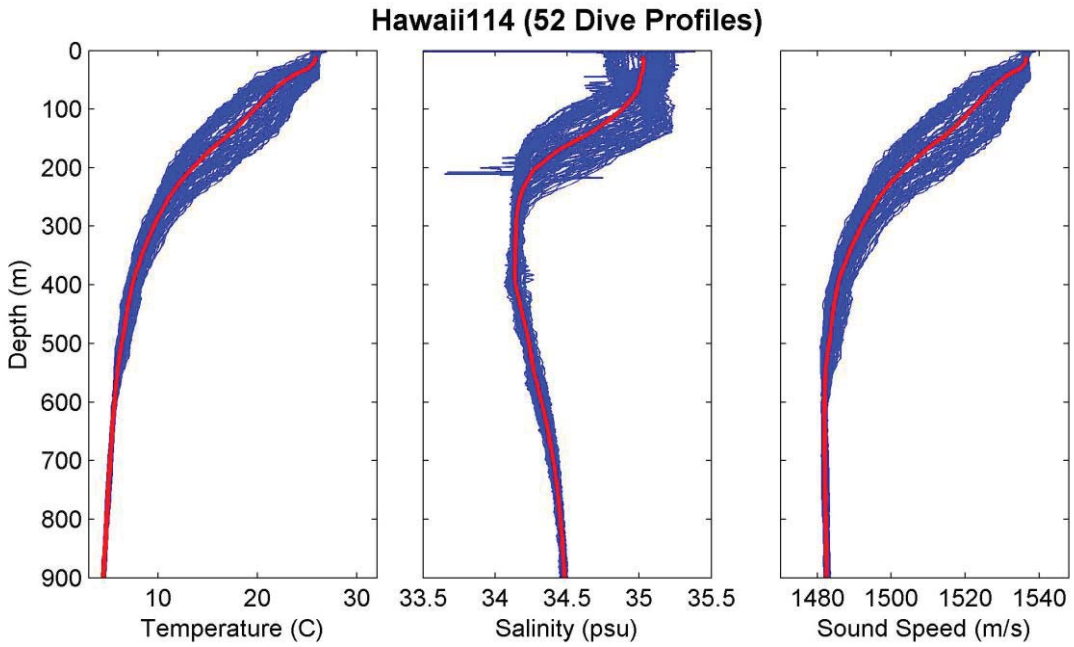

Figure 29. Glider 114 temperature, salinity, and sound speed profiles for 52 dives.

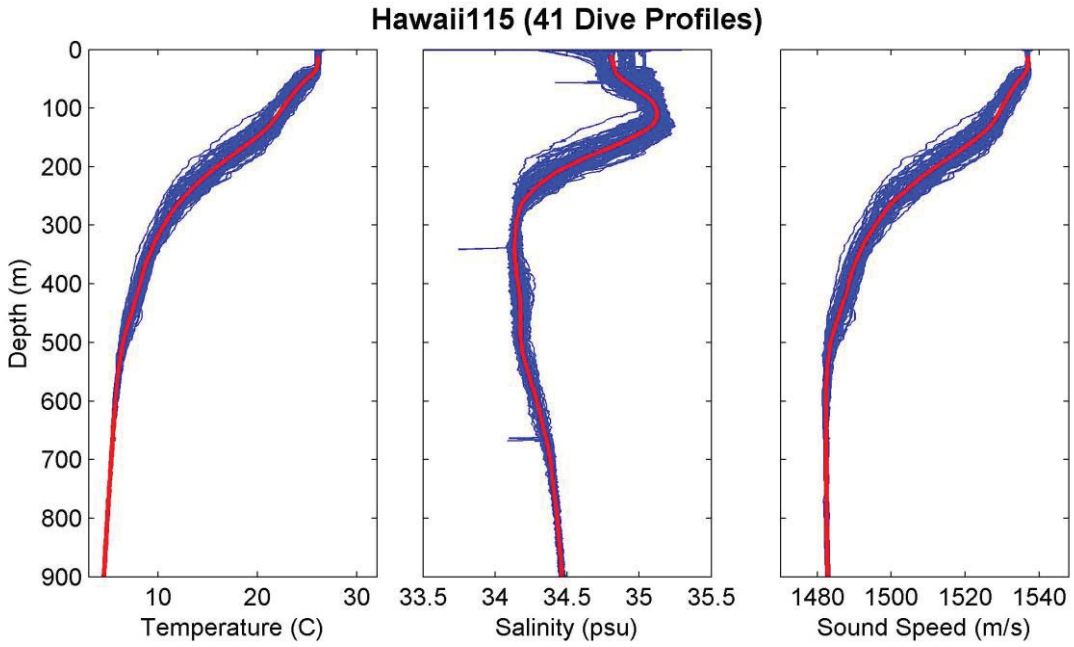

Figure 30. Glider 115 temperature, salinity, and sound speed profiles for 41 dives.

4. Okinawa

Two USN sea gliders were deployed off the east coast of Okinawa by NAVO on November 1 through the December 6, 2007 in support of Ship Anti-submarine Warfare Readiness and Evaluation Measurement (SHAREM) (Mahoney et al. 2009b). Glider 135 was deployed in the vicinity of 25.50N, 129.54E (blue circle) and Glider 136 (red line) was deployed in the vicinity of 26.01N, 131.57E (red circle) (see Figure 31). Glider 135 starts of going north for approximately 60nm and then turns southward and ends up at 24.69N, 129.68E (blue star). Glider 136 start of going south west and makes a turn to the north then turn to south ending its voyage at 24.70N, 129.70E (red star). The total lateral voyages for glider 135 is 202.47nm (see Figure 32). Glider 136 total lateral voyage is 279.81nm.

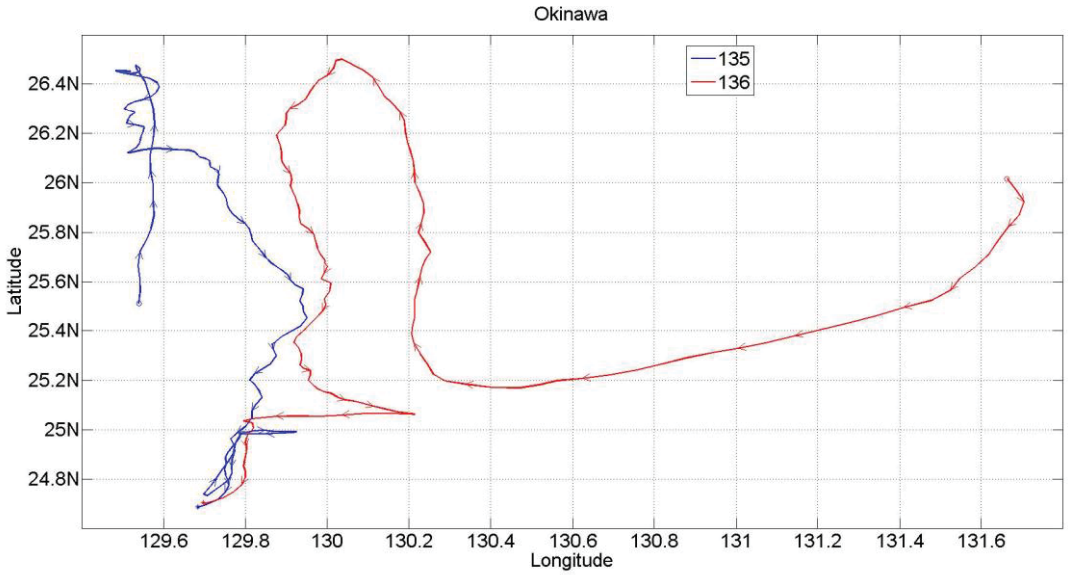

Figure 31. Starting points, path taken, and end points for gliders 135 and 136.

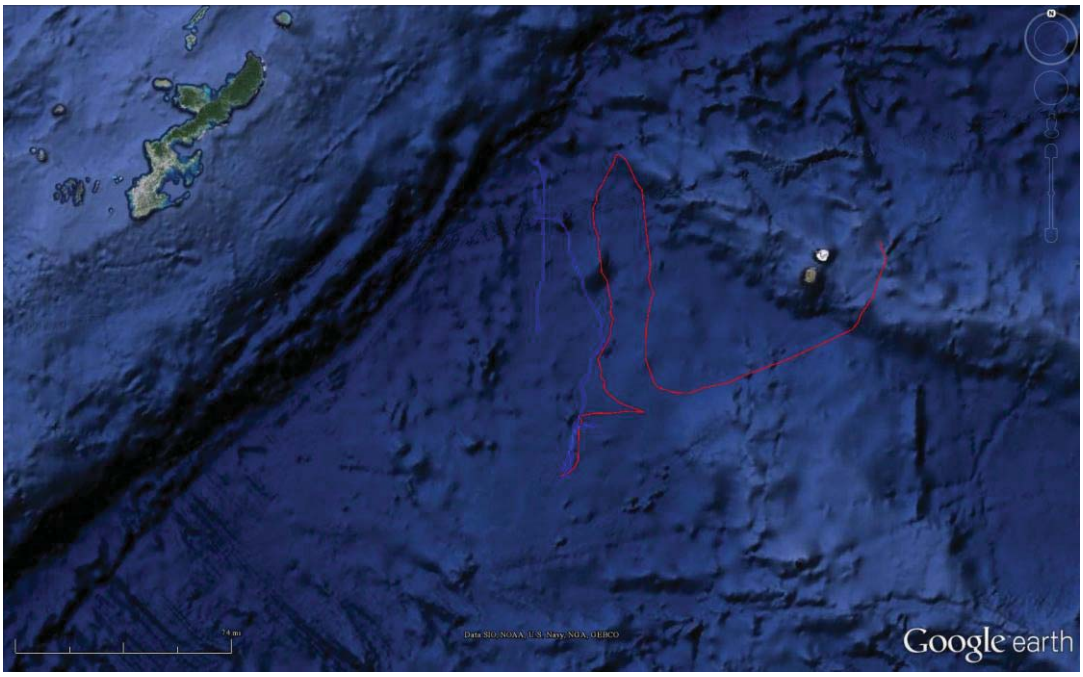

Figure 32. Glider 135 and 136 path overlaid onto globe (after Google Earth 2014).

a. SPM and SLD

The SPM for the Okinawa data set is similar for the different gliders. The SPM of the sea gliders downward profiles are plotted on the top graph in Figure 33. The middle graph is the sea gliders upward profile and the bottom is the two profiles combined. The sound speed maximum is between 1535.5 m/s to 1540.7 m/s for two the gliders.

Figure 34 has the same layout has the SPM, but we are plotting the SLD depth versus the day. The SLD for both gliders are close even though they are in different parts of the ocean.

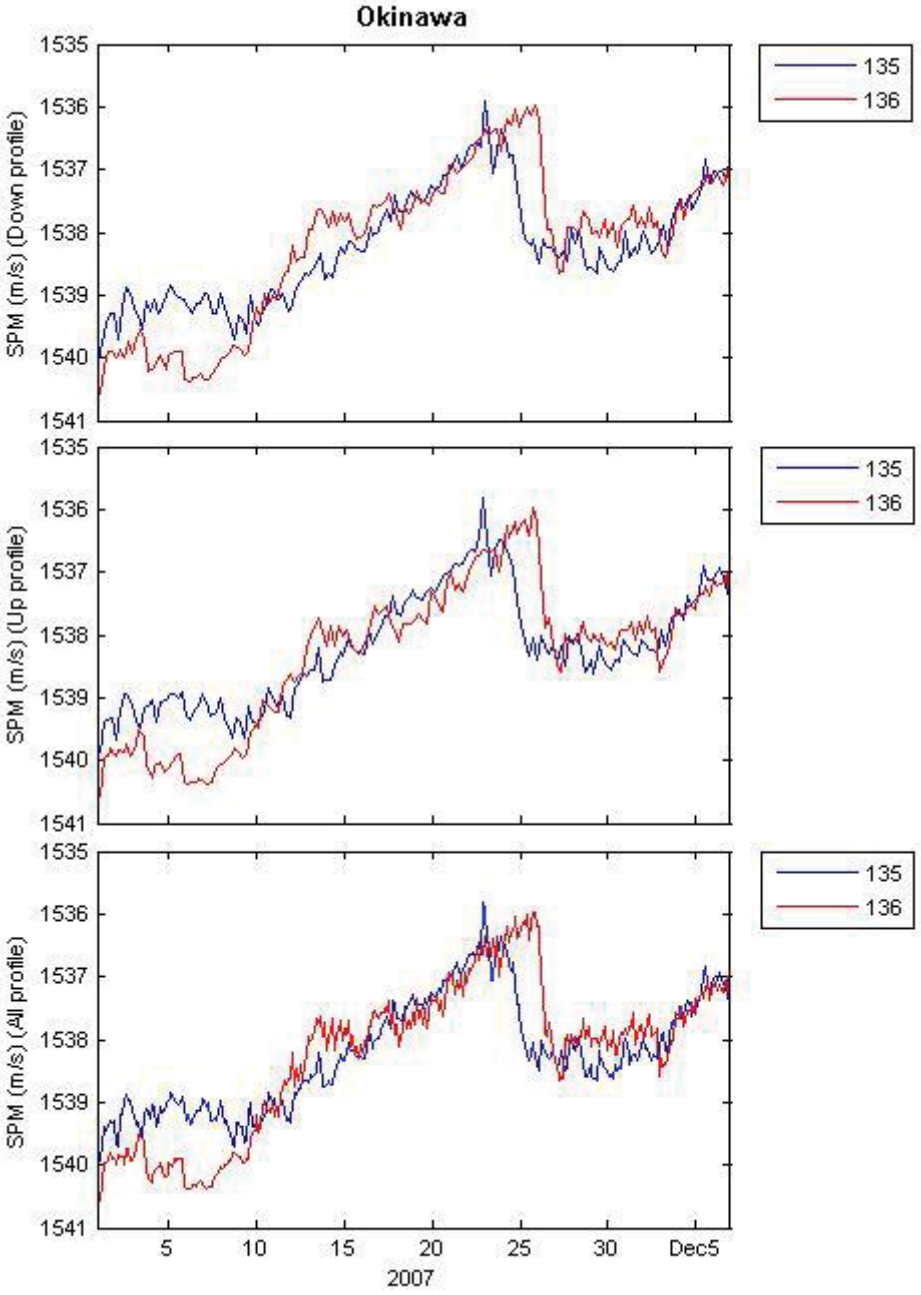

Figure 33. The SPM for the Okinawa data set by day for the downward part of the dives, the upward parts, and both combined.

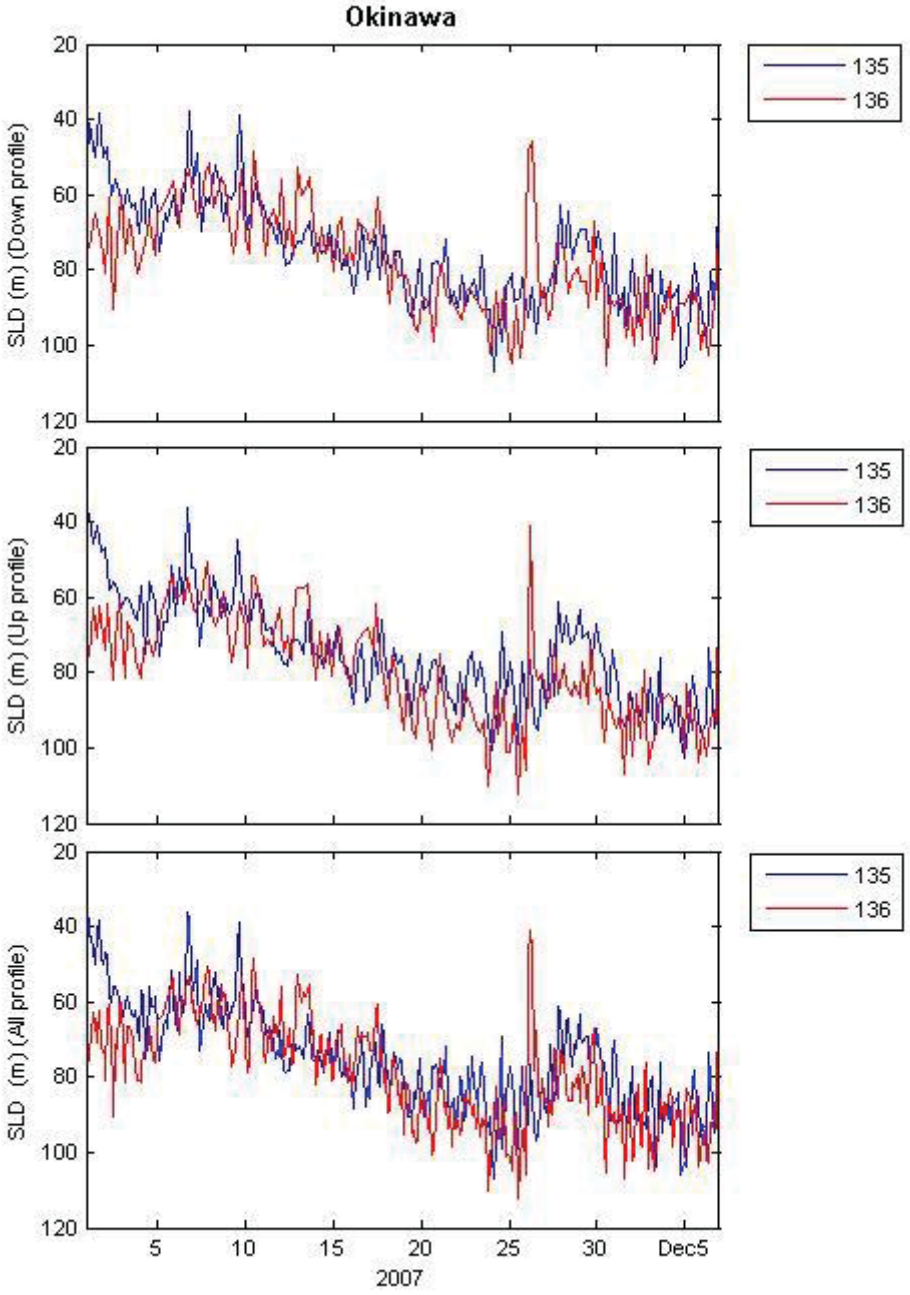

Figure 34. The SLD for the Okinawa data set by day for the downward part of the dives, the upward parts, and both combined.

b. Dive Profile

Figure 35 is the dive profile from 03NOV07. It shows a dive profile that took approximately five and half hours to go down to 995m and back to the surface.

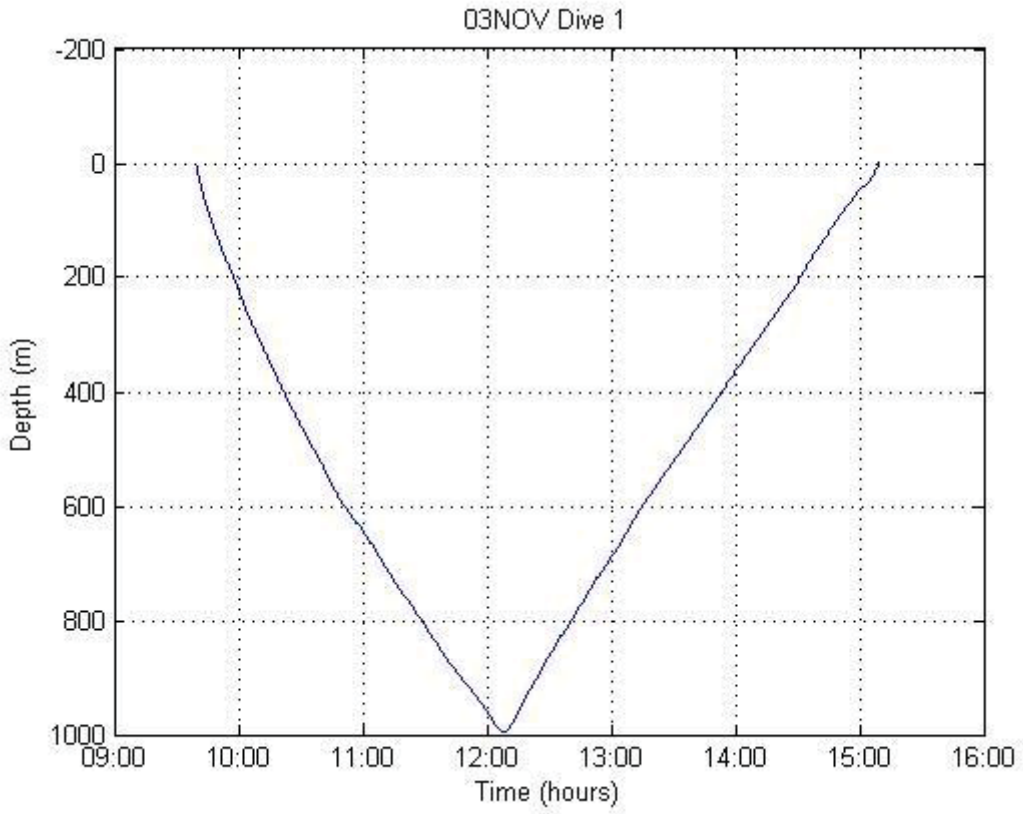

Figure 35. November 3 dive profile for SHAREM 07

c. Temperature, Salinity, and Sound Speed Profiles

Figures 36 and 37 show each of the dive profiles by glider for temperature, salinity, and sound speed (blue lines). The red lines are the average of the respective variables. As one can see from the profiles the blue lines are in a tight grouping. There is also a clear mixed layer, thermocline/halocline, and deep layer in Figures 36 and 37 a well-defined SLD at approximately 80m.

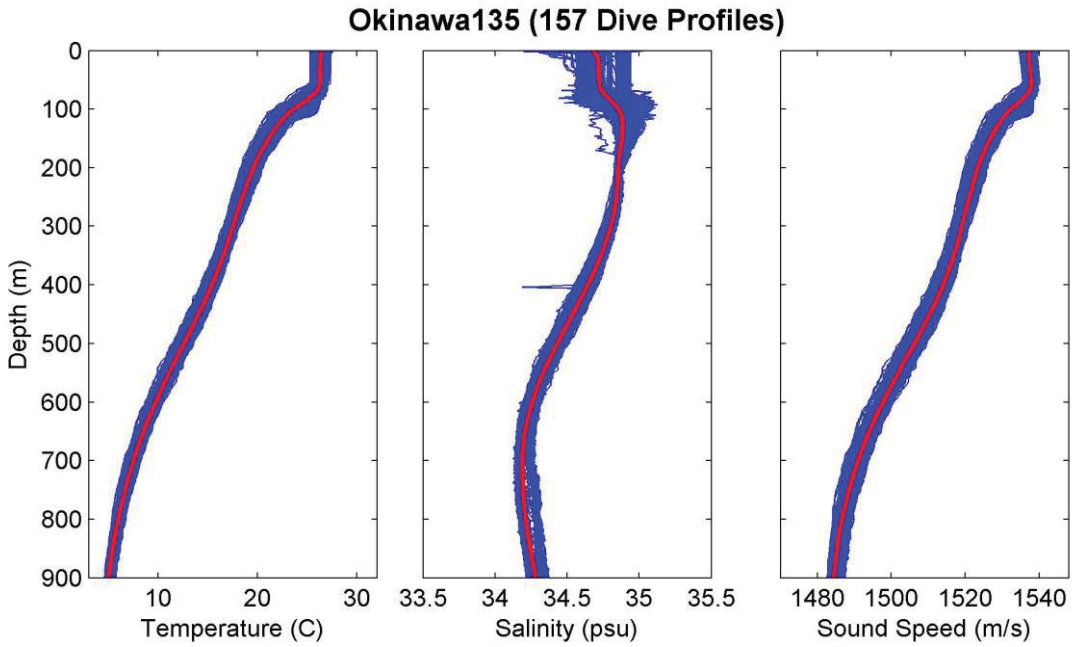

Figure 36. Glider 135 temperature, salinity, and sound speed profiles for 157 dives.

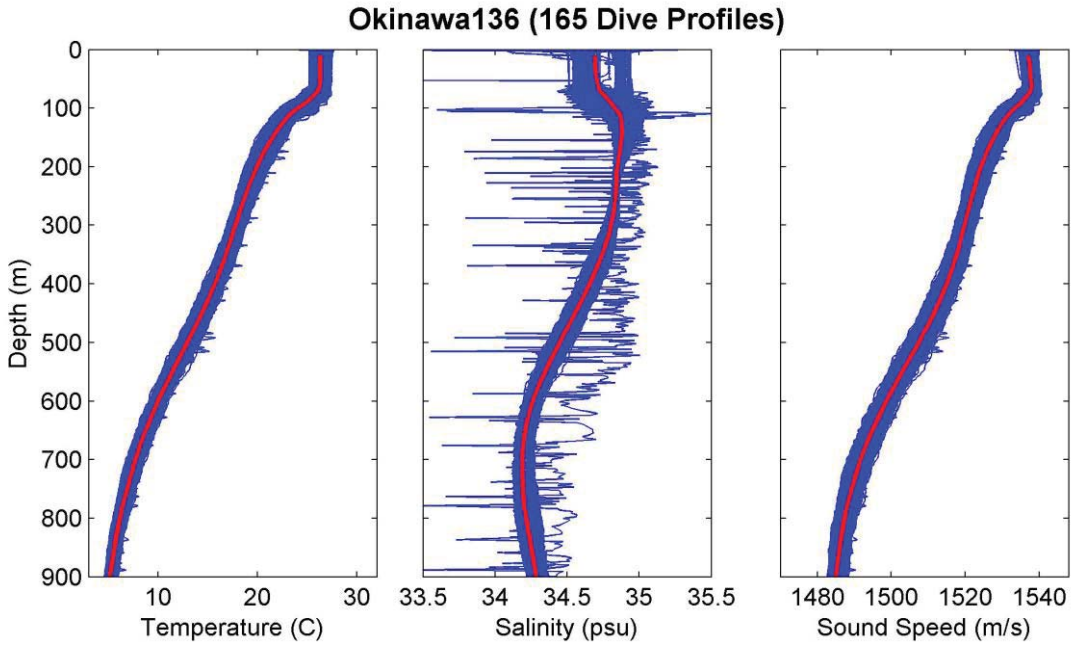

Figure 37. Glider 136 temperature, salinity, and sound speed profiles for 165 dives.

5. RyukYu

Six USN sea gliders were deployed off the coast of Ryukyu island chain by NAVO on the September 6, 2007 through the October 31 in support of exercise Annual Exercise 07 (ANNUALEX) (Mahoney et al. 2009b) (see Figure 39). The color coding is as follows: Glider 131 (left blue line), Glider 132 (red line), Glider 133 (black line), Glider 134 (pink line), Glider 135 (green line), and Glider 137 (right blue line) were all deployed in the vicinity of Ryukyu island (see Figure 38). Each starting point is indicated by a color coded circle. The color coded stars in the figure are where each glider finished its mission.

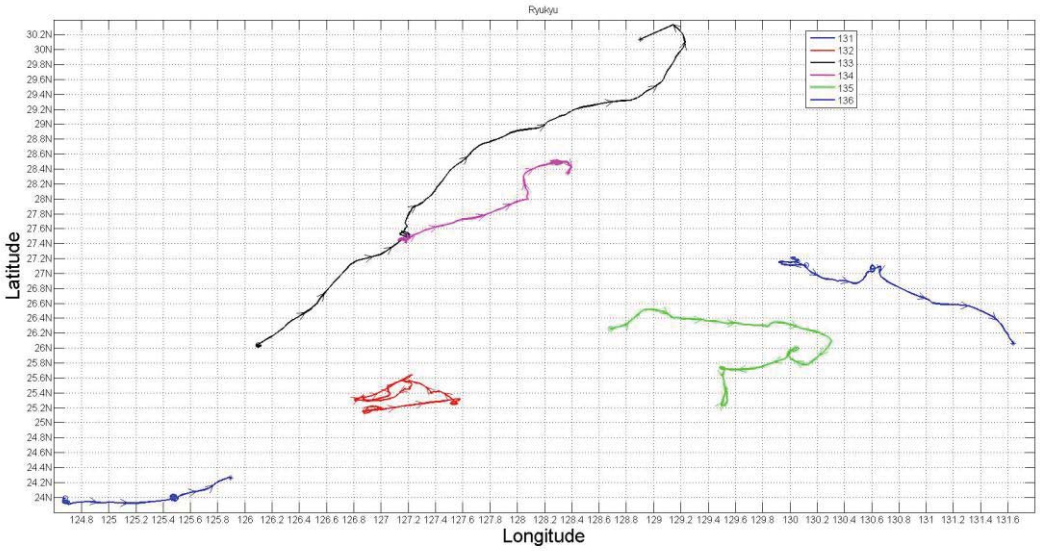

Figure 38. Starting points, path taken, and end points for gliders 131 through 136.

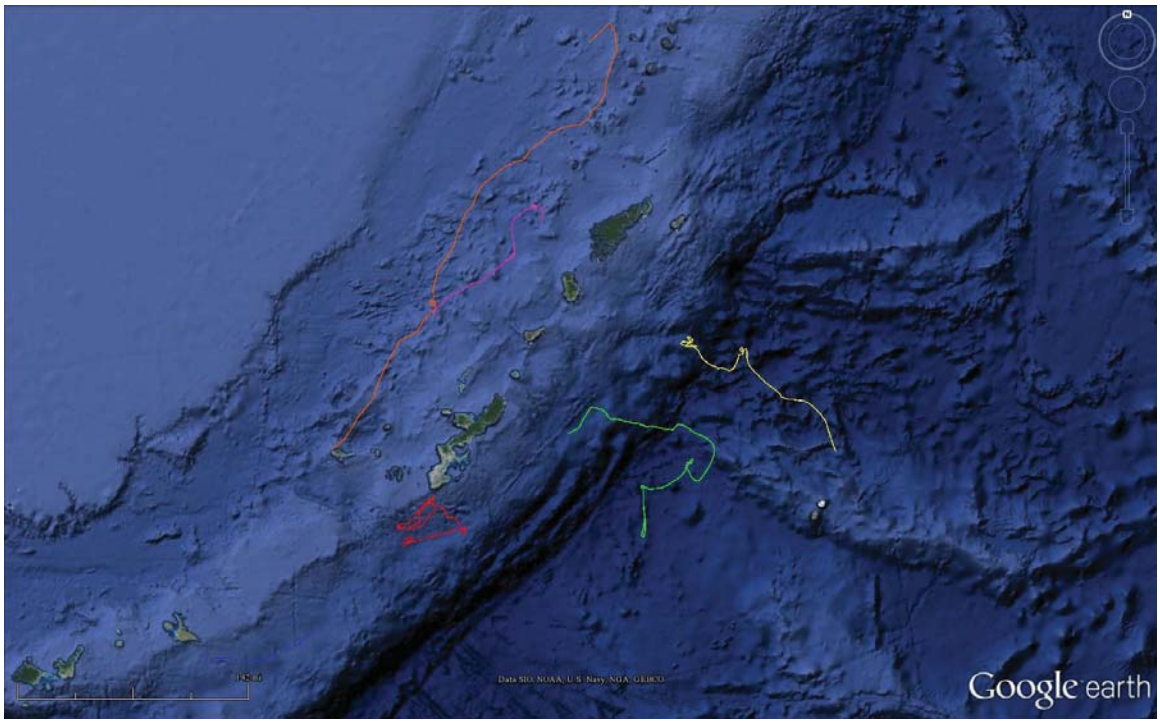

Figure 39. Glider 131 through 136 paths overlaid onto globe (after Google Earth 2014).

a. SPM and SLD

The SPM for the Ryukyu Islands data set are different for each of the gliders. The SPM of the sea gliders downward profiles are plotted on the top graph in Figure 40. The middle graph is the sea gliders upward profile and the bottom is the two profiles combined. The sound speed maximum is between 1538.3 m/s to 1544.7 m/s for two the gliders.

Figure 41 is the same layout has the SPM, but we are plotting the SLD depth versus the day. The SLD for the different gliders are far off because they were deployed in different water and different dates.

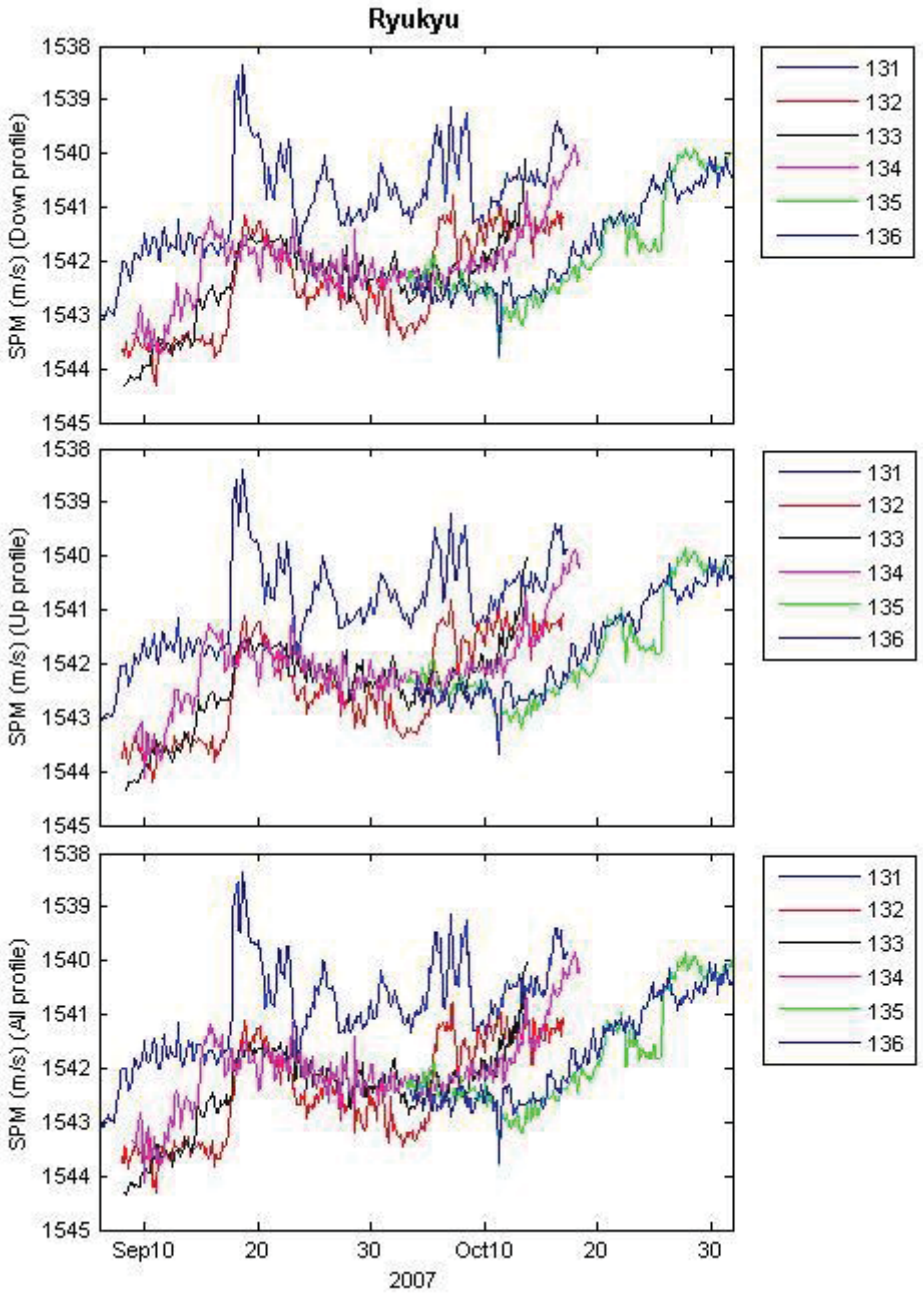

Figure 40. The SPM for the Hawaii data set by day for the downward part of the dives, the upward parts, and both combined.

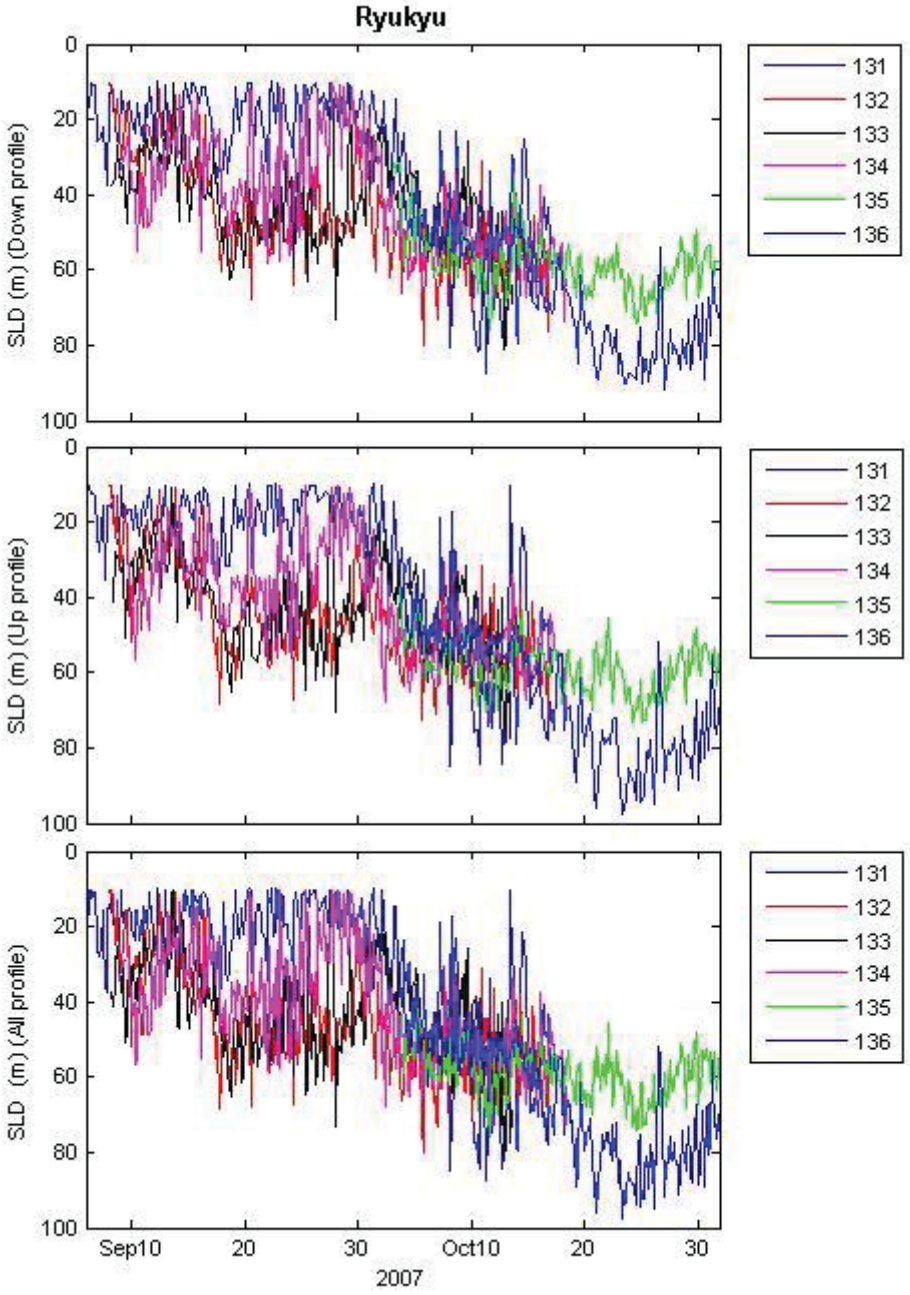

Figure 41. The SLD depths for the Ryukyu Island chain data set by day for the downward part of the dives, the upward parts, and both combined.

b. Dive Profile

Figure 42 is the dive profile from 01OCT07. It shows a dive profile that took approximately four and half hours to go down to 990m and back to the surface.

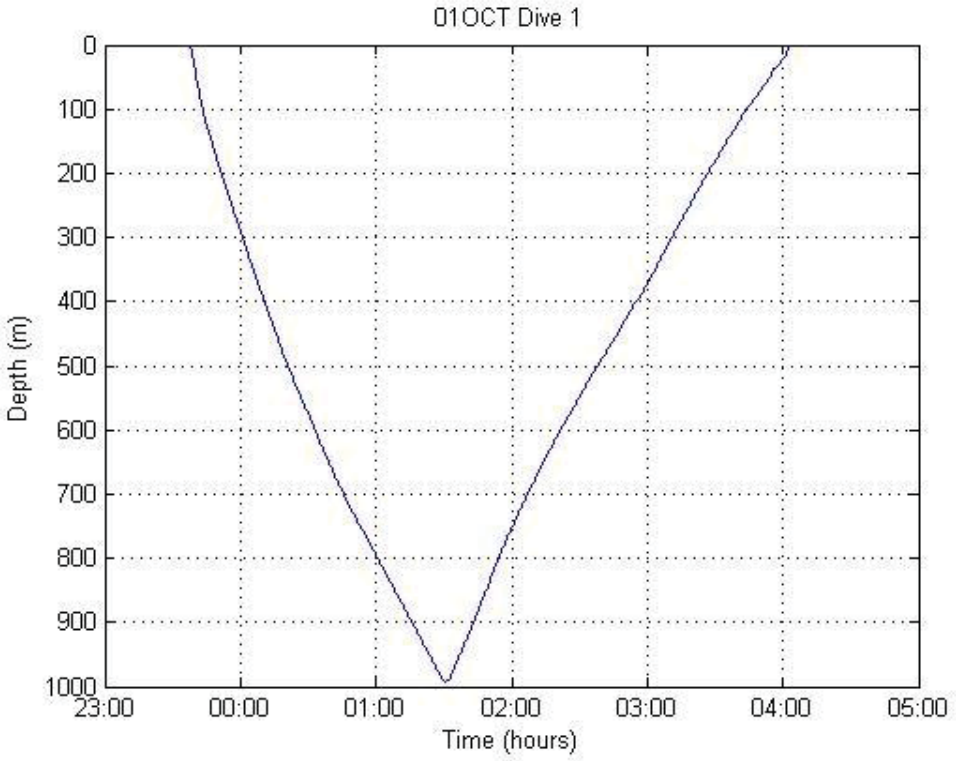

Figure 42. 01 October dive profile for ANNUALEX 07

c. Temperature, Salinity, and Sound Speed Profile

Figures 43–48 show each of the dive profiles by glider for temperature, salinity, and sound speed (blue lines). The red lines are the average of the respective variables. The profiles highlight the tight grouping of the blue lines. There is also a clear mixed layer, thermocline/halocline, and deep layer in most of the figures. Glider 131 profile (Figure 43) the MLD and SLD is not as defined as in the other figures.

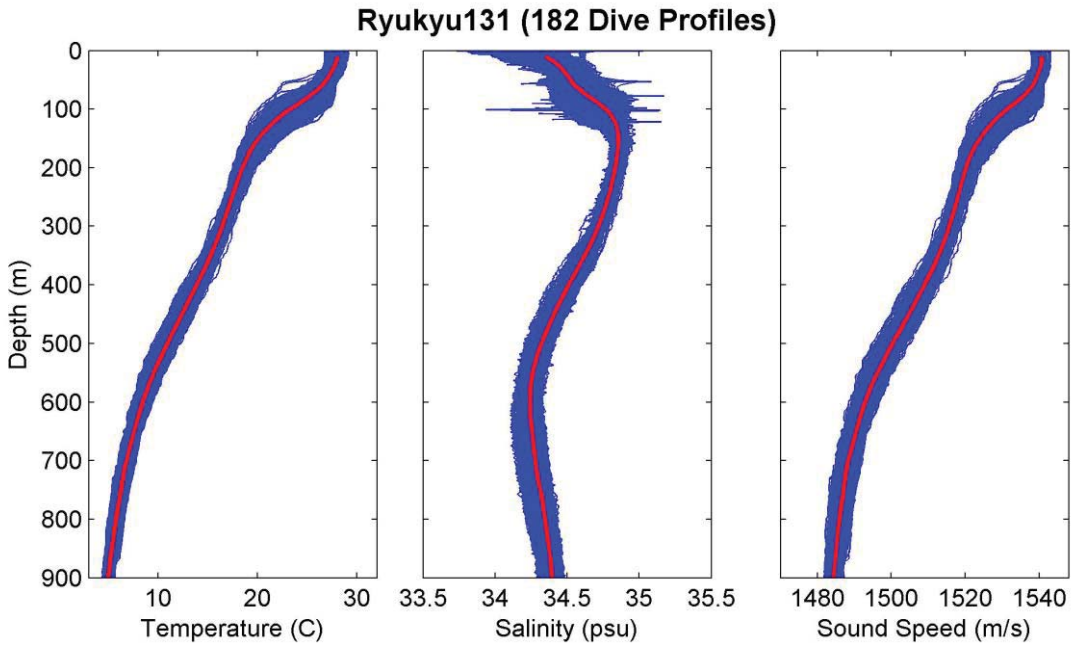

Figure 43. Glider 131 temperature, salinity, and sound speed profiles for 182 dives.

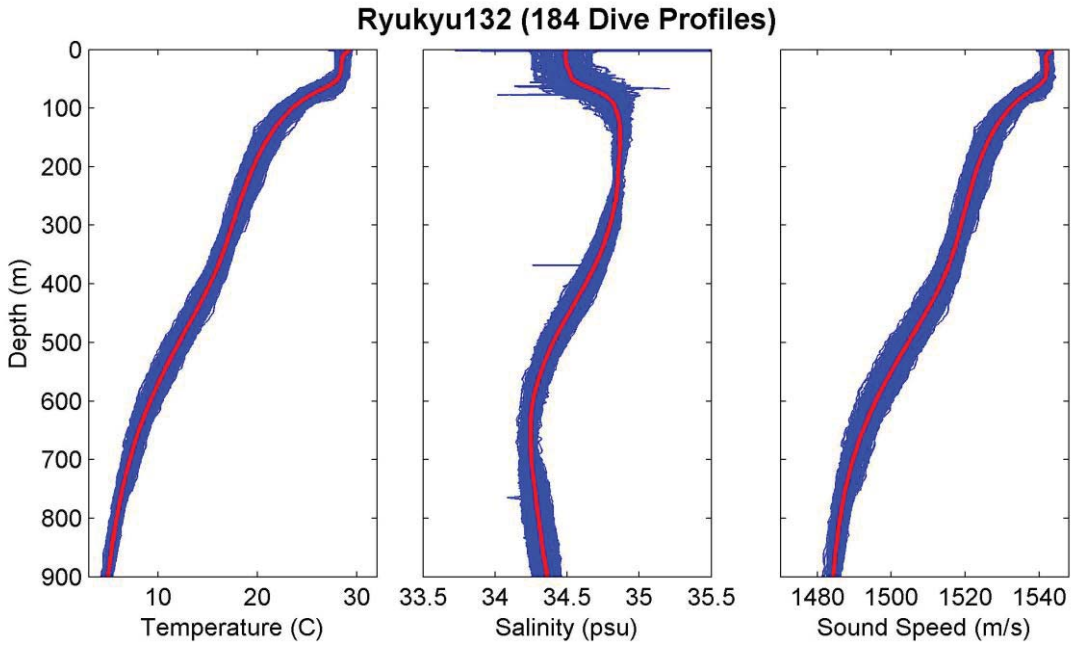

Figure 44. Glider 132 temperature, salinity, and sound speed profiles for 184 dives.

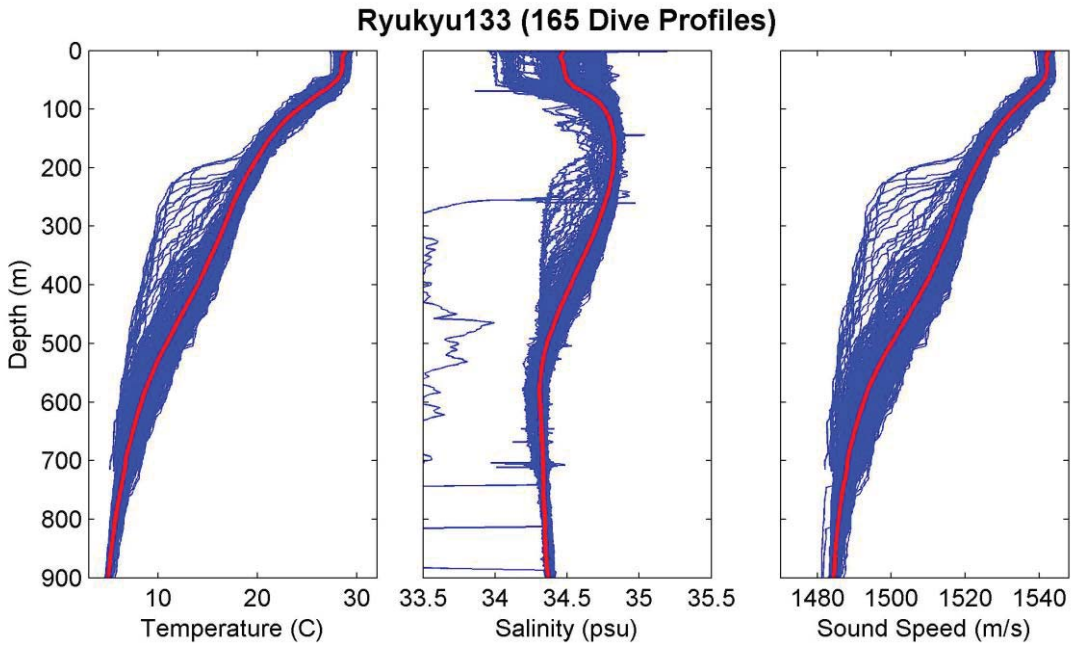

Figure 45. Glider 133 temperature, salinity, and sound speed profiles for 165 dives.

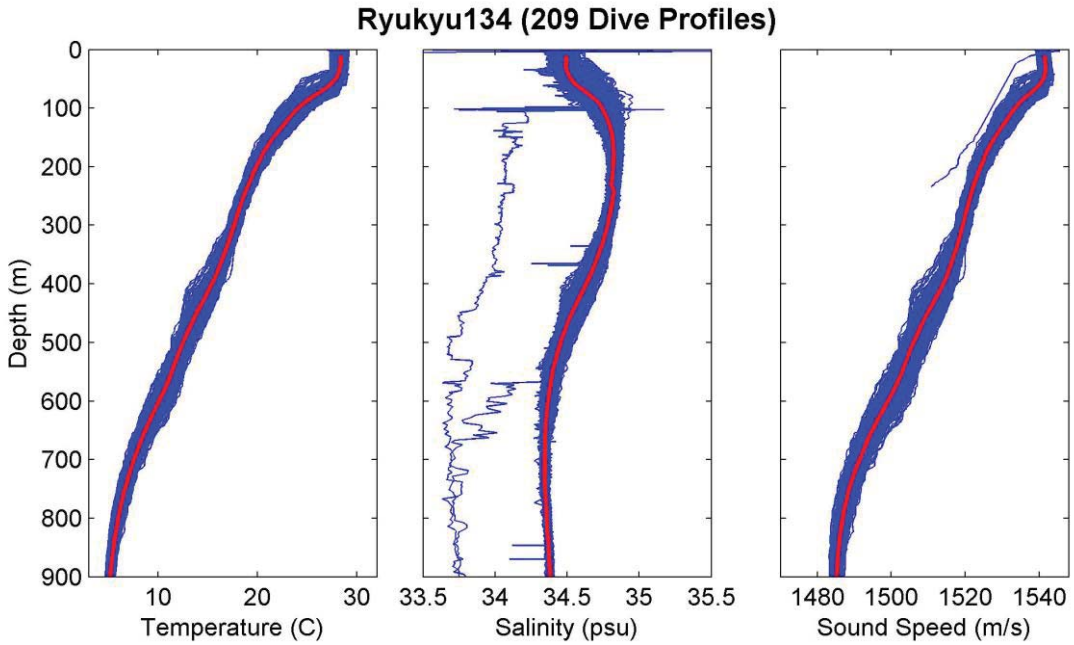

Figure 46. Glider 134 temperature, salinity, and sound speed profiles for 209 dives.

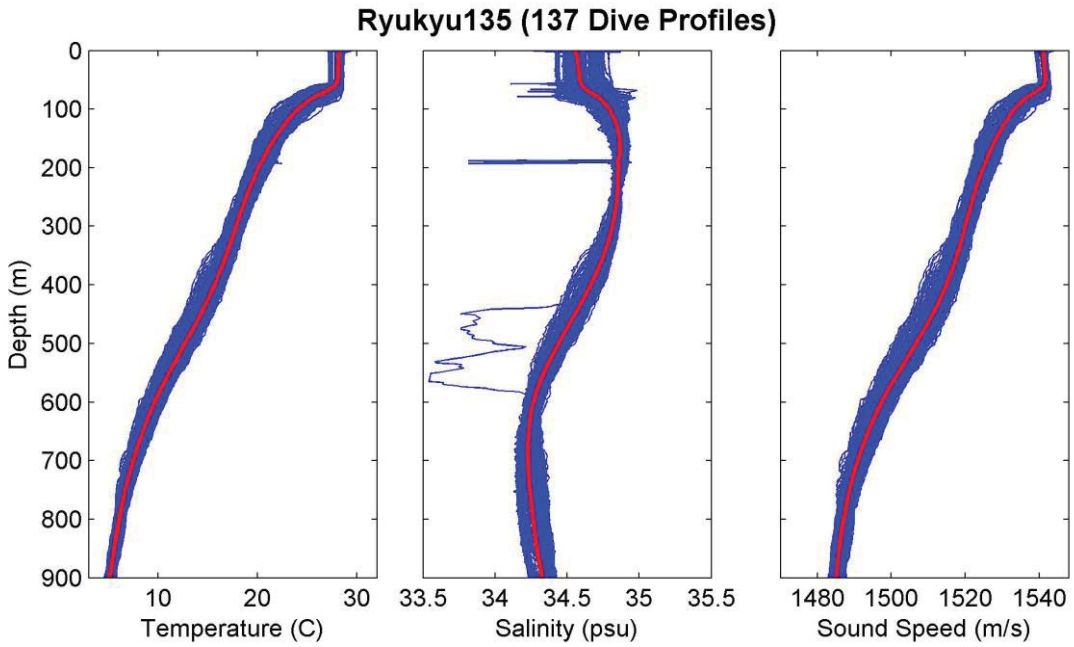

Figure 47. Glider 135 temperature, salinity, and sound speed profiles for 137 dives.

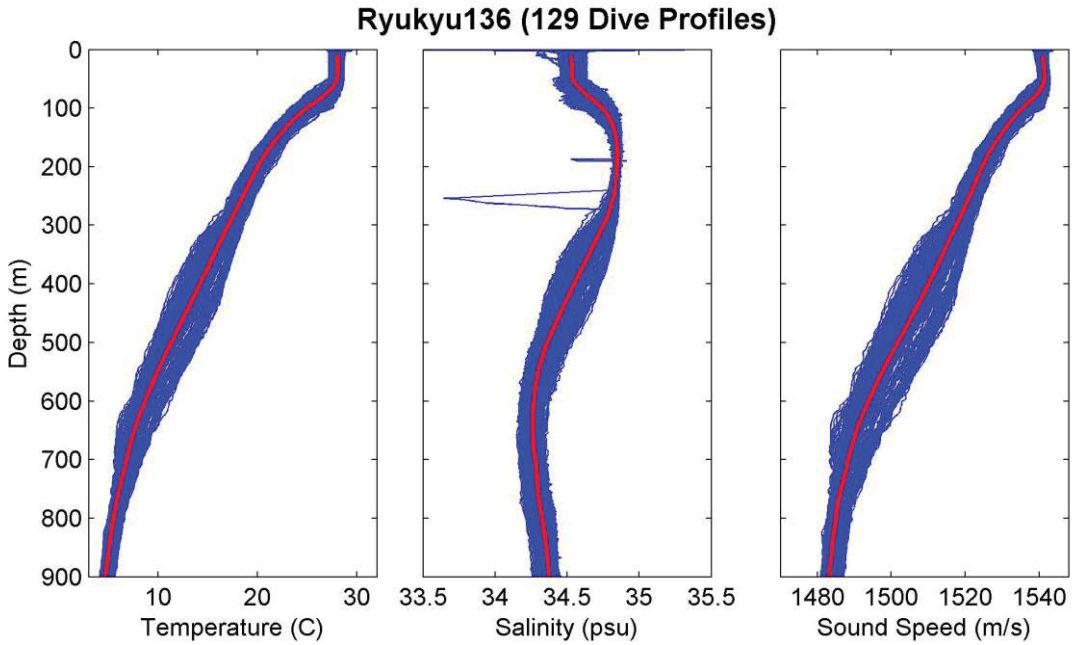

Figure 48. Glider 135 temperature, salinity, and sound speed profiles for 129 dives.

THIS PAGE INTENTIONALLY LEFT BLANK

III. METHODS AND MODELS

This chapter describes and defines the different methods we used to obtain the MLD and SLD. It explains each method step by step and details the limitations and short comings of each one.

A. DIFFERENCE METHOD

The first method we looked at to determine the MLD was the difference method. The difference method is the simplest and fastest way we looked at to identify the MLD. There are a few basic steps to the method. The first step is to choose a parameter to measure. We can use either density or temperature; however, for this thesis we used temperature. After choosing the parameter, we choose a reference depth. We choose three different starting depths: 0m, 3m, and 10m. We selected these three depths to match different experiments that other researchers have conducted in the past.

The next step is to determine the threshold (ΔT) value. We choose six different ΔT values: .1, .2, .5, .8, and1.0 degrees Celsius. Again we matched these to our different reference depths to align with the previous experiments (see Table 1).

Reference Depth (m)	ΔT(°C)	Authors
10	0.1	(Sprintall and Roemmich 1999)
0	0.2	(Chu and Fan 2010b)
3	0.2	(Thompson 1976)
10	0.2	(Boyer 2004)
0	0.5	(Obata et al. 1996)
10	0.5	(B. Meltzer et al. 2014, unpublished manuscript)
0	0.8	(Chu and Fan 2010b)
10	0.8	Kara et al. 2006)
0	1	(Rao et al. 1989)
10	1	(Rao et al. 1989)

Table 1. Difference method determinations

Next, we looked for a zone of constant temperature in the temperature profile obtained from the gliders. In other words if T_n and T_{n+1} at adjacent depths, are less than our ΔT, then they are of a constant temperature. If an area of constant temperature is found, "the value of the reference temperature T_{ref} is updated to the temperature value T_n at the shallower of the pair of the profile points. This is done for every occurrence of a pair of points occurring within the first uniform temperature region, so that the reference temperature is that at the base of the" constant area of temperature (Kara et al. 2000).

1. Shortcomings for the Difference Method

There are a few issues that could arise in this method. If we have our start point set to 10m and the MLD is above that, the difference method will not work. This is also true for the 3m start point. Our ΔT might be too large for the difference method to pick up a small change of temperature, which could indicate the end of the MLD. Lastly, the difference method could miss the MLD if a small jump in temperature occurs in the MLD; if the ΔT is too small the difference method could make the MLD to shallow. A clear MLD must also be present for this method to work.

B. CURVATURE METHOD

The second method we looked at to determine the MLD was the curvature method (Kara et al. 2009). The parameter we choose to measure for this method was temperature. The curvature method requires that the second derivative of temperature be a minimum at the base of the MLD (Chu and Fan 2010a).

1. Shortcomings for the Curvature Method

The issues facing the curvature method are that there must be a mixed layer and that the data cannot have "noise" since we are dealing with the second derivative (Chu and Fan 2010a).

C. GETSLOP17 MATLAB FUNCTION

The "getslop17" MATLAB function is a function where the inputs of depth and temperature will yield several outputs; namely the slope between 10 to 70 percent (see

Figure 49) of the temperature curve, start point, midpoint, end point, how many steps it took to calculate the slope, and any flags (flags will be discussed in a latter section) in the data. We need to use the outputs of this function as inputs for the max angle (MA) method and for quality control for our data.

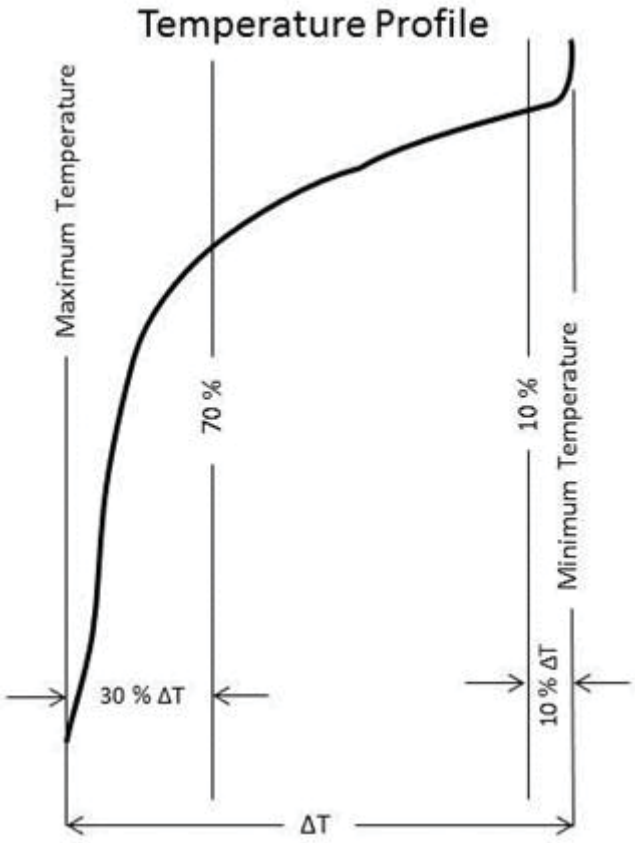

Figure 49. A visual of the Getslop17 MATLAB Function.

D. MAX ANGLE METHOD

The MA method (Chu and Fan 2011) has three basic steps to it. Again, we have the option to use temperature or density, but for this experiment we used temperature. The first step is to use linear fitting to get two vectors both pointing downward. The first vector is at some upper level pointing downward to a deeper depth. The second vector is at the deeper depth of the first one pointing downward to a deeper depth. Next, we calculate the tangent of the angle between the two vectors for all points. Lastly, we

calculate which temperature depth corresponds to the maximum value of the tangent angle (Chu and Fan 2011) (see Figure 50).

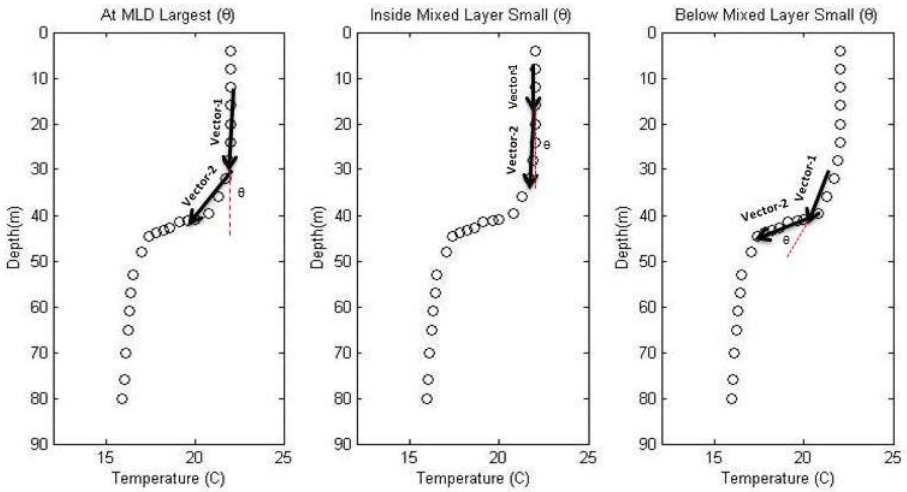

Figure 50. An example of how the max angle method works.

1. Shortcomings for the MA Method

The MA method depends on a linear regression, which could cause some issues for low resolution data set (Chu and Fan 2011).

E. GRADIENT METHOD

The first step of the gradient method is to take the change in temperature (°C) over the change in depth (meters), also known as the first derivative of temperature. Then those values are compared to a certain predetermined fixed value; when those values are larger than the predetermined fixed values one has reached the bottom of the MLD. This is similar to the difference method. We choose three previous used predetermined values and two of our own for this experiment, they are listed below:

'G (0.015); (Defant 1961)

'G (0.020); (Bathen 1972)

'G (0.025); (Lukas and Lindstorm 1991)

'G (0.030); (B. Meltzer et al. 2014, unpublished manuscript)

'G (0.050); (Chu et al. 2002)

1. Shortcomings for the Gradient Method

The gradient method has the same issues as the curvature method. In addition, the gradient method faces the same issue of difference method in the fact that a change of temperature indicating the MLD not triggering the function because the predetermined threshold value is too large, or getting a false positive because the threshold value is too small.

F. SOUND SPEED

For determining the sound speed, we used Mackenzie 1981 nine term equation:

$$\begin{aligned} c &= 1448.96 + 4.591T - 5.304\times10^{-2}T^2 + 2.374\times10^{-4}T^3 \\ &+ 1.340(S-35) + 1.630\times10^{-2}D + 1.675\times10^{-7}D^2 \\ &- 1.025\times10^{-2}T(S-35) - 7.139\times10^{-13}TD^3 \end{aligned} \tag{1}$$

Sound speed, c is in meters per second temperature (T) is in degrees Celsius, salinity (S) is in particle salinity units, and depth (D) is in meters. The SLD is located where the sound speed is at a maximum.

G. QUALITY INDEX

We included a quality index (QI) for all our methods in this thesis. We used Lorbacher et al. (2006) method.

$$QI = 1 - \frac{rmsd(T_k - \hat{T}_k) \;|(H_1, H_{mix})}{rmsd(T_k - \hat{T}_k) \;|(H_{1.5}, H_{mix})} \tag{2}$$

H_{mix} equals the MLD. The Lorbacher method is one minus the ratio of the root-mean square difference (rmsd) between the observed and the fitted temperature in the depth range from the surface to the MLD to the rmsd between the observed and fitted temperature from the surface to a depth of 1.5×MLD. The highest possible QI is 1.0. The lower the number goes the less the quality of the output of the function. A well-defined

MLD has a QI > 0.8. Any MLD with a QI between 0.5 and 0.8 and determining the MLD becomes difficult (Chu and Fan 2010b) (see Figure 51).

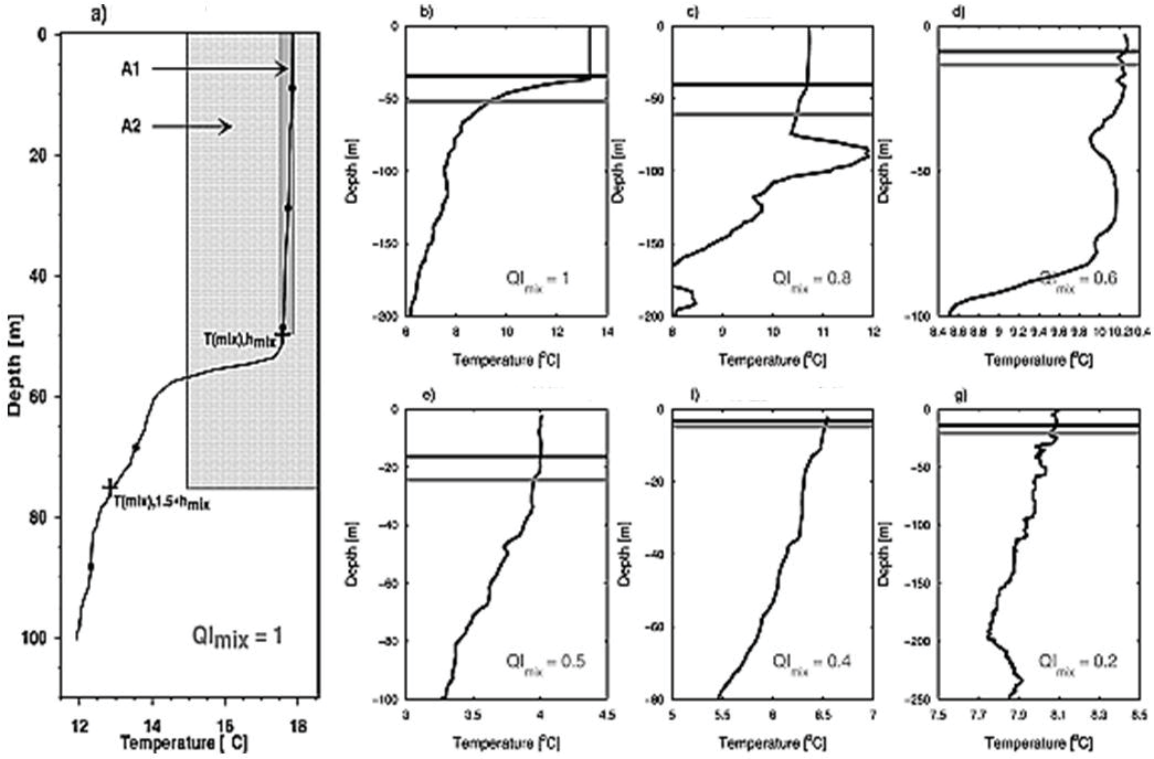

Figure 51. (a) Sketch of a notional profile QI_{mix}. (b)–(g) are examples of different QI_{mix} for different types of profiles. Black solid lines are H_{mix} and grey solid lines are 1.5 H_{mix} (after Lorbacher et al. 2006, p.13).

Calculating H_{mix} is centered on the idea that there is an ideal temperature profile see figure 51(a) where there exist an ideal mixed layer that has ideal homogenous properties in which the standard deviation of the property being measured about its vertical mean is zero. Below the H_{mix} depth the property variance should increase rapidly about its vertical mean (Lorbacher et al. 2006). Figure 28 (b)–(g) shows decreasing values of QI_{mix} as the temperature profile becomes less defined.

H. FLAGS

Flags are the result of lines of code that were inserted into our program to help quality control our data. Flags are an indicator issues with our data set. There are eight possible flags and they are as follows:

0: normal

1: Points between 10m to 40m <=2

2: Total observation points <=5

3: Max depth <20m

4: Start point deeper than 50m

5: Difference of above 20m > difference of under 20m

6: Max difference < 1 (temp)

7: No thermocline

8: Thermocline gradient is too small

If we received any of these flags other than zero or one in our data set, we threw out that dive profile completely. A dive profile is either the up or down part of one dive from one glider.

I. FILTERS

After the flags had been applied our data set it was relatively clean, but we had to apply four filters more filter to get rid of the "garbage" data. The first one we applied get rid of all the "not a number(s)" it MATLAB. The second was getting rid of the numbers that were approaching infinity. The third was to throw out all depth data that was not changing appropriately with a change in depth. Examples of these are when the sea glider was diving down and the depth values would become shallower or vice versus. We also threw out the data when the depth stayed the same on a descending or ascending sea glider. Lastly, we threw out any data from any variable that was greater than three times the standard deviation of that variable.

THIS PAGE INTENTIONALLY LEFT BLANK

IV. IDENTIFICATION OF THE MIXED AND SONIC LAYER DEPTHS

This chapter reveals our findings of the MLD and the SLD from our experiment. It presents the results in several different graphs and illustrations.

A. MLD FINDINGS

After running all 17 techniques these were the results (Table 2):

#	Florida	Guam	Hawaii	Okinawa	Ryukyu	Method	Average	Rank
1	0.87734	0.551396	0.748699	0.933675	0.846689	0.1 10	0.7915599	3
2	0.871289	0.510163	0.74089	0.932698	0.83423	0.2 0	0.777854	6
3	0.871289	0.510163	0.74089	0.932698	0.83423	0.2 3	0.777854	5
4	0.877574	0.545859	0.792117	0.934053	0.86056	0.2 10	0.8020326	2
5	0.838233	0.519606	0.756421	0.910017	0.832636	0.5 0	0.7713828	8
6	0.841325	0.577724	0.786521	0.910741	0.834801	0.5 10	0.7902225	4
7	0.814115	0.610262	0.731461	0.875765	0.803968	0.8 0	0.7671142	10
8	0.815457	0.650638	0.734348	0.876629	0.803535	0.8 10	0.7761215	7
9	0.78036	0.627683	0.697652	0.851363	0.781392	1.0 0	0.7476899	12
10	0.78126	0.63594	0.70139	0.852501	0.780725	1.0 10	0.7503633	11
11	0.680407	0.252591	0.318074	0.742257	0.457551	0.015	0.4901762	17
12	0.758348	0.304312	0.380785	0.814973	0.522947	0.02	0.5562729	16
13	0.802194	0.343575	0.426249	0.866077	0.58293	0.025	0.6042049	15
14	0.833778	0.378081	0.461591	0.899251	0.622681	0.03	0.6390763	14
15	0.873202	0.473546	0.616078	0.941502	0.722086	0.05	0.7252828	13
16	0.912486	0.504753	0.684139	0.933355	0.819399	Curvature	0.7708265	9
17	0.910701	0.607679	0.790172	0.94742	0.867573	Max Angle	0.8247089	1

Table 2. MLD findings and results.

Numbers 1 through 10 in the table are all of the difference method with the first number under the method column being the ΔT and the second number being the reference depths in meters. Numbers 11 through 15 are the different gradient methods, and 16 and 17 are the curvature method and the MA method. The top four most accurate method for determining the MLD is the MA method followed by the difference method 0.2 ΔT reference depth 10m, then 0.1 ΔT 10m, and finally 0.5 ΔT 10m.

The MA method was the first or second best method in four out of the five areas and the difference method of 0.2 ΔT and reference depth 10m placed top three methods in four out of the five areas. Figure 52 is a snapshot of the MLD MATLAB program running and identifying the MLD using the 17 different techniques. The blue star is method 13, the red star is method 16, the blue circle is method 1, the red circle is method 6 and the black circle is method 17.

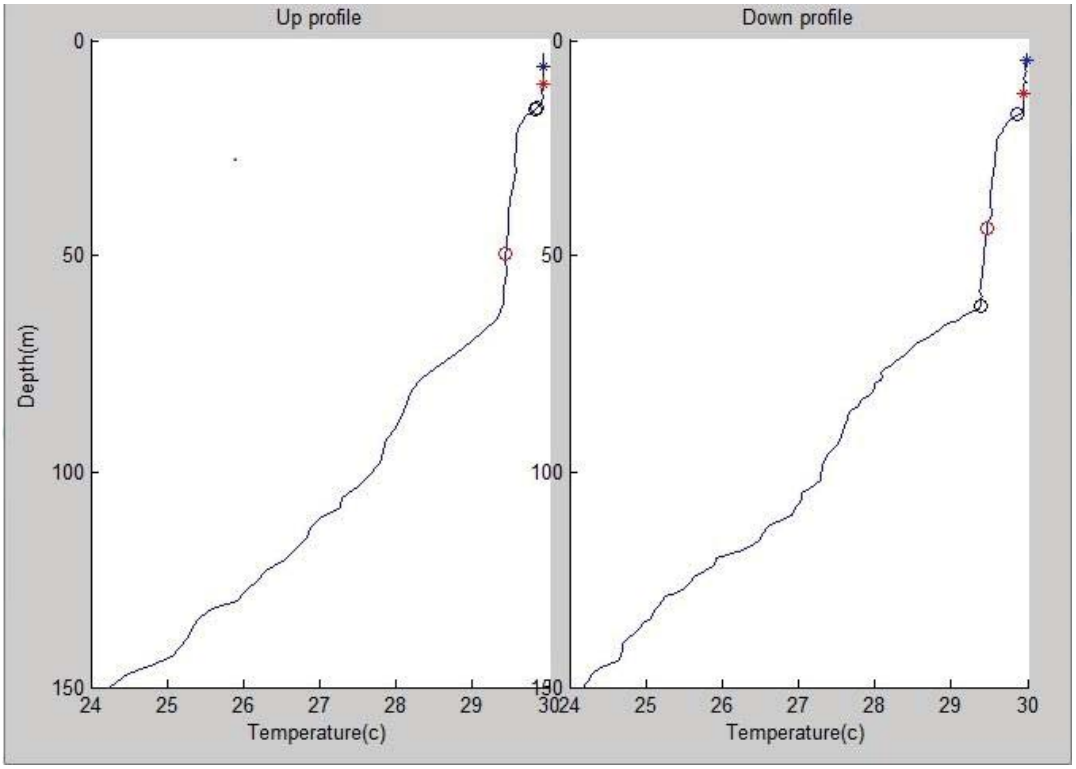

Figure 52. A snapshot of a random dive profile of Guam with the MLD program identifying the MLD based on the different methods.

The MA method, difference method of Δ.2 reference 10m, and difference method of Δ.8 reference 10m are graphed in Figures 53 through 57. As a reminder, their respective over all rankings were first, second, and seventh. These ranking were chosen to graph to show how close the first and second places were in relationship to each other and to one that was in the middle of the pack. They were also chosen because the MA method was the best at determining the MLD for Okinawa and Ryukyu, while the difference method of Δ.2 reference 10m was the best for Hawaii, and the difference method of Δ.8 reference 10m was the best method for determining the MLD in Guam.

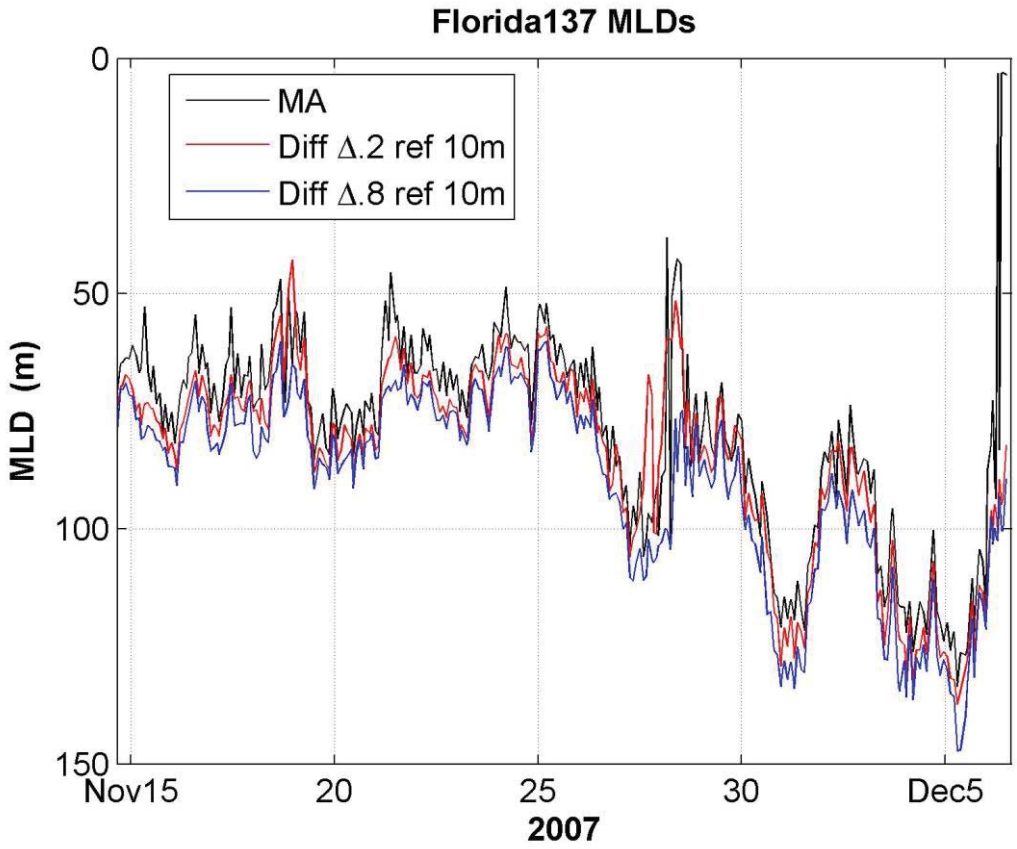

Figure 53. A graph of MA, difference Δ.2 reference 10m, and difference Δ.8 reference 10m methods for Florida Glider 137.

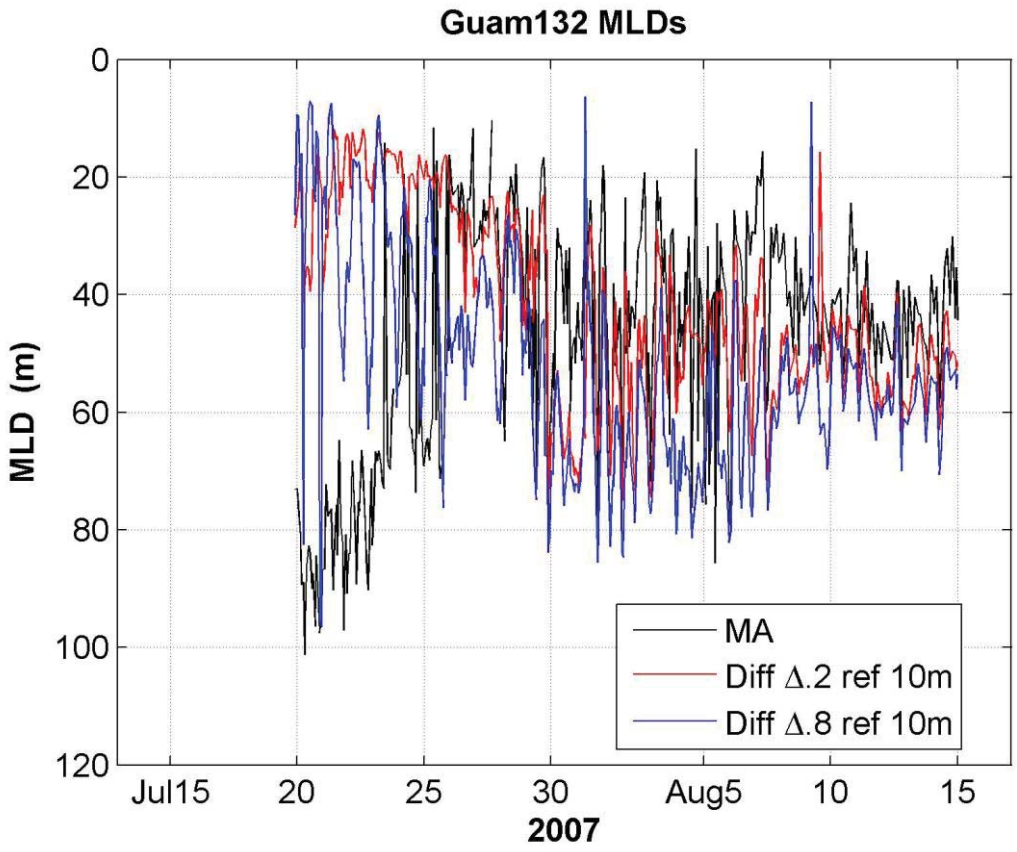

Figure 54. A graph of MA, difference Δ.2 reference 10m, and difference Δ.8 reference methods 10m for Guam Glider 136.

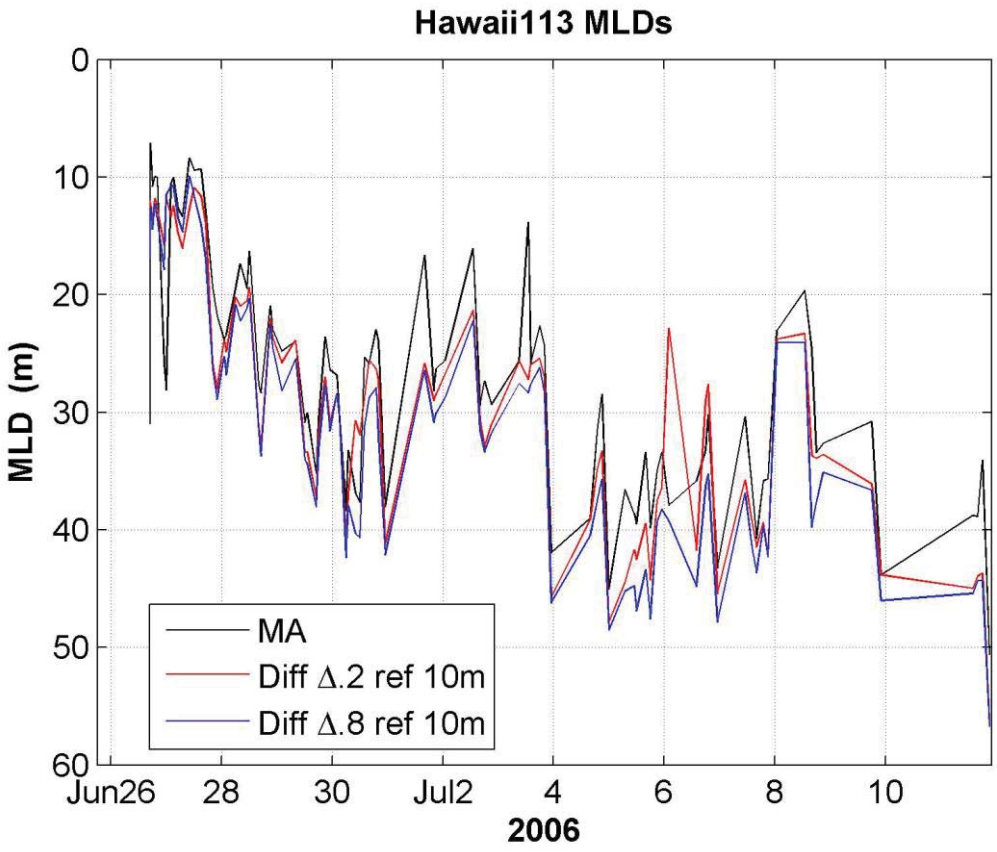

Figure 55. A graph of MA, difference Δ.2 reference 10m, and difference Δ.8 reference 10m methods for Hawaii Glider 113.

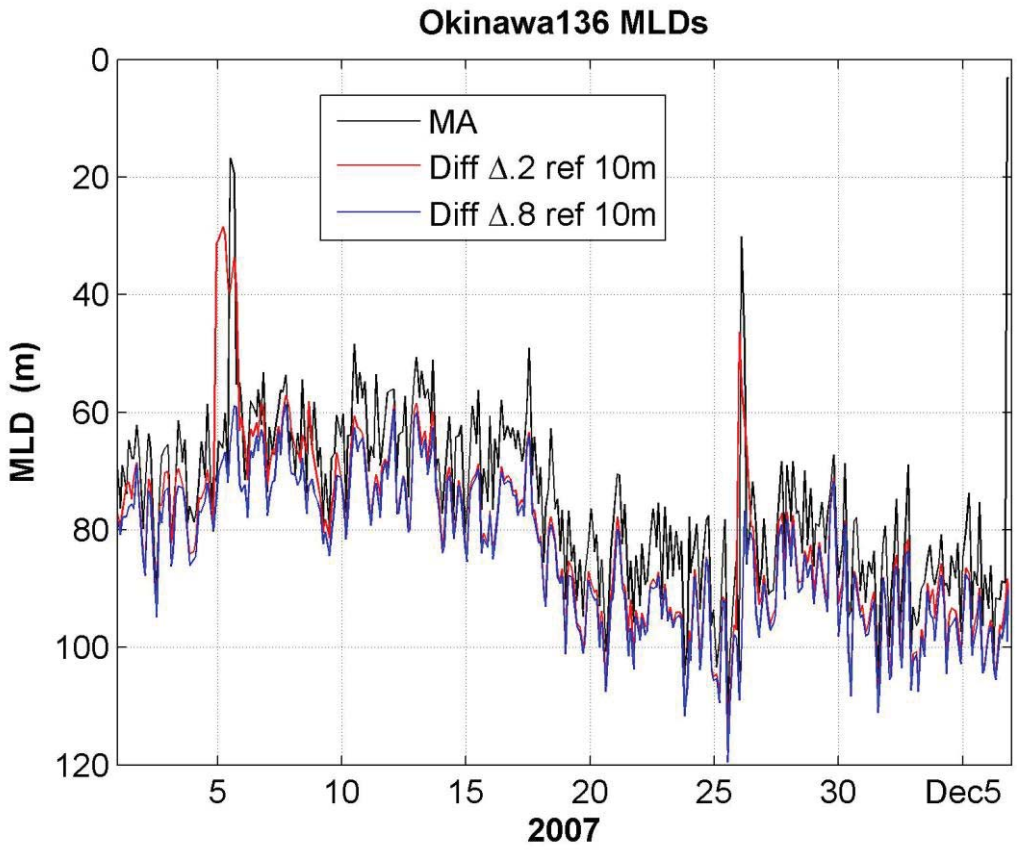

Figure 56. A graph of MA, difference Δ.2 reference 10m, and difference Δ.8 reference 10m methods for Okinawa Glider 136.

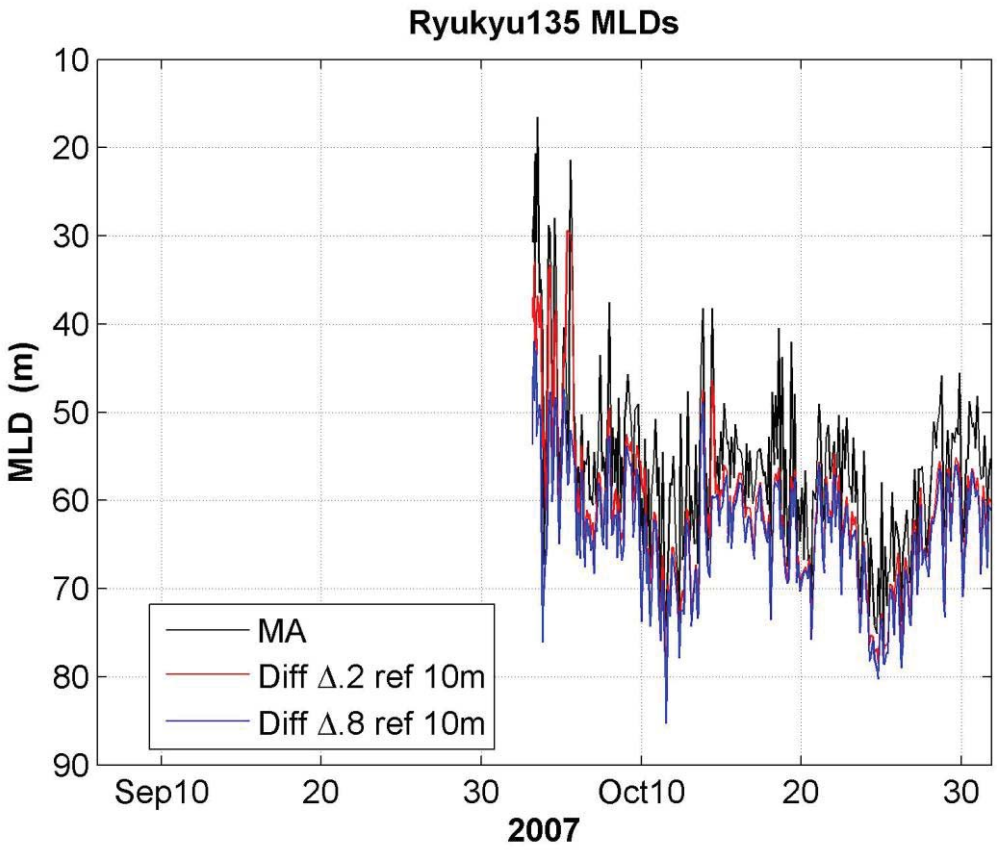

Figure 57. A graph of MA, difference Δ.2 reference 10m, and difference Δ.8 reference 10m methods for Ryukyu Glider 135.

B. SLD FINDINGS

We ran into an issue in our results with the SLD. As one can see in Figure 58 the SLD is above the MLD at most points of the graph. This issue was present in each and every dive profile at all five locations. The SLD should be deeper than the MLD at most points due to the inclusion of salinity into the equation of sound speed. An increase in salinity leads to an increase in sound speed. After looking at the data, we determined that this was happening was because of some sporadic salinity measurements in the top 100 meters of the water column. By our definition on the SLD is where the sound speed is at its max. Therefore, there was a small horizontal spike (or bump) in sound speed that was throwing off our SLD determination equation. To correct for this, we applied the same MA method that we used for determining the MLD to the sound speed profile to determine the SLD. Theoretically speaking, the two different ways of calculating the

SLD should be the same; however, in the real world they are not. As one can see in Figure 59, the SLD is now correctly below the MLD at most points in the graph.

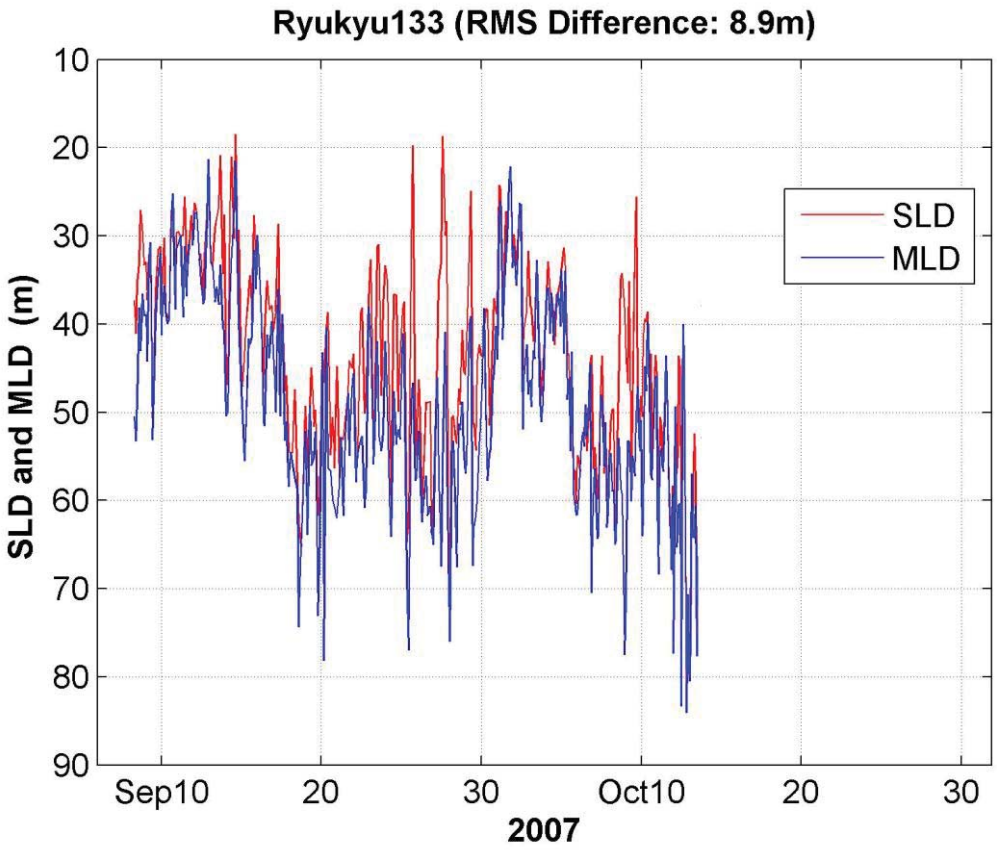

Figure 58. SLD and MLD plotted together for Ryukyu Glider 133.

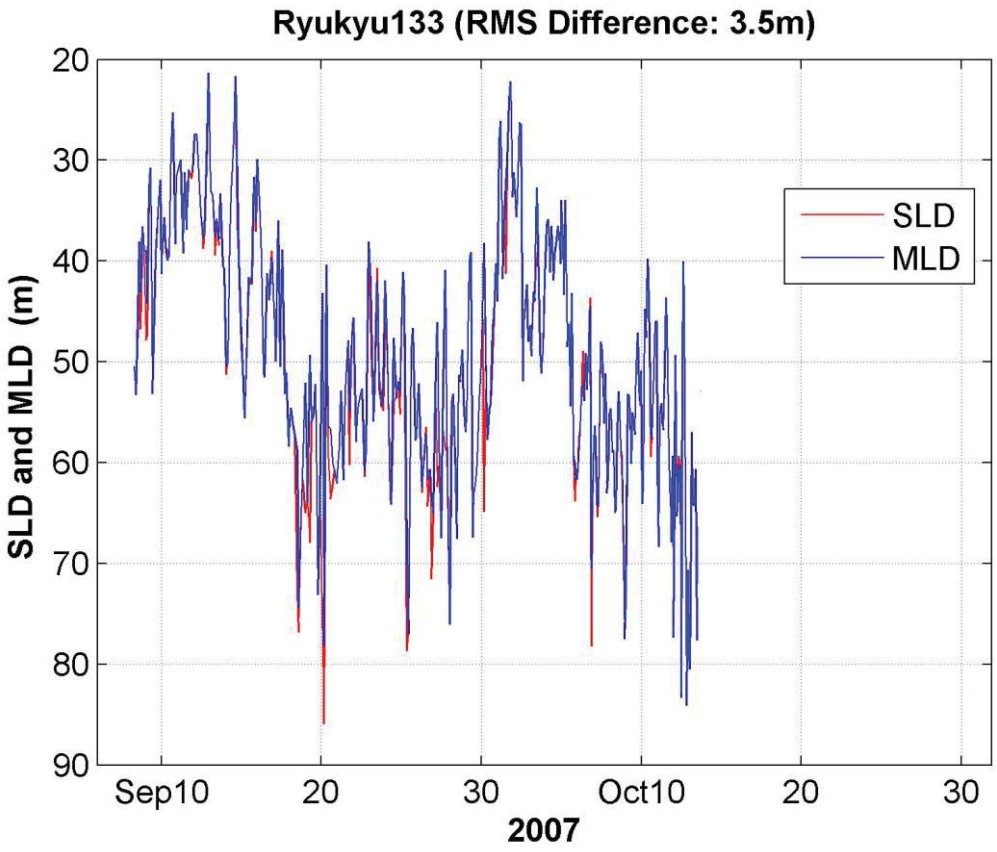

Figure 59. SLD and MLD plotted together for Ryukyu Glider 133 with SLD corrected.

C. MLD COMPARISON TO THE SLD

Figures 60-80 show the MLD plotted against the SLD for each of the glider profiles in each of the areas. The RMSD is computed on the top of each graph. As one expects, the higher the QI of the area is, the smaller the RMSD is (Okinawa>Florida>Ryukyu>Hawaii>Guam). In Hawaii, there were not as many data points taken in the exercise. There are also some days when certain gliders did not take temperature or salinity data (figures 69 and 72).

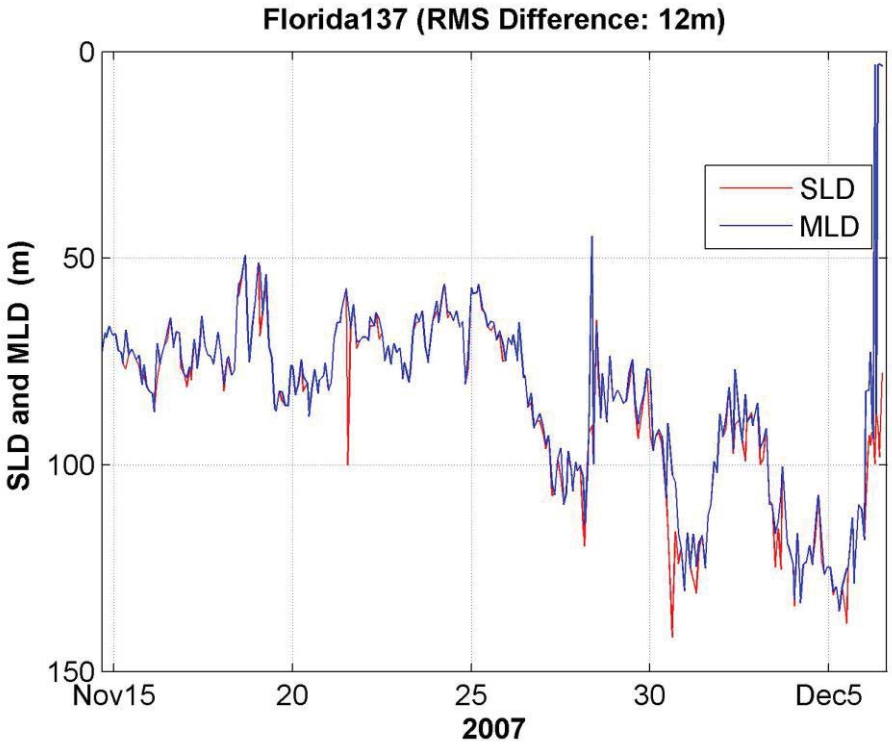

Figure 60. Glider 137 MLD and SLD for Florida.

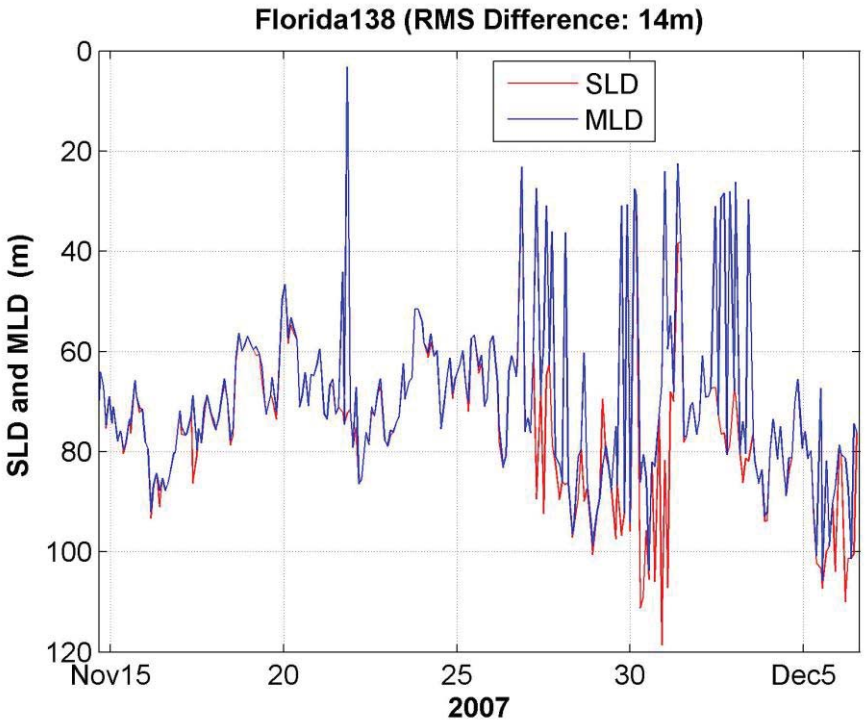

Figure 61. Glider 138 MLD and SLD for Florida.

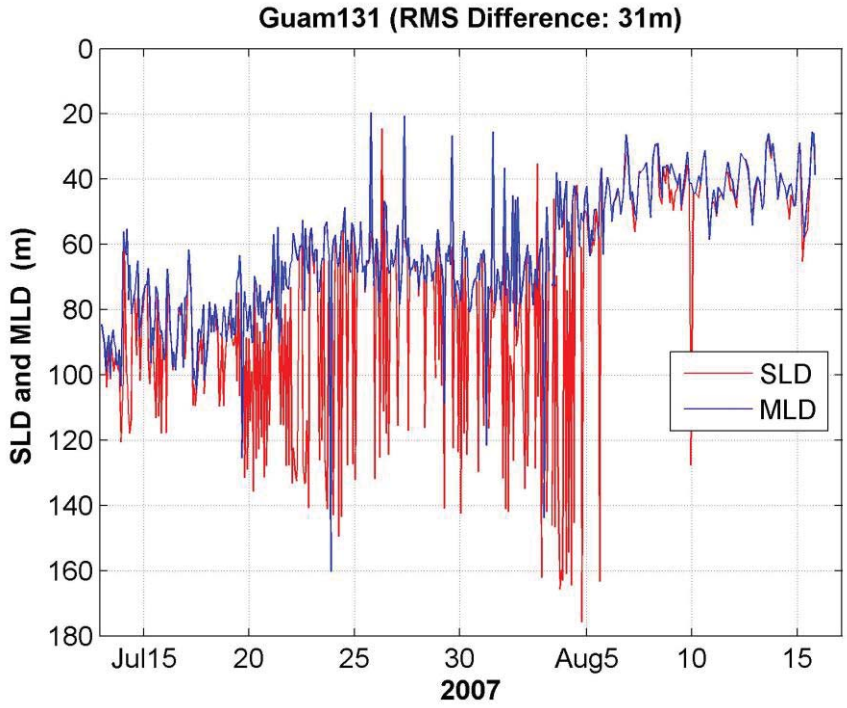

Figure 62. Glider 131 MLD and SLD for Guam.

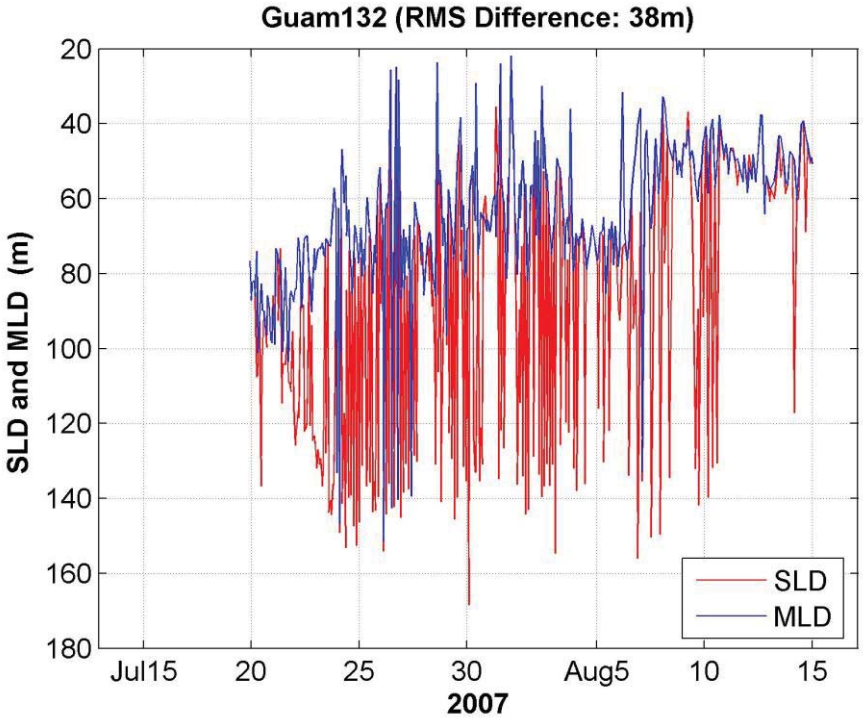

Figure 63. Glider 132 MLD and SLD for Guam.

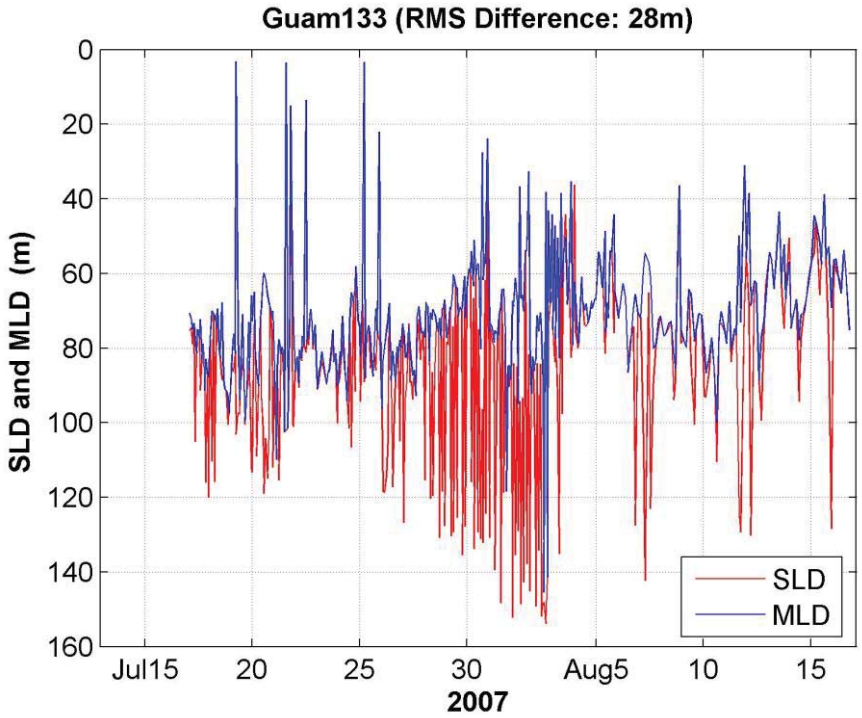

Figure 64. Glider 133 MLD and SLD for Guam.

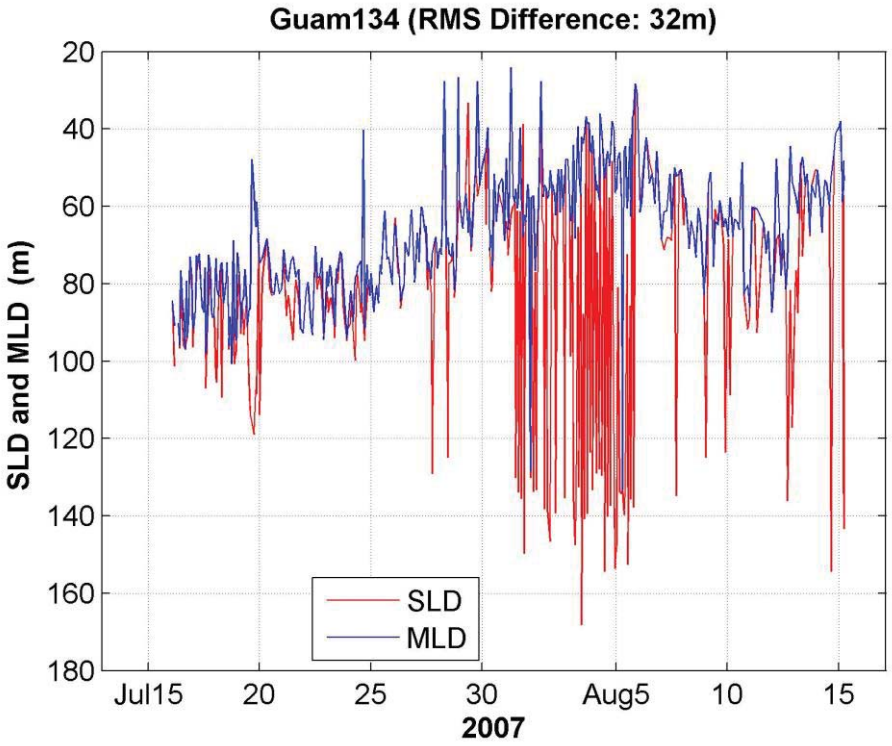

Figure 65. Glider 134 MLD and SLD for Guam.

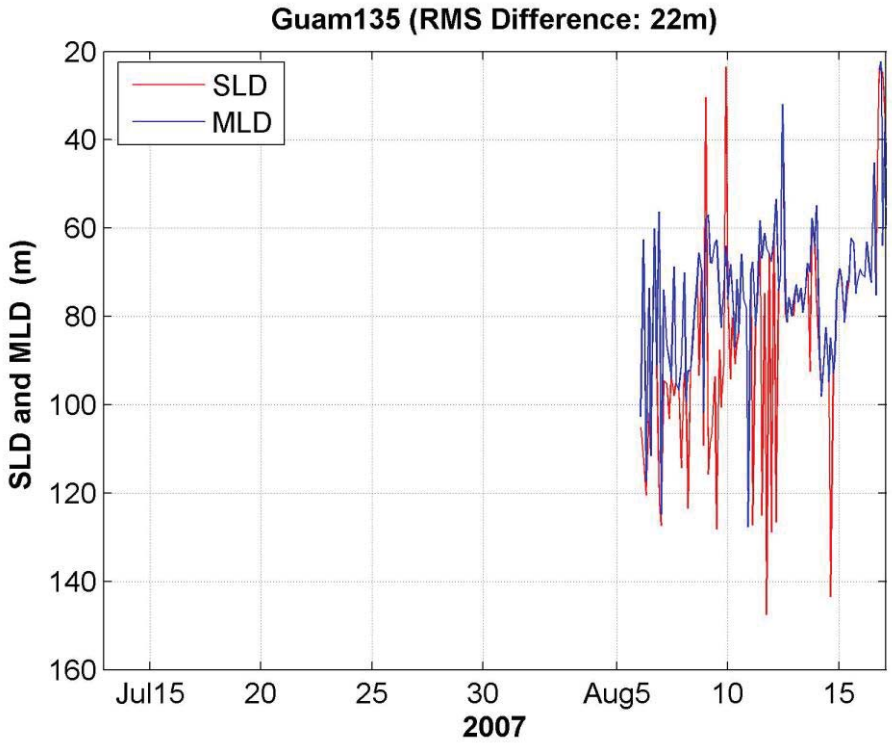

Figure 66. Glider 135 MLD and SLD for Guam.

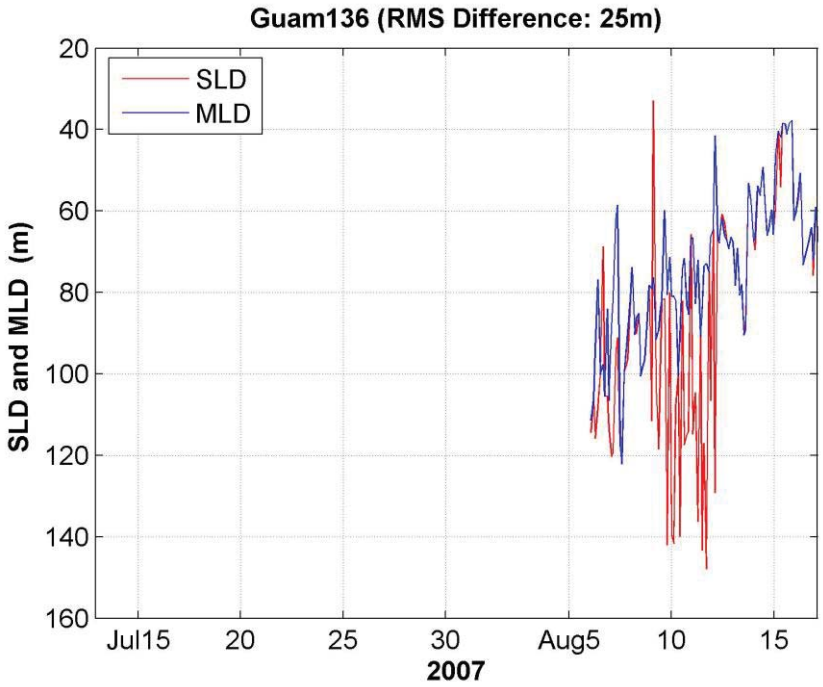

Figure 67. Glider 161 MLD and SLD for Guam.

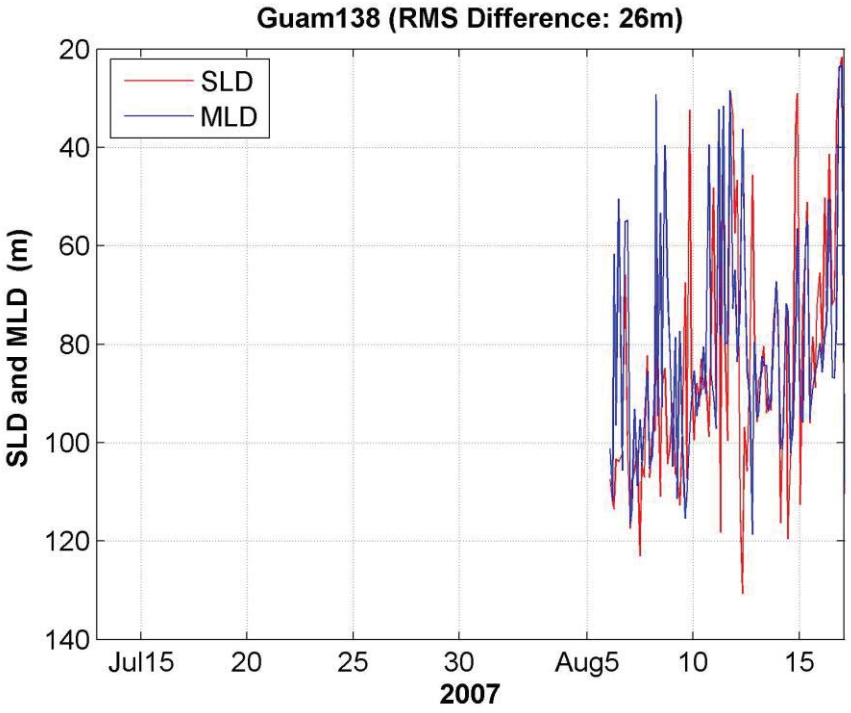

Figure 68. Glider 138 MLD and SLD for Guam.

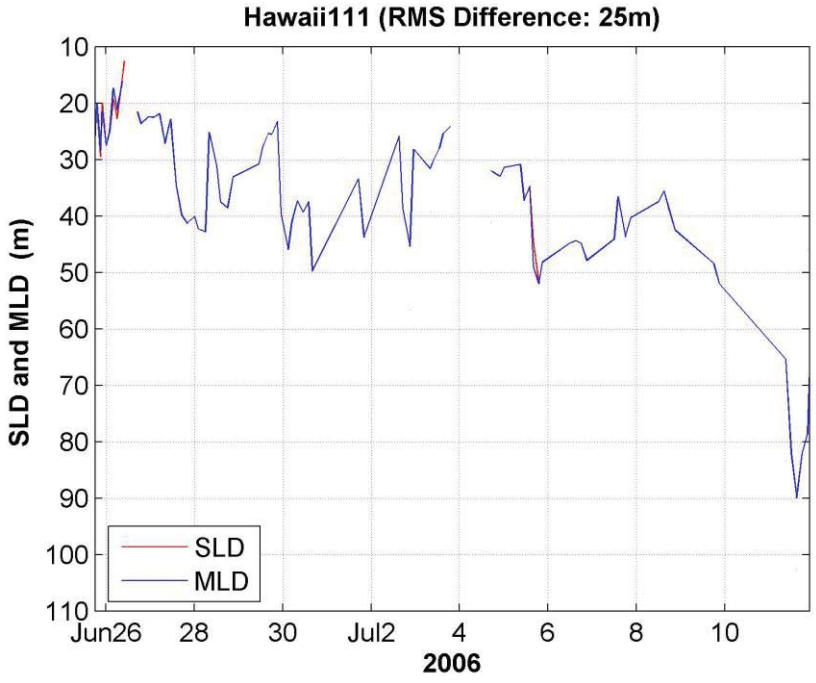

Figure 69. Glider 111 MLD and SLD for Hawaii.

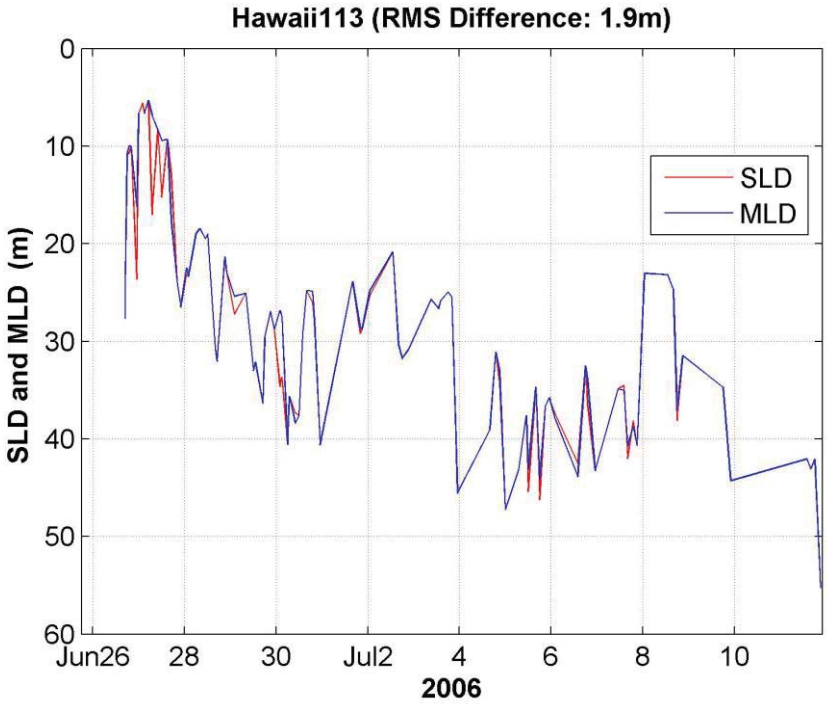

Figure 70. Glider 113 MLD and SLD for Hawaii.

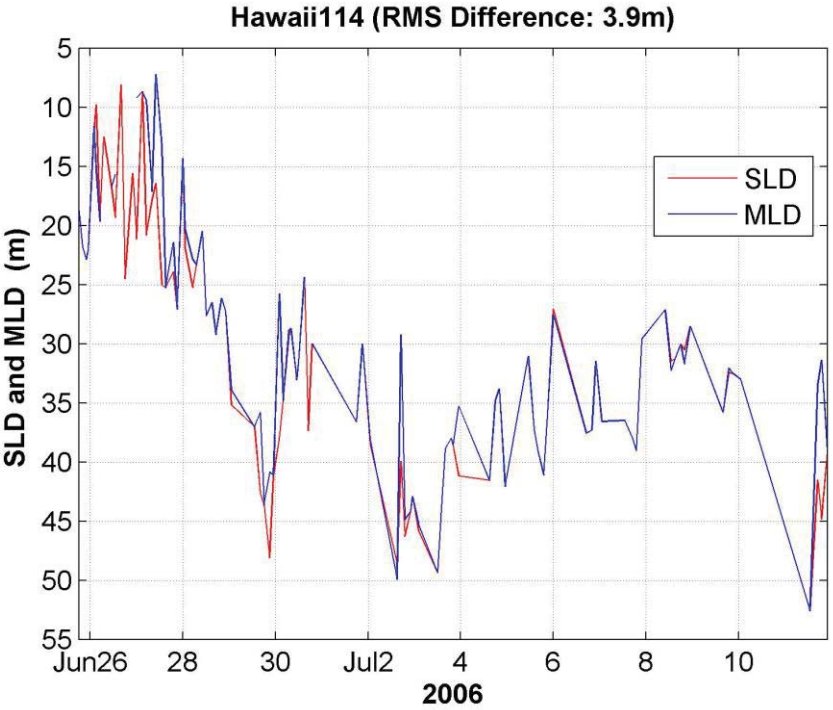

Figure 71. Glider 141 MLD and SLD for Hawaii.

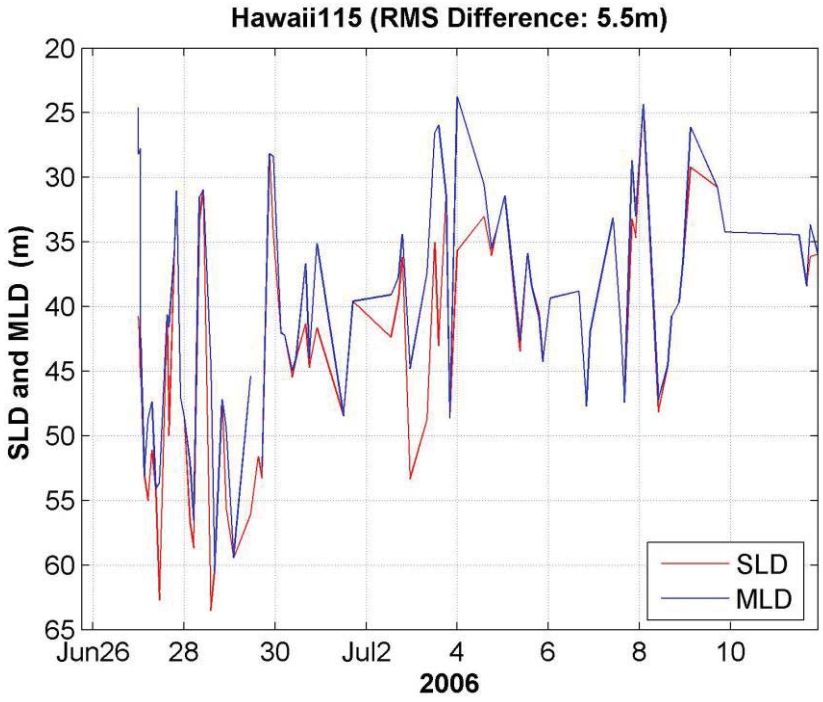

Figure 72. Glider 115 MLD and SLD for Hawaii.

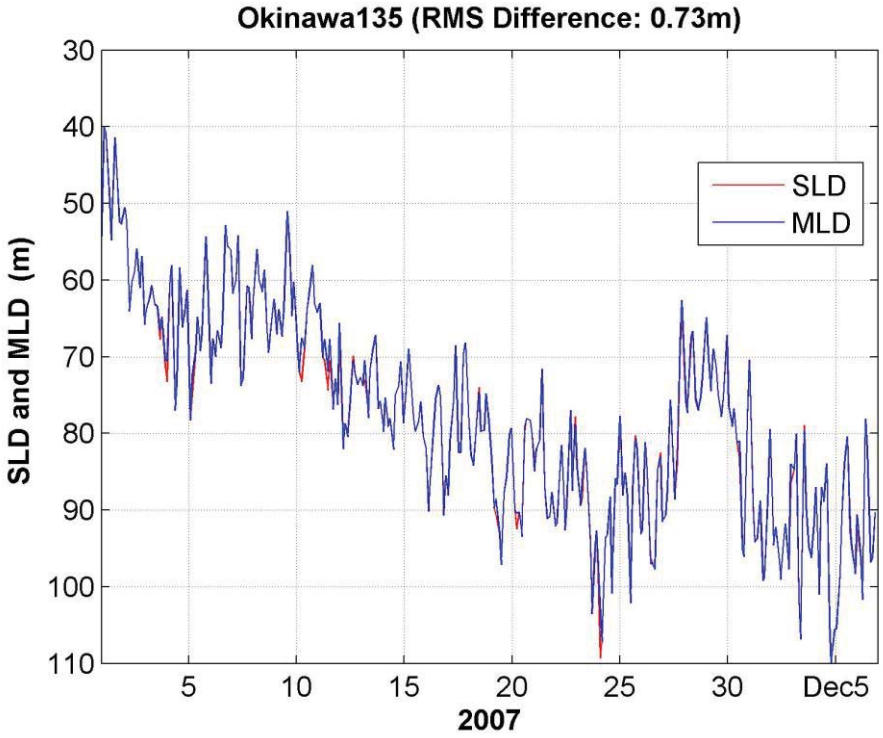

Figure 73. Glider 135 MLD and SLD for Okinawa.

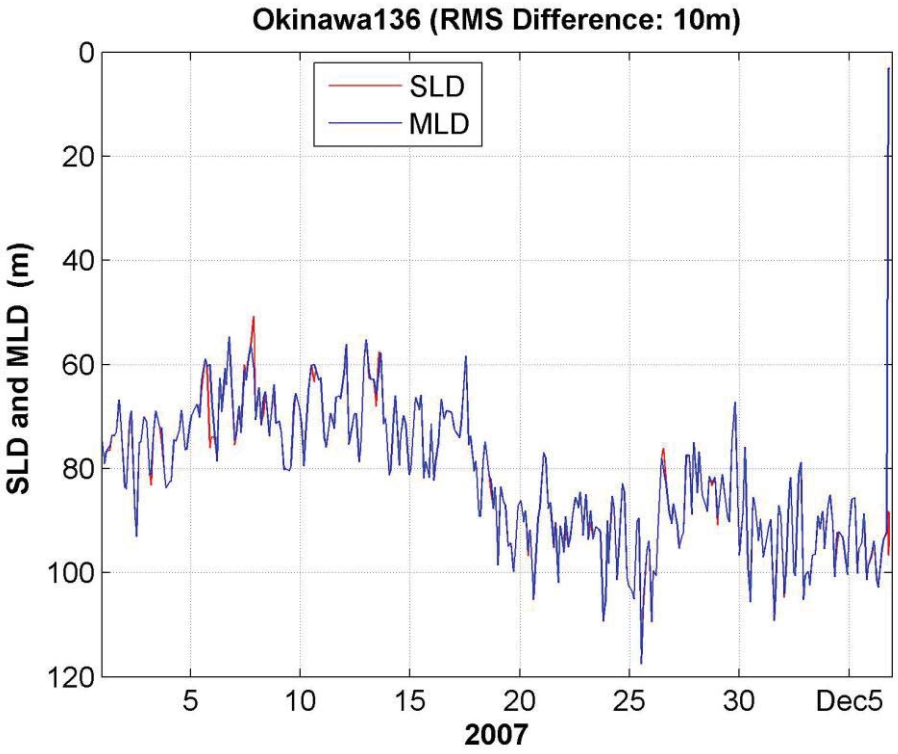

Figure 74. Glider 136 MLD and SLD for Okinawa.

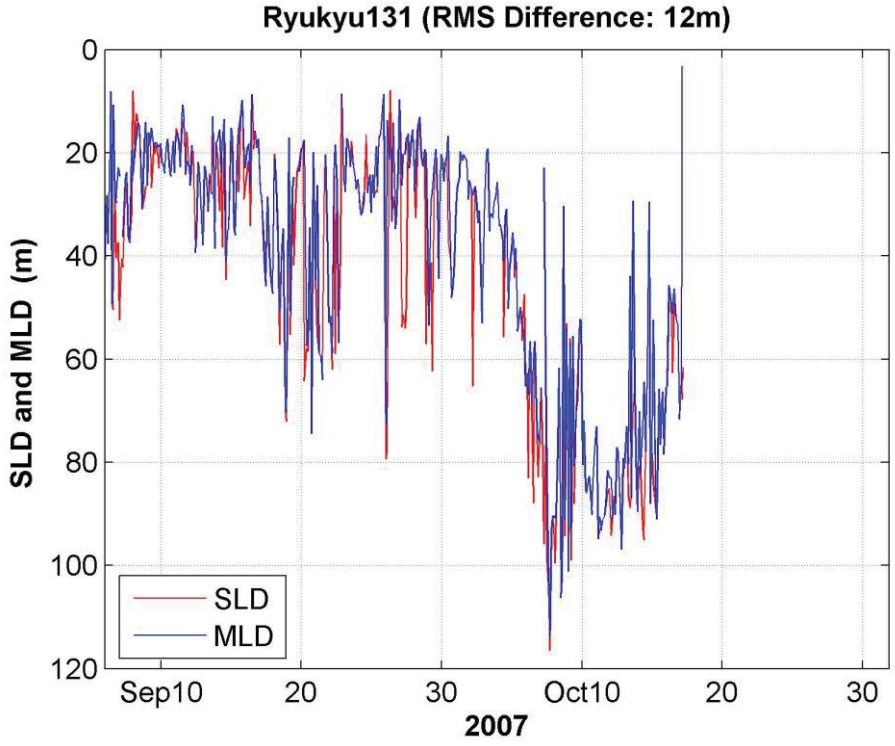

Figure 75. Glider 131 MLD and SLD for Ryukyu.

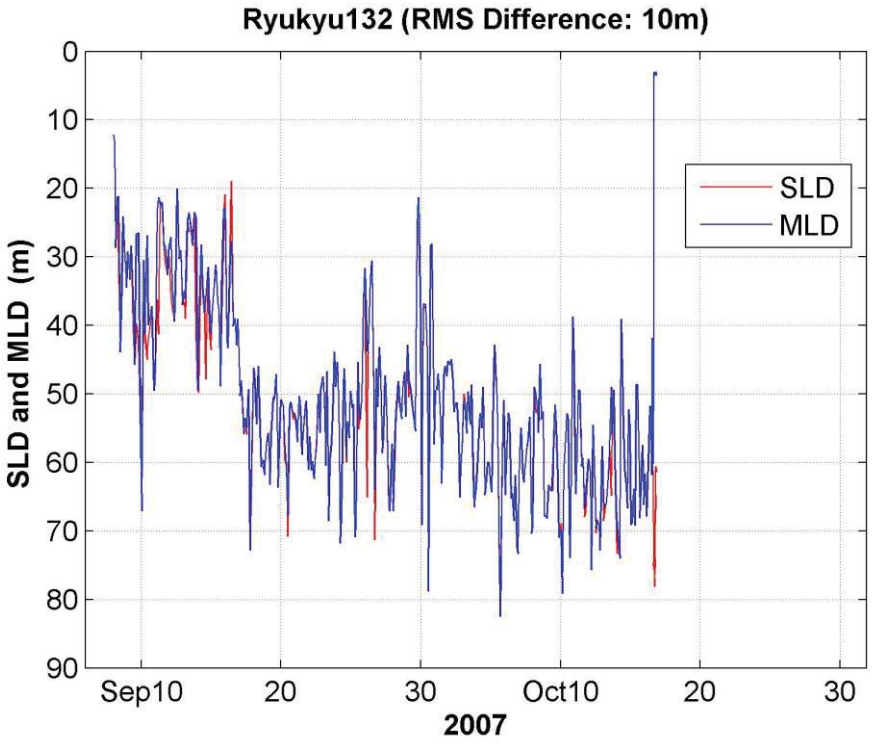

Figure 76. Glider 121 MLD and SLD for Ryukyu.

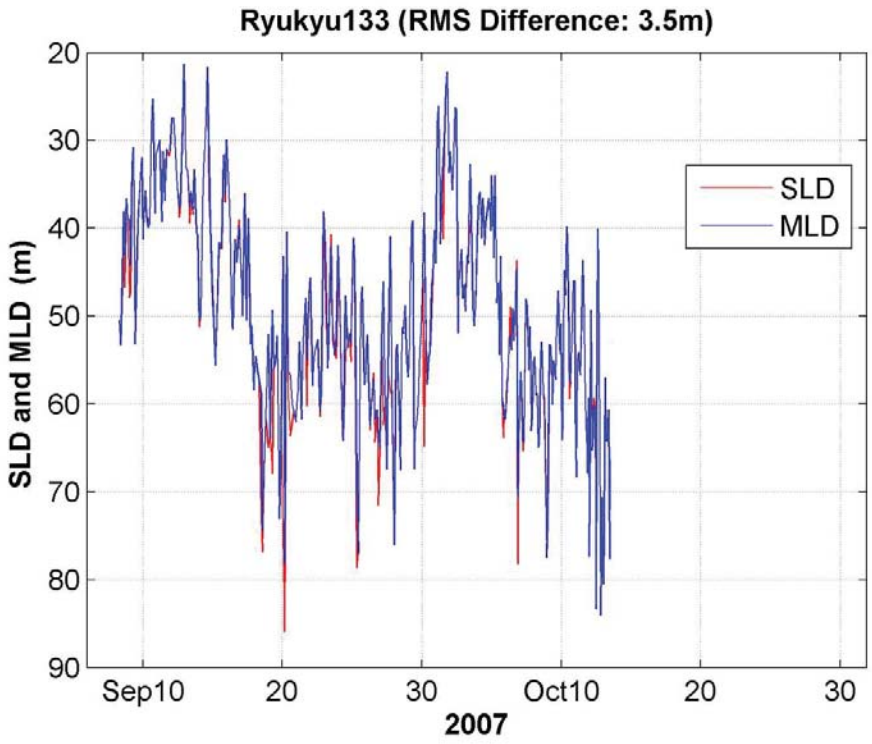

Figure 77. Glider 133 MLD and SLD for Ryukyu.

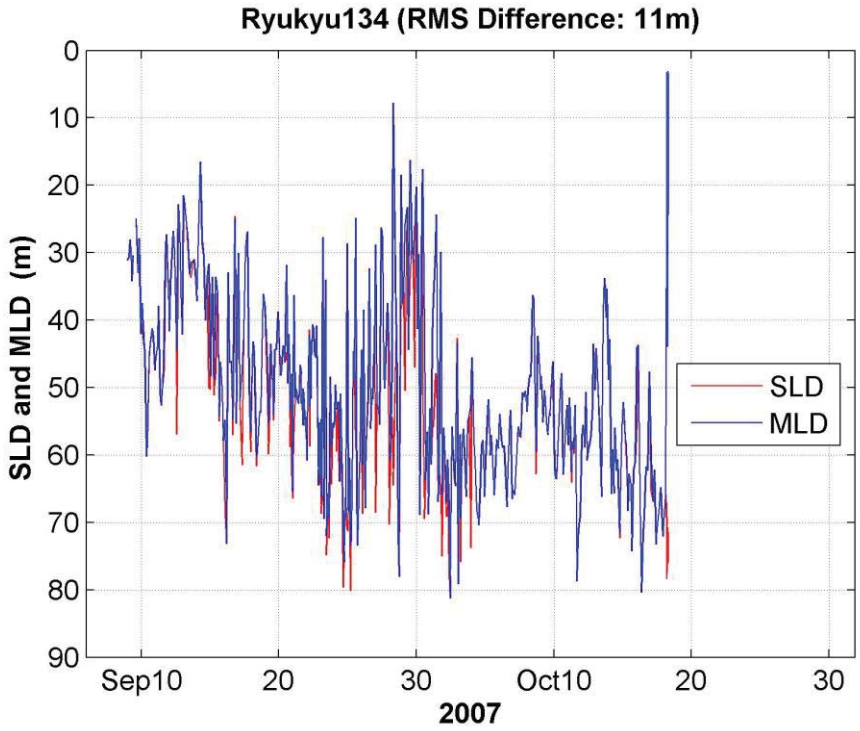

Figure 78. Glider 141 MLD and SLD for Ryukyu.

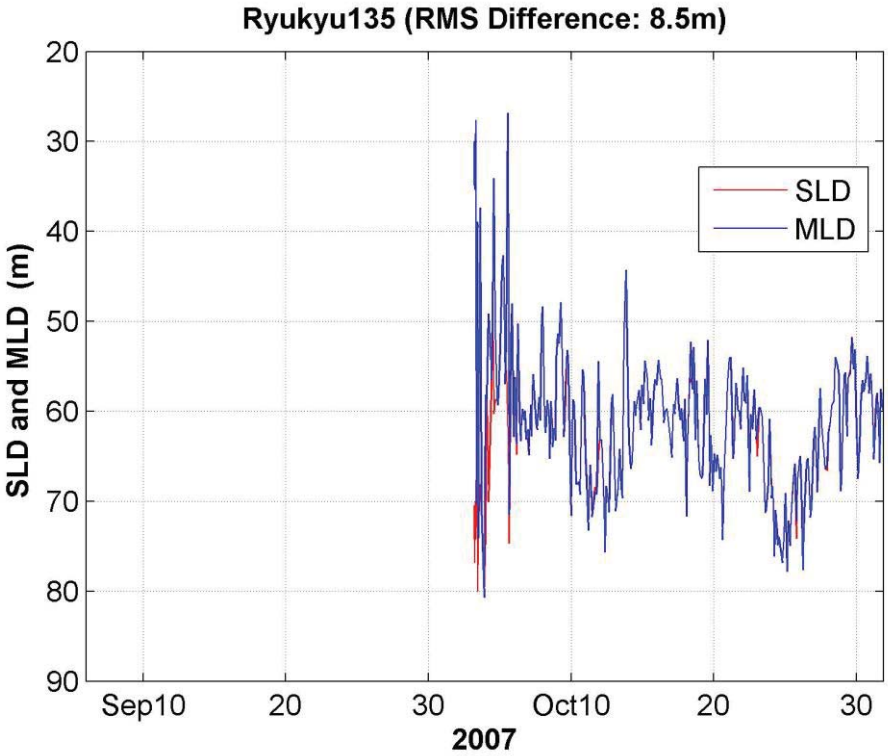

Figure 79. Glider 135 MLD and SLD for Ryukyu.

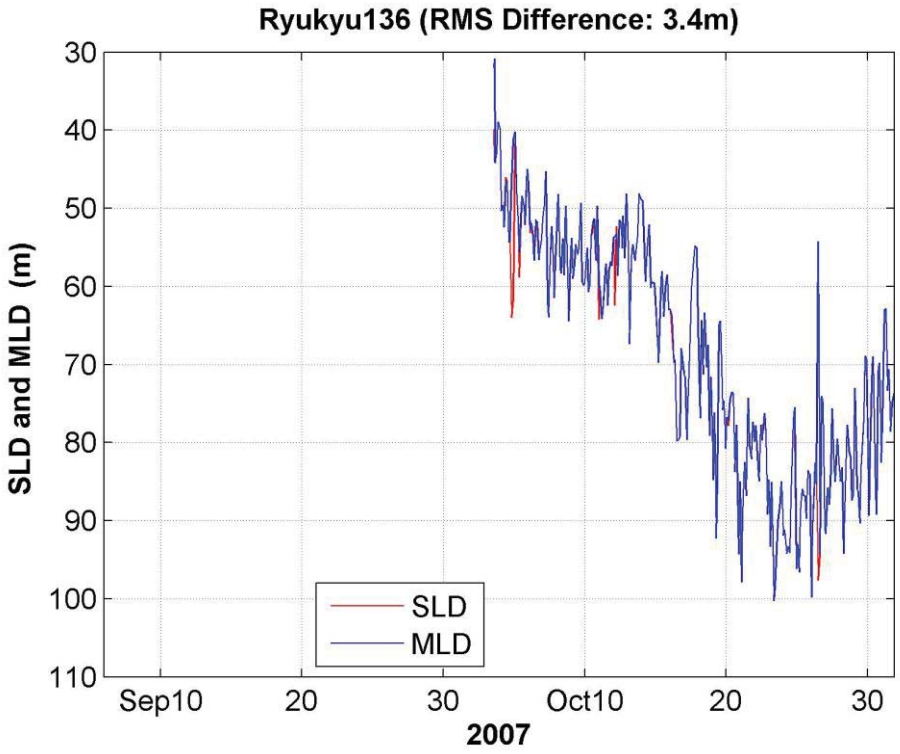

Figure 80. Glider 131 MLD and SLD for Ryukyu.

To get a better feel for the comparison of the MLD to the SLD we plotted the linear regression of the MLD for all areas. In the below six graphs (Figures 81-86) the red line is the linear regression for the MLD. The equation of the line at the bottom right of each graph is the equation of the line for the linear regression. The black line is the ideal line for MLD versus SLD. If everything were perfect, all the blue dots would fall on that line. The number at the top of the graphs is the absolute mean distance of the blue dots from the black line. As one would expect most of the blue dots fall above the black line, due to the SLD being below the MLD at most points in our data set.

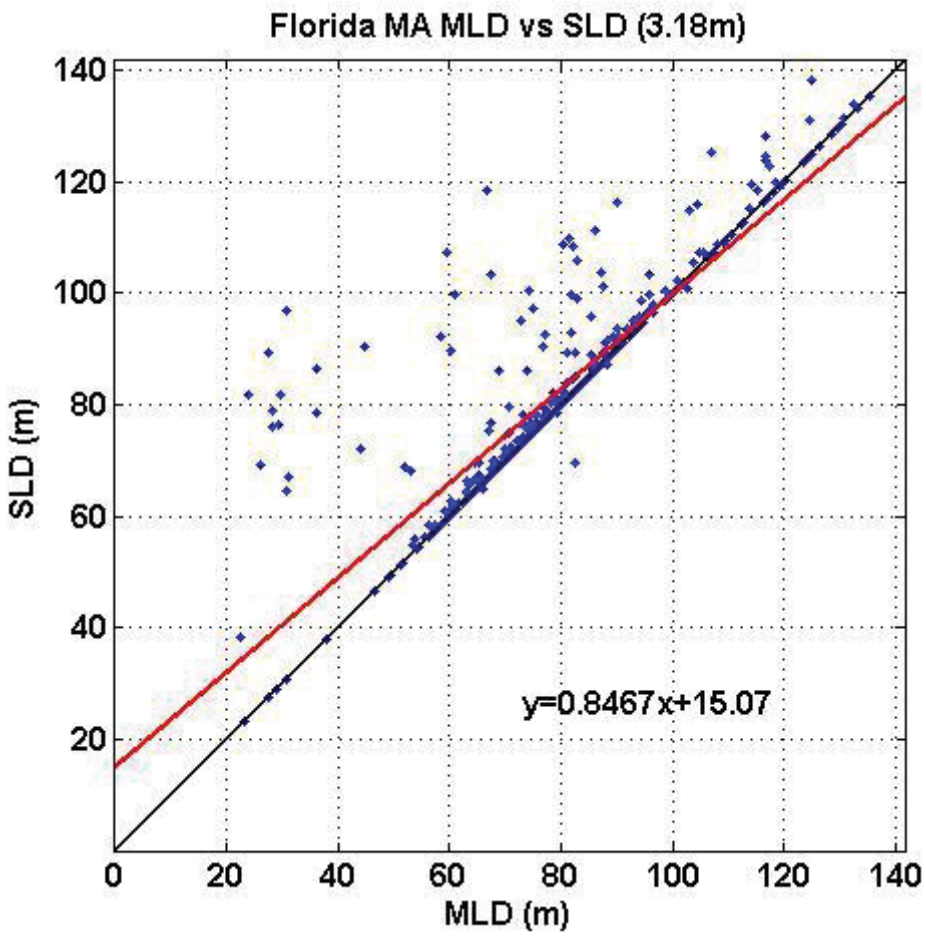

Figure 81. A plot of the liner regression line for the MLD vs SLD for all of Florida.

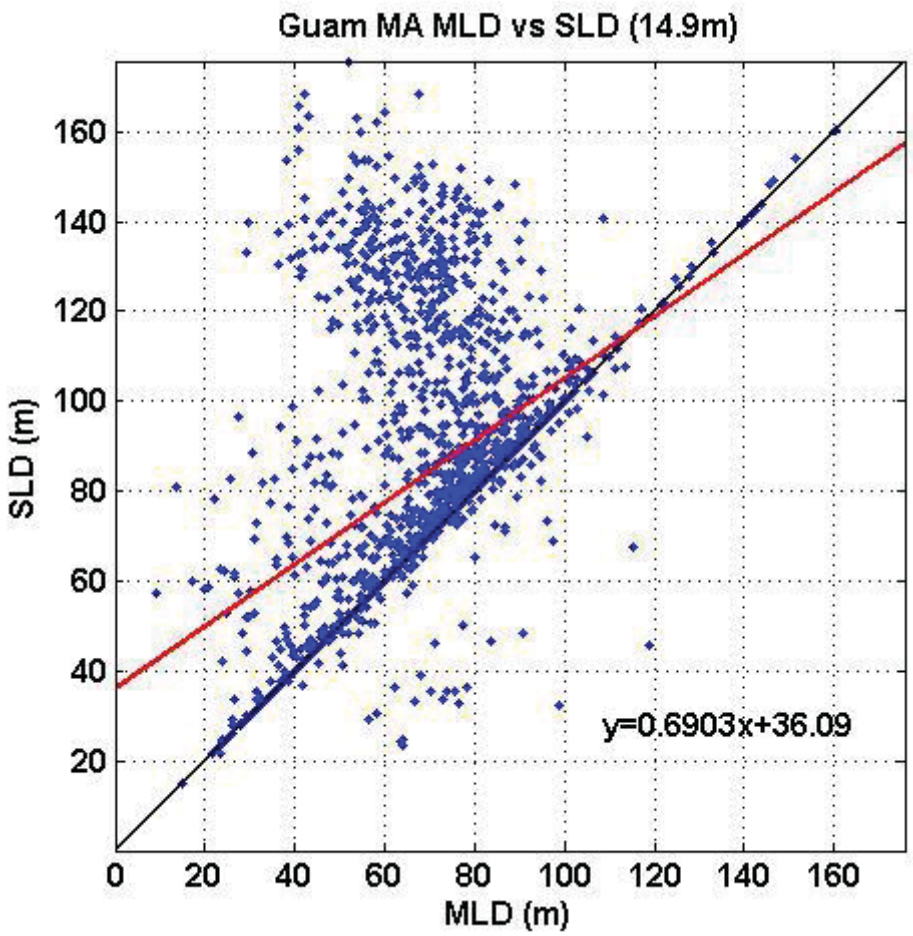

Figure 82. A plot of the liner regression line for the MLD vs SLD for all of Guam.

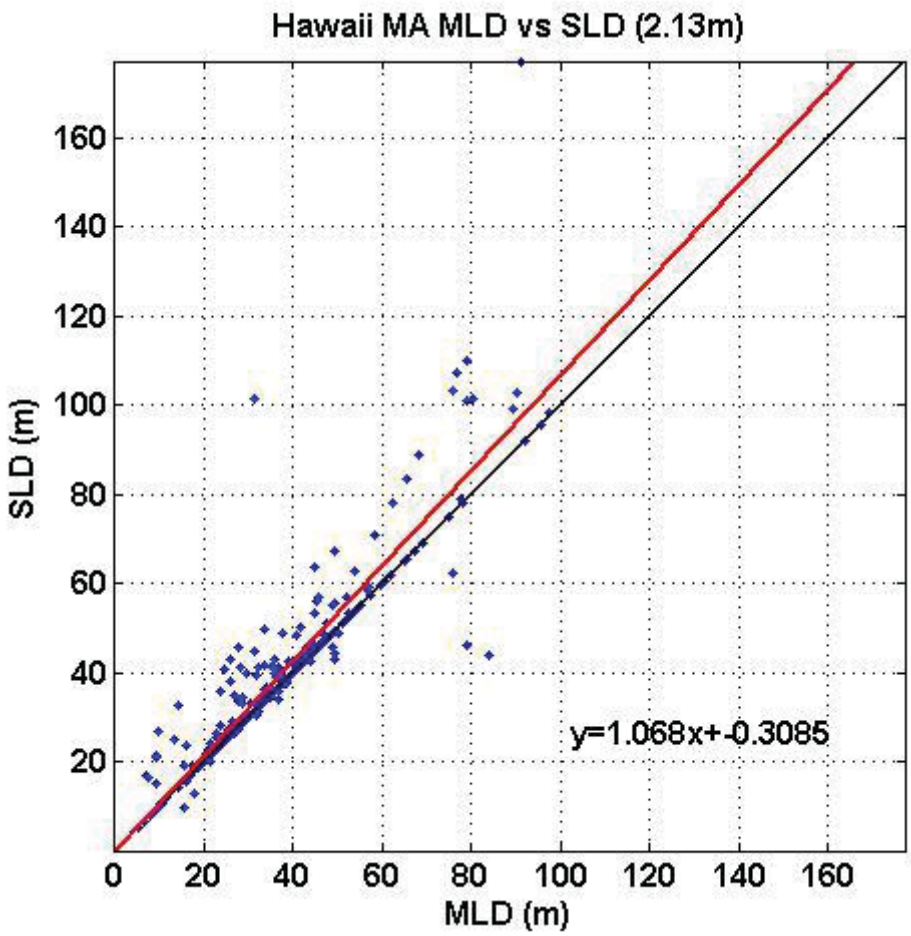

Figure 83. A plot of the liner regression line for the MLD vs SLD for all of Hawaii.

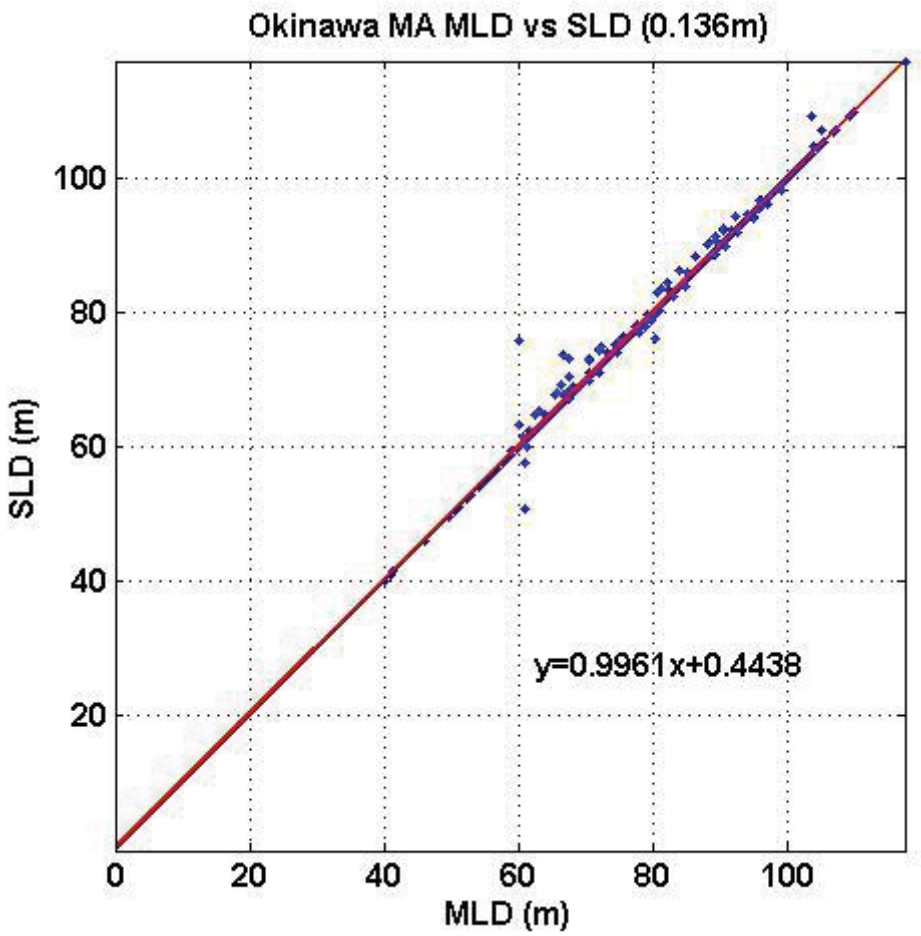

Figure 84. A plot of the liner regression line for the MLD vs SLD for all of Okinawa.

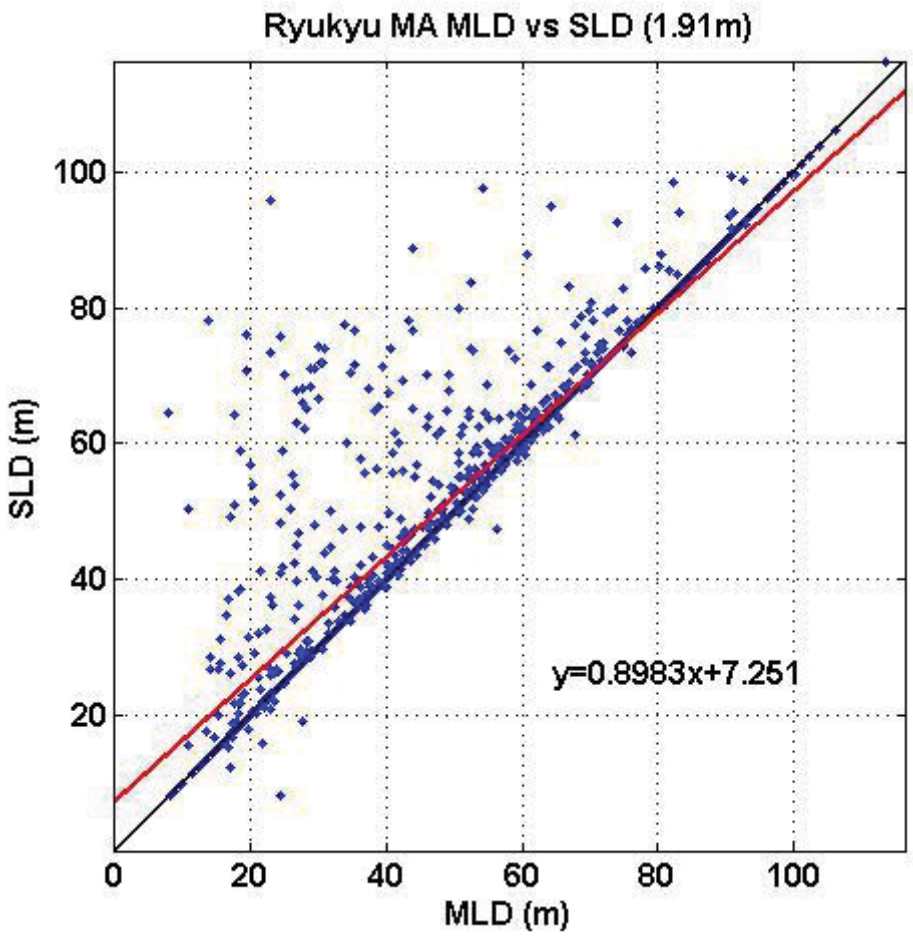

Figure 85. A plot of the liner regression line for the MLD vs SLD for all of Ryukyu.

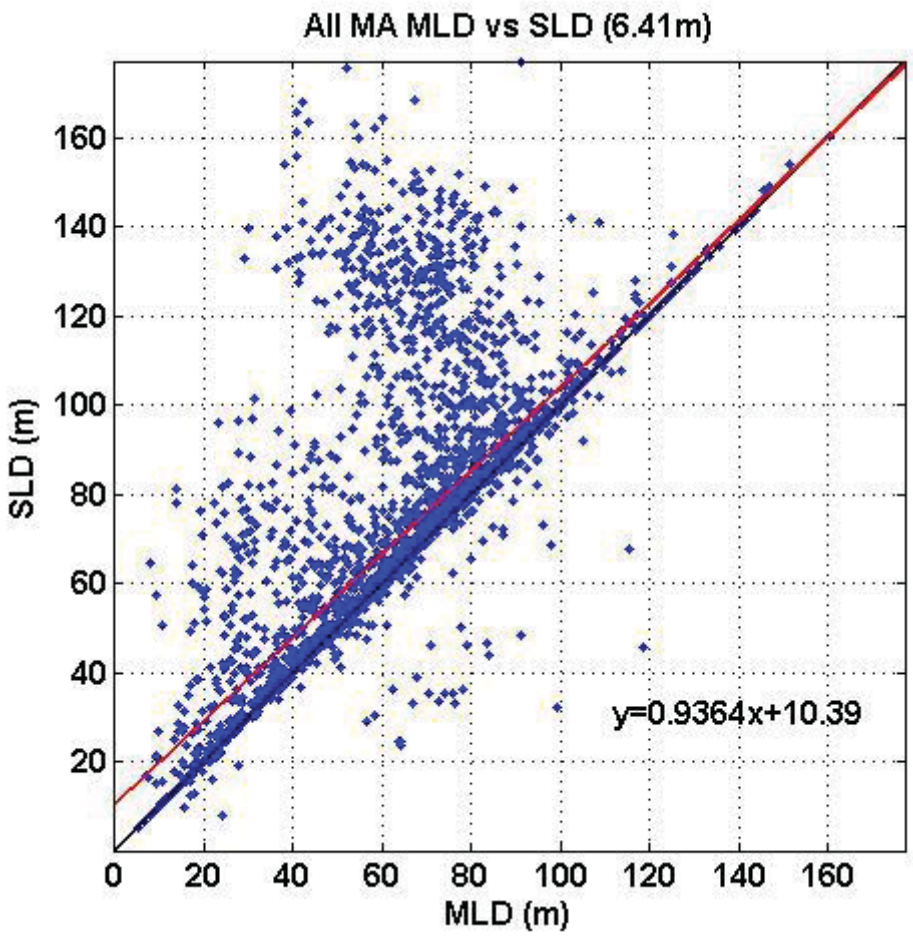

Figure 86. A plot of the liner regression line for the MLD vs SLD for all five of the areas.

THIS PAGE INTENTIONALLY LEFT BLANK

V. ANALYSIS

This chapter presents the analysis of our data set of the MLD and compares them to the SLD. It also outlines possible reasons and explanation for the outcomes that we received.

A. BEST METHOD

It is quite clear that the MA method is the best method for determining the MLD. The MA was first place finisher in four out of five areas and second in the other. If one looks at Figure 87, over 4,000 dive profiles from all five areas of the MA MLD where within a meter or less of the of the SLD. That is approximately 80 percent of the data points and 90 percent of them are within 10 meters (See Figure 87).

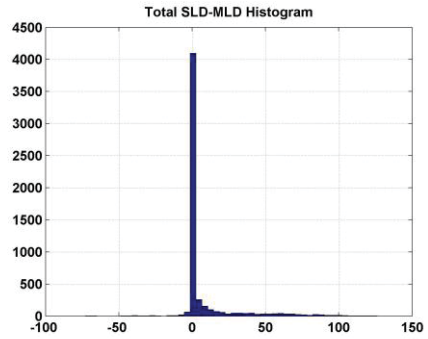

Figure 87. SLD minus the MA MLD histogram for every dive profile.

If one looks at Guam, the difference of Δ.8 reference 10m method was the second best method to determine the MLD. The reason for this was the low QI for Guam (.608 MA). All QI references in this thesis will refer to the MA QI as a benchmark. There are three contributing factors to the low QI score at Guam. For whatever reasons there was not a well-defined mixed layer in the region, which lowered the QI. The second was that the underwater environment at Guam was particular "noisy" throwing off the data measurements. The last reason and least likely was that there could have been some erroneous measurements from the sea gliders that lowered the score of the QI.

If the QI is below .7, than the difference method of Δ.8 reference 10m method will out due other difference methods as it is not as sensitive to sporadic temperature readings, or too large of a ΔT to pass up the MLD. The best examples of this can be seen in figure 53. Although the MA was the second best method for Florida, one can clearly see that both the MA method and the difference method of Δ.2 reference 10m have sharp vertical spikes at points in the graph where a change in temperature triggered their programs to identify the MLD higher than it actually was. For this reason the difference method of Δ.8 reference 10m method will work better than the other difference methods, gradient methods, and the curvature method in a low QI environment.

B. OTHER FINDINGS

It is also clear from the data that the gradient method is by far and consistently the worst method to determine the MLD. With the lone exception being the 0.05°C/m threshold that was the second best in Okinawa. Of key note was Okinawa had the highest QI (.948) out of all the areas we considered for this thesis. When one averages out the scores of all five gradient methods, including the 0.05°C/m threshold across the five areas, they round out the bottom of the 17 methods used with the 0.05°C/m threshold being 13th to the 0.015°C/m threshold being 17. This also shows that the less sensitive the gradient method is the better it seems to do.

The results also show that for the difference method it is much better to use 10 meters as the reference depth rather than 0 meters. There are four different situations where the same ΔT was used but the reference depths were either 0 meters or 10 meters. In each of the four situations where the same Δ was used the references of 10 meters scored better than the 0 meter reference techniques.

While the curvature method came in ninth overall when we averaged all five of the areas together, it did score first overall in Florida and ranked high in Okinawa. This is due to the curvature method being sensitive to “noisy” data. In both Florida and Okinawa the QI was above .9. From the results it would be a safe assumption that if the QI is above .9, then the curvature will closely match or exceed the difference methods.

C. OTHER SIGNIFICANT POINTS

One surprising result in the data was that the difference method of Δ.2 reference depth 0 meters was the exact same as the Δ.2 reference depth 3 meters in each of the areas. This is due to the measurements between 0 and 3 meters in depth being the same for all five areas. In other words there was no temperature change greater than 0.2 degrees Celsius between the surface of the water and 3 meters in depth.

D. SLD FINDINGS

It was a surprise when we got the results back from the Mackenzie 1981 nine-term equation used to calculate the SLD that most of the point would be above the MA MLD. In the perfect world it would not have mattered which way we measured the SLD, as they should be one and the same. At first we could not determine the exact cause for the SLD being above the MLD in the majority of points on the graph, but after some investigation we determined that very "noisy" salinity measurements present in most areas were throwing off the sound speed profile (SSP). They were creating small unauthentic horizontal spikes (or bumps) in the SSP that were high enough to throw off the SLD. In some of the profiles the two SLD differed by more than 40 meters.

In the perfect world the max value SLD determination would work 100 percent of the time and there would be no need for MA determination of the SLD. However, this is a real world data set, and real world data sets have flaws and errors in them. To help correct these issues the MA SLD determination is a better method for determining the SLD when using a real world data set because it allows for the data to have flaws but still be viable.

THIS PAGE INTENTIONALLY LEFT BLANK

VI. CONCLUSIONS

This chapter takes our results and explains how it can benefit the USN and its missions now and in the future. Next, it summarizes our results. Lastly, it suggests future area of works that can be researched that are related to our thesis.

A. IMPACTS TO THE NAVY

The following sections describe how the USN can use the MA method to their advantage. We detail three specific examples below (Expendable bathythermograph, Wave Glider, and operations).

1. Expendable bathythermograph

In standard practices the USN uses an instrument called an Expendable bathythermograph (XBT) to determine the SLD from their ships, aircraft, and submarines. The XBT has seen in Figure 88 is a small torpedo look devices that measures temperature as it falls through the water column. It has a weight at the "nose" of the torpedo and probe to measure temperature. It sends the information collected back to the platform via a copper wire. To measure depth, the XBT uses a fall rate equation to determine where it is in the water column. In other words, it knows approximately how fast it is falling and how long it has been falling. Speed equal distance times time; therefore, the system is able to back out distance/depth. The advantages of using an XBT are that it is inexpensive, simple, and the platform can be moving while it is being used.

Figure 88. A picture of a standard XBT (from NOAA 2014).

The data form the XBT is transferred to the sonar suite onboard the navy platform and plugged into a function to determine the SLD from temperature only. I have not been able to determine the exact equation used by the USN, but it is safe to assume that it is not the MA method, which was developed by Chu and Fan in (2010). Most likely the USN uses some form of the difference method. I am also unaware as to whether they are able to manually change the ΔT or the reference depth in the function. In either case the MA would perform better than the difference method that they are using. The locations in this thesis where specially chosen because the USN is consistently operating in those waters. We wanted to show that the MA method as a direct and real impact on the way the USN operates. If the USN were to adopt the MA method, the results would be a more accurate and objective measurements for the SLD for the platform to conduct its ASW and ASUW missions. This would be a relative simple and inexpensive software upgrade that would result in better determination of the SLD for the USN.

2. Wave Glider

The Wave Glider began development in 2005 with its lead inventor Roger Hine. It was developed to be a new class of persistent ocean vehicles that could constantly sample the ocean environment and do it with less money and more effectively then moorings or ships could. In 2007, Roger Hine and company founded Liquid Robotics Incorporated (LRI) to further develop the Wave Glider for scientific, commercial, and military applications (Hine et al. 2009). The defining attribute of the Wave Glider is its ability to

harvest energy from the ocean waves to provide basically limitless propulsion. This provides an entirely new approach to deploying ocean instruments and opens the door to new ocean applications (Manley et al. 2010).

Figure 89. Wave Glider major component and physical layout (from Rochholz 2012, p.4).

a. The Basics

The Wave Glider is an ocean wave-propelled unmanned autonomous vehicle with a two-body design (Rochholz 2012). The float body floats on the ocean's surface and looks similar to a surfboard see Figures 89. The other half is the "sub." It is about seven meters below the float attached by an umbilical cord. The combination of the "float" and the "sub" working together provide the propulsion. It is the open architect design that permits a variety of sensors and instruments to be placed on it, allowing it to measure many different parameters in the ocean and atmosphere.

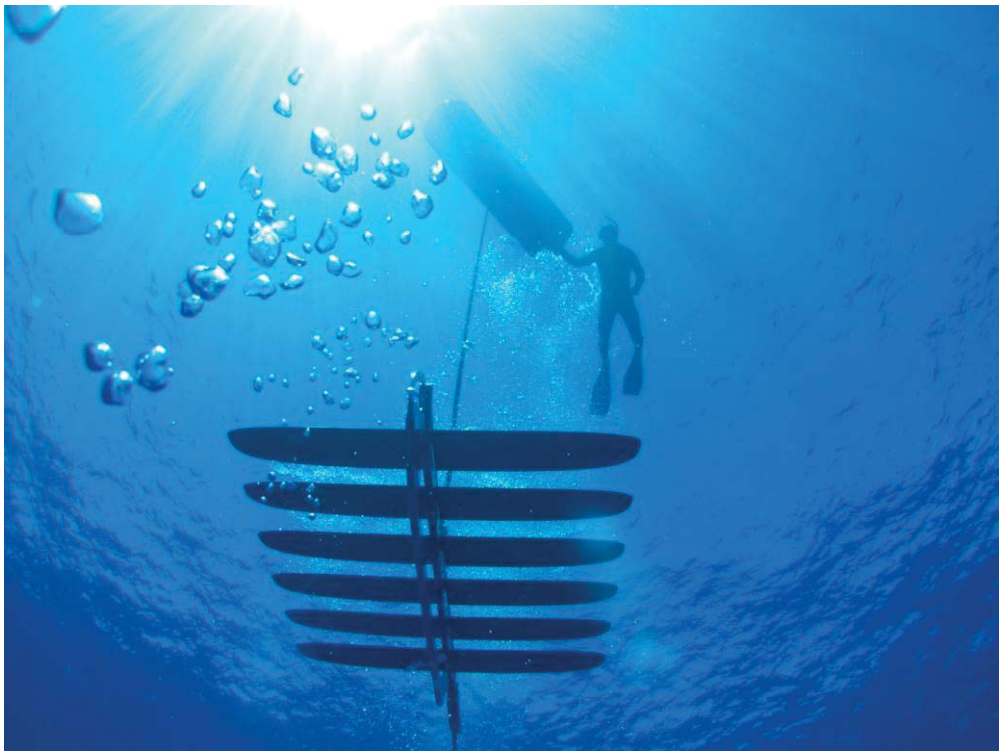

Figure 90. Wave Glider from below (from LRI 2014).

Liquid Robotics' Wave Gliders were the first unmanned autonomous vehicle to use the natural wave motion of the seas for energy (Dillow 2013). It is a simple and novel propulsion method. The "sub" and "float" simply convert the wave energy to thrust. The crest of a wave passes under the "float" and the tethered "sub" is lift vertically. The lower water movement at the subs depth acts on spring-loaded wings pressing them down creating a forward motion pulling the float. As the sub drops with the passing wave, its wings pivot up and the sub continues moving forward (Manley et al. 2010). This is done independent of wave direction.

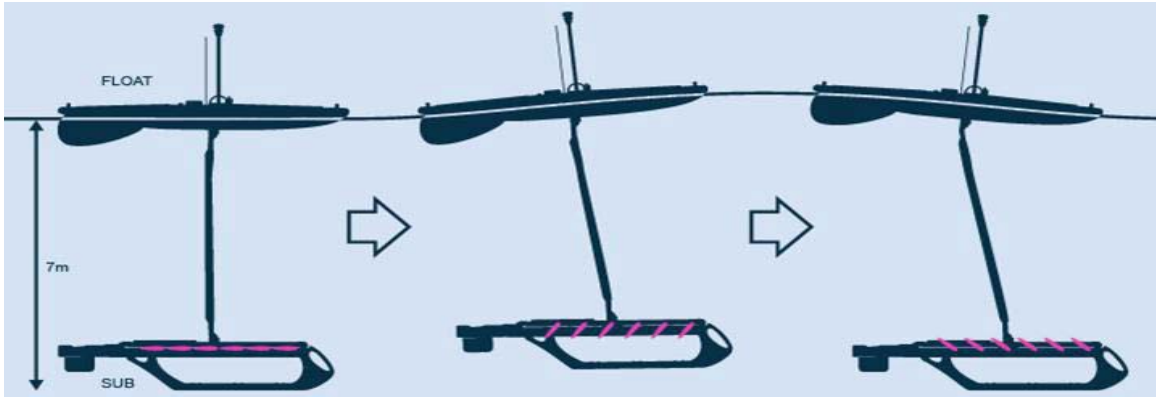

Figure 91. How the wave glider works (from LRI 2014).

LRI currently has two versions of the wave glider, the older surface vehicle two (SV2) and the surface vehicle three (SV3). The SV2 is a proven platform with over 200 produced and over 100 customer missions accomplished. They have survived five hurricanes, three cyclones, and over 300,000 nautical miles (LRI 2014).

b. The SV3

The SV3 is a superior model to the SV2. The biggest improvements are the addition, of an auxiliary thruster, an extra solar panel, and onboard computing power. With its powerful "computational capabilities for real-time onboard processing of large volumes of data at sea, the SV3 can transmit "just the answer" back to shore, representing a big step forward in unmanned ocean monitoring and exploration (LRI 2014)." With more power available to the sensors the SV3 can now handle more power hungry payloads and support a wider array of sensors.

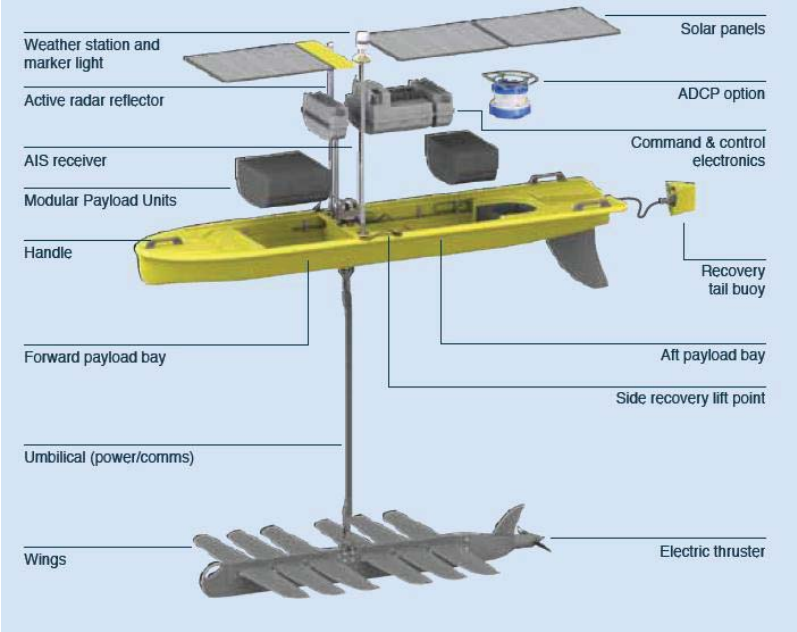

Figure 92. The SV3 components (from LRI 2014).

The SV3 float is 290cm x 67cm and its sub is 21cm x 190cm. The combined float and sub weighs about 90kg. Its speed is again dependent on the sea state, but is generally between 1kts-2kts. With its auxiliary thruster on the SV3, it can run about at 1.5-2.3 knots.

The SV3 can also briefly submerge to a depth of 2m. Its battery power is 980Wh rechargeable Li-ion and a peak solar power of 170W. It also deploys for up to year at a time. For more information about the speciation of the SV3 please see Table 3.

Wave Glider SV3: Basic specifications

GENERAL

Vehicle configuration
Sub & Float joined by 4m (13ft) tether

Dimensions
Float: 290cm x 67cm (114in x 26in)
Sub: 21cm x 190cm (8in x 75in)
Wings: 143cm wide (56in)

Weight
122kg (270lb)

Endurance
Operate for years at sea (with regularly scheduled maintenance)

Water speed
Aux. thruster off:
1.0kts (SS1) - 2.0kts (SS4)
Aux. thruster on:
1.5kts (SS1) - 2.3kts (SS4)

Depth rating
Continuous wash and spray
Brief submergence to 2m (6.5ft)

Observability
Visibility mast, with flag, marker light and radar target enhancer

Transportation & shipping
Air freight compatible
Ships in 3 wooden crates
Crate dimensions: 305cm x 61cm x 61cm (10ft x 2ft x 2ft)
Crate 1: 136kg (300lb)
Crate 2: 104kg (230lb)
Crate 3: 73kg (160lb)

COMMUNICATIONS

Over-the-horizon
Iridium® 9602
RUDICS (option)
Cellular (option)

Local
802.11g WiFi

POWER

Propulsion
Conversion of wave energy into thrust
Auxiliary thruster

Battery
980 Wh rechargeable Li-Ion standard
Increments (980 Wh) up to 7.8kWh

Solar power
170W (peak)

SAFETY

Emergency location
Shore-activated light
Redundant RF beacons
2-Year redundant Iridium® tracker

Health sensors
Pressure, temperature & leak sensors in dry boxes

Battery compliance
Batteries isolated from each other
Automatic charge/discharge cut-off (for temperature and/or voltage)

NAVIGATION

Heading
Solid state magnetometer

GPS
12 channel WAAS capable

Accuracy
3m radius CEP50

Station keeping
40m radius CEP90
(SS3: current <0.5kts)

PAYLOAD

Architecture
Standard mechanical, electrical & software Modular Payload Unit (MPU) architecture for easy integration and configurability

Base integration
Water speed sensor
AIS receiver
Airmar 200WX weather station
Wave data
Radar reflector, light, and flag

Payload ports
Float: 4
8-pin 5/8" wet mateable connector
13.2V, 3A, RS232/422/485, GPS, PPS

High voltage payload ports
Float: 1
6-Pin 5/8" wet mateable connector 48V, 3A, RS232/422/485

Expansion ports
Float: 4; Sub: 1
12-pin wet mateable connector
14-22V, 10A, RS 232/485, 10/100 Ethernet

Max. discrete payloads
7 (MPUs in float)

Max. payload weight (float)
45kg (100lb)

Max. payload volume (float)
93L (3.3ft^3)

Peak payload power
400W

OPERATION

Mission control
Chart-based GUI
Multi-vehicle display
Waypoint & course generation

Status monitoring
Text & visual status indicators accessible via web interface
SMS and email alerts
Programmable inclusion & exclusion zones

Autonomous navigation
Programmable waypoint course
Follow course and hold/loop
Station keeping at target

SOFTWARE

Operating system
Regulus

Features
Multi-tenant
Mesh
Swarm
Collision avoidance autonomy
High availability
On-board data processing
In-situ application updates

Table 3. SV3 specifications (from LRI 2014).

c. Wave Glide, Sea Gliders and the USN

The USN currently has a fleet of sea gliders that are being used more and more out in the fleet. The USN currently has a handful of Wave Gliders that have limited use. There are many concerns that operators face when using the sea gliders. Some of the issues are time on station, determining the exact location in the water column, battery power, and computing power. The SV3 can solve most of these concerns. In 2012, T. W. Rochholz wrote a thesis titled "Wave-Powered Unmanned Surface Vehicle as a Station-

Keeping Gateway Node for Undersea Distributed Networks." In his thesis, he describes his findings for the Wave Glider to be a gateway node between UUV. He states,

> Because of the surface/subsurface interface design that the Wave Glider embodies, it provides a platform that would be useful for communication with UUVs deployed in nearby areas. One difficulty in UUV operation is the ability to operate at or near the surface. The Wave Glider could provide a useful link in communication with UUVs via an acoustic path, allowing the UUV to stay submerged completely while communicating. This would eliminate the need for the UUV to surface or extend a mast above the water line to transmit comms to decision makers. (Rochholz 2012)

The Wave Glider can bridge the gap between the "decision makers" and the UUV. The SV3 is fully capable and has the power, data processing, and communications to have a sea gliders send it its temperature data via an acoustic path and have the Wave Glider apply the MA method and send to nearby USN assets for use. By doing this, the UUV and Wave Glider can exchange information without the UUV surfacing. This will save the UUV's battery power, getting a GPS fix, and increases its time on station.

LRI has developed, engineered, and fielded a prototype vertical depth profiler for the SV3. Operating in a command-activated or fully-autonomous mode, the profiler deploys to a depth of up to a mile, rewinds, and uploads the cast upon docking. The SVP casts are then available via Iridium or other available communications paths, or can be used on board as part of a decision-making algorithm. Thus the Wave Glider could not only be a gateway subsea-to-surface-to-"decision makers" node for UUVs, but it could also determine the MLD and many other deeper depth environmental parameters by itself (D. Jagoe (LRI), 2014, personal communications).

The USN can benefit from both of these cases. For example, they would no longer need a platform on station to determine the MLD. This would prove helpful in waters around the world that are not friendly to U.S. forces. Knowing the SLD and its trends before the USN enters it could have huge advantage in the USN ASW and ASUW roles. In addition, having real time data from platforms that are able to move is a huge advantage for areas around the world that there are drastic changes in temperature and

salinity. In both cases, the Wave Glider using the MA method would improve the USN ability to wage undersea warfare (USW).

3. Operations

Using the MA method will improve the accuracy of our SLD. While this is a simple statement it has huge implications for officers out in the fleet. Take for example a dive officer on a submarine going to periscope depth. He has to adjust the trim of the submarine from a Sound Velocity Profile (SVP). The SLD is a good indicator of a pcynocile and halocline and this can help the dive officer from broaching when he is going to periscope depth. In addition, the tactical action officer in combat on a surface ship can better prosecute a submarine if he better knows where the SLD is. With an improvement to the location of the SLD, the tactical action officer will better know where to put the tail and also where the submarine has a possibility to expose itself. Furthermore, a pilot or mission commander on an aircraft could better deploy his fleet of sonobuoys if he has a better approximation of the SLD. By air, sea, and subsea improving the USN approximation of the SLD would improve its advantage in its ability to wage USW.

B. SUMMARY

In this thesis we looked at 17 different techniques with four different methods: difference, curvature, gradient, and MA to determine the MLD. These methods will only work when there is a present and defined thermocline in the water column being sampled. This will work in most areas of the world except at high latitudes where there is not always a defined thermocline. We looked at five different locations from around the world: Florida, Guam, Hawaii, Okinawa, and Ryukyu and over 6,000 dive profiles. Out of all the methods tested the MA method was the best for determining the MLD. The MA method scored first in four out of the five areas and second in the other. In second was the difference method of $\Delta.2$ reference 10m that scored second or third best in three out of the five areas. Both of these methods performance declined as expected when the QI was below.7 because they became too sensitive for the "noisy" data. In Guam the difference method of $\Delta.8$ reference 10m worked the second behind the MA method

because it is not as susceptible to "noisy data" as the other difference methods, curvature method, and gradient method. The difference method always worked better when the reference depth was at 10 meters vice zero meters. The gradient method was by the far the worst method it determining MLD and rounded out the bottom five slots out of the 17 different ways we calculated the MLD. The curvature method was only a factor when the QI was above .9. The MA determined MLD on average differed from the SLD in a great QI (>.95) environment by less than a meter.

While in practice the max sound speed determination of the SLD should work 100 percent of the time. But when it is used in real-world with a noisy data set it can be fooled. The best way to deal with a noisy real world data set is to apply the MA determination of the SLD to it. It will allow for most of the erroneous horizontal spikes/bumps to be over looked while maintaining the validity of the data set.

C. FUTURE RECOMMENDATIONS

There are several areas of this thesis that can be researched further. One area is to apply a smoothing function to the temperature profile before running all 17 different calculations. Another future area of study is to use a data set that comes from XBTs from USN assets from around the world. Another objective determination of the MLD exists. The method is called the optimal linear fitting (Chu et al. 2010b) was not evaluated in this thesis. It possesses many of the same pros of the MA method and should be evaluated against it.

Another area that can be further explored is to create a function that changes the ΔT in the difference method using a reference depth of 10 meters to maximize the QI and comparing that result to the MA angle method. This could give the edge to the difference with method with its ability to tweak the ΔT for the area.

It would also be worth looking at some higher predetermined threshold for the gradient method. The QI increase for the gradient method in every area that we looked at when we raise the threshold number. While this would not work in a perfect profile, it would behoove someone to see how high we could raise the threshold number and still get dependable data.

LIST OF REFERENCES

Bathen, K. H. 1972: On the seasonal changes in the depth of the mixed layer in the North Pacific Ocean. *J. Geophys. Res*., **77**, 7138–7150.

Chen, D., Busalacchi, A. J., and Rothstein, L. M. 1994: The roles of vertical mixing, solar radiation, and wind stress in a model simulation of the sea surface temperature seasonal cycle in the tropical Pacific Ocean. *J. Geophys. Res.: Oceans (1978–2012)*, **99**, 20345–20359.

Chu, P. C., Q. Liu, Y. Jia, and C. W. Fan, 2002: Evidence of a barrier layer in the Sulu and Celebes Seas. *J. Phys. Oceanogr.*, **32**, 3299–3309.

Chu, P.C., and C. W. Fan, 2010a: Objective determination of global ocean surface mixed layer depth. *OCEANS.* 1001–1007

Chu, P.C., and C. W. Fan, 2010b: Optimal linear fitting for objective determination of ocean mixed layer depth from glider profiles. *J Atmos Oceanic Technol.* **27**, 1893–1898.

Chu, Peter C., and C. W. Fan, 2011: Maximum angle method for determining mixed layer depth from seaglider data. *J.of Oceanogr.* **67**, 219–230.

de Boyer Montegut, C., G. Madec, A. S. Fischer, A. Lazar, and D. Iudicone, 2004: Mixed layer depth over the global ocean: An examination of profile data and a profile-based climatology. *J. Geophys. Res.: Oceans (1978–2012)*, **109**, doi:10.1029/2004JC002378.

Defant, A. 1961: *Physical Oceanography*, **1**. Pergamon Press, 729 pp.

Dillow, C., cited 2014: Drones come to the high seas. [Available online at http://fortune.com/2013/04/11/drones-come-to-the-high-seas/]

Garrett, C. 1996: Processes in the surface mixed layer of the ocean. *Dyn. Atmos. Oceans*, **23**, 19–34.

Google Inc., 2014: Google Earth Version 7.0.3.8542. Google Inc.

Guest, A., cited 2014: Direct path propagation. [Available online at http://www.oc.nps.edu/~bird/oc2930/acoustics/directpath.html]

Helber, R. W., C. N. Barron, M. R. Carnes, and R. A. Zingarelli, 2008: Evaluating the sonic layer depth relative to the mixed layer depth. *Journal of Geophysical Research: Oceans (1978–2012)*, **113**, doi:10.1029/2007JC004595.

Helber, R. W., A. B. Kara, C. N. Barron, and T. P. Boyer, 2009: Mixed layer depth in the Aegean, Marmara, Black and Azov Seas: Part II: Relation to the sonic layer depth. *J. of Marine Sys.*, **78**, 181–190.

Hine, R., S. Willcox, G. Hine, and T. Richardson, 2009: The wave glider: A wave-powered autonomous marine vehicle. *OCEANS 2009*, 1–6.

Holli, R., cited 2014: The ocean's carbon balance. [Available online at http://earthobservatory.nasa.gov/Features/OceanCarbon/]

Liquid Robotics Inc., cited 2014: Liquid Robotics. [Available online at http://liquidr.com/ and http://liquidr.com/technology/waveglider/how-it-works.html]

Kara, A. B., P. A. Rochford, and H. E. Hurlburt, 2000: An optimal definition for ocean mixed layer depth. *J. Geophys. Res.: Oceans (1978–2012)*, **105**, 16803–16821.

Kara, A. B., and H. E. Hurlburt, 2006: Daily inter-annual simulations of SST and MLD using atmospherically forced OGCMs: Model evaluation in comparison to buoy time series. *J. of Marine Sys.*, **62**, 95–119.

Kara, A. B., R. W. Helber, T. P. Boyer, and J. B. Elsner, 2009: Mixed layer depth in the Aegean, Marmara, Black and Azov Seas: Part I: general features. *J. of Marine Sys.*, **78**, 169–180.

Lorbacher, K., D. D. Dommenget, P. P. Niiler, and A. Kohl, 2006: Ocean mixed layer depth: A subsurface proxy of ocean-atmosphere variability, *J. Geophys. Res*., **111**, doi:10.1029/2003JC002157.

Lukas, R., and E. Lindstrom, 1991: The mixed layer of the western equatorial Pacific Ocean. *J. Geophys. Res.h: Oceans (1978–2012)*, **96**, 3343–3357.

Mackenzie, K. V. 1981: Nine-term equation for sound speed in the oceans. *The Journal of the Acoustical Society of America*, **70**, 807–812.

Mahoney, K. L., O. Schofield, J. Kerfoot, T. Giddings, J. Shirron, and M. Twardowski, 2007: Laser line scan performance prediction. *Optical Engineering+ Applications*, **6675**, doi:10.1117/12.734617.

Mahoney, K., R. Arnone, P. Flynn, B. Casey, and S. Ladner, 2008: Ocean Optical Forecasting in Support of MCM Operations. *Proc. of 8th Int. MINWARA Conference of Technology and the Mine Problem*.

Mahoney, K. L., and N. D. Allen, 2009: Glider observations of optical backscatter in different Jerlov water types: Implications to US naval operations. *OCEANS 2009, MTS/IEEE Biloxi—Marine Technology for Our Future: Global and Local Challenges,* 1–8.

Mahoney, K. L., K. Grembowicz, B. Bricker, S. Crossland, D. Bryant, M. Torres, and T. Giddings, 2009: RIMPAC 08: Naval Oceanographic Office Glider Operations. *SPIE Defense, Security, and Sensing*, **7317**, doi:10.1117/12.820492.

Manley, J., and S. Willcox, 2010: The wave glider: A persistent platform for ocean science. *OCEANS 2010 IEEE-Sydney*, 1–5, doi:10.1109/OCEANSSYD.2010.5603614

National Oceanic and Atmospheric Administration, cited 2014: EXpendable BathyThermograph (XBT) and Conductivity Temperature Depth (CTD) observations. [http://www.aoml.noaa.gov/phod/goos/xbtscience/images/xbt_fig_clear.png]

Obata, A., J. Ishizaka, and M. Endoh, 1996: Global verification of critical depth theory for phytoplankton bloom with climatological in situ temperature and satellite ocean color data. *J. Geophys. Res.: Oceans (1978–2012)*, **101**, 20657–20667.

Rao, R. R., R. L. Molinari, and J. F. Festa, 1989: Evolution of the climatological near-surface thermal structure of the tropical Indian Ocean: 1. Description of mean monthly mixed layer depth, and sea surface temperature, surface current, and surface meteorological fields. *J. Geophys. Res.: Oceans (1978–2012)*, **94**, 10801–10815.

Rochholz, T. W. 2012: Wave-powered unmanned surface vehicle as a station-keeping gateway node for undersea distributed networks. M.S. thesis, Dept. of Applied Physics, Naval Postgraduate School, 62pp.

Sprintall, J., and D. Roemmich, 1999: Characterizing the structure of the surface layer in the Pacific Ocean. *J. Geophys. Res.: Oceans (1978–2012)*, **104**, 23297–23311.

Thompson, R. O. 1976: Climatological numerical models of the surface mixed layer of the ocean. *J. Phys. Oceanogr.*, **6**, 496–503.

THIS PAGE INTENTIONALLY LEFT BLANK

INITIAL DISTRIBUTION LIST

1. Defense Technical Information Center
   Ft. Belvoir, Virginia

2. Dudley Knox Library
   Naval Postgraduate School
   Monterey, California